

ABSTRACT

Title of Document: **ESTABLISHING LINK BETWEEN
TRANSLATIONAL RECODING AND HUMAN
DISEASE.**

Vivek Manoharlal Advani, Doctor of Philosophy, 2015

Directed By: **Professor and Chair, Jonathan Dinman
Department of Cell Biology and Molecular Genetics**

Gene expression can be controlled at the level of mRNA stability, and prior studies from our laboratory have explained how Programmed -1 Ribosomal Frameshifting (-1 PRF) fits within this paradigm. Computational analyses suggest that 10-15% of eukaryotic mRNAs contain at least one potential -1 PRF signal. The overwhelming majority of predicted “genomic” -1 PRF events are predicted to direct translating ribosomes to premature termination codons. We have demonstrated that these can function as mRNA destabilizing elements through the Nonsense-Mediated mRNA Decay (NMD) pathway. In published work we have explored the biological significance of the connection between -1 PRF and NMD on telomere maintenance in yeast. More recently we extended this line of inquiry to human cells, demonstrating that a sequence element in the mRNA encoding Ccr5p harbors a -1 PRF signal which functions as an mRNA destabilizing element through NMD. In the current work we are exploring the link between global changes in -1 PRF rates and human health using yeast and human cell-based models of two diseases, X-linked Dyskeratosis Congenita

(X-DC) and Spinocerebellar ataxia 26 family (SCA26) as models. Preliminary findings suggest these genetically inherited defects result in translational fidelity defects (i.e. changes in rates of -1 PRF, +1 PRF, and stop codon recognition), with attendant effects on mRNA abundance, gene expression and telomere maintenance. These studies establish a paradigm for understanding the linkage between translational fidelity and human disease.

ESTABLISHING LINK BETWEEN TRANSLATIONAL RECODING AND
HUMAN DISEASE

By

Vivek Manoharlal Advani

Dissertation submitted to the Faculty of the Graduate School of the
University of Maryland, College Park, in partial fulfillment
of the requirements for the degree of
Doctor of Philosophy
2015

Advisory Committee:

Professor Jonathan D. Dinman, Chair
Associate Professor Douglas A. Julin
Associate Professor Stephen M. Mount
Assistant Professor Antony M. Jose
Professor Iqbal Hamza, Dean's Representative

© Copyright by
Vivek Manoharlal Advani
2015

Dedication

Dedicated to my parents for their love and nurture.

Acknowledgements

I wish to express my sincere thanks to Dr. Dinman for sharing expertise, valuable guidance, humor and encouragement extended to me. Without his mentorship and persistent help this work would not have been possible. I would also like to thank my committee members for their time and assistance. A big thank you to all past and present Dinman lab members, for years of fun and assistance.

This work was supported in part by a National Institute of Health grant to Dr. Jonathan Dinman and Graduate Deans Dissertation Fellowship from University of Maryland to Vivek Advani.

Table of Contents

Dedication	ii
Acknowledgements	iii
Table of Contents	iv
List of Tables	vi
List of Figures.....	vii
Chapter 1	1
Introduction.....	1
The Translation cycle.....	2
Translational Recoding.....	8
Nonsense Mediated (mRNA) Decay Pathway.....	18
Ribosome Biogenesis and Ribosomopathies.....	25
Scope of work and Thesis Summary	26
Chapter 2	29
Telomere maintenance is globally controlled by programmed ribosomal frameshifting and the nonsense- mediated mRNA decay pathway	29
Introduction.....	29
Results.....	33
Discussion.....	48
Methods Summary	53
Chapter 3	56
When Translation Goes Bad.....	56
Introduction.....	56
Results.....	60
Discussion.....	66
Methods Summary	69
Chapter 4	71
Conclusion and Future Directions	71
Chapter 5.....	77
Experimental Procedures	77
Cell Culture.....	77
Dual Luciferase Assays.....	77
Quantitative Real Time Reverse transcriptase PCR	78
Transfections.....	79
Transformations	80
Appendix 1: Yeast Strains Used	81
Appendix 3: Mammalian plasmids.....	85
Appendix 4: Oligonucleotides for Cloning.....	87
Appendix 5: Oligonucleotides for Site-Directed Mutagenesis	89
Appendix 6: Oligonucleotides used for qPCR.....	91
Appendix 7: Phylogenetic analysis of predicted -1 PRF signals in ORFs involved in yeast telomere maintenance	93
Appendix 8: RNAi Oligonucleotides.....	99

Appendix 9: Additional validated -1 PRF signals in Humans.....	100
Appendix 10: Summary of the additional validated -1 PRF signals in Humans ..	101
Appendix 11: Human -1 PRF being cloned by the FIRE class.....	105
References.....	107

List of Tables.

Table 1. Clinical characteristics of different ribosomopathies.	26
Table 2. Most predicted -1 PRF signals in ORFs involved in yeast telomere maintenance promote efficient -1 PRF in yeast cells.	36
Table 3. Predicted -1 PRF signals in ORFs involved in human telomere maintenance promote efficient -1 PRF in yeast cells.	48
Table 4. Yeast strains used in chapters 2 and 3. Appendix 2: Yeast based plasmids	82
Table 5. Yeast based plasmids used in chapters 2 and 3.	84
Table 6. Mammalian plasmids used in the study.	86
Table 7. Oligos used for cloning.	88
Table 8. Oligos used for site-directed mutagenesis.	90
Table 9. Oligos used for qPCR in this study.	92
Table 10. Phylogenetic analysis of predicted -1 PRF signals in ORFs involved in yeast telomere maintenance.	98
Table 11. RNAi oligonucleotides used in this study.	99
Table 12. Additional validated -1 PRF signals in Humans.	100
Table 13. Additional -1 PRF signals being cloned by the FIRE class.	106

List of Figures

Figure 1. Model of canonical eukaryotic translation initiation pathway.....	4
Figure 2 The positions of the tRNAs during the elongation cycle: the Hybrid States model.....	5
Figure 3 Overview of the eukaryotic translational elongation.....	6
Figure 4. The model of eukaryotic translation termination.....	7
Figure 5. Viral -1 PRF: Organization and regulation of gene expression	10
Figure 6. Structure and mechanism of -1 PRF.....	12
Figure 7. Kinetic partitioning of mechanisms of -1 PRF.....	13
Figure 8. Pipeline for predicting and validating genomic -1 PRF signals.....	14
Figure 9. Programed +1 ribosomal frameshift signal in yeast EST3 gene.....	16
Figure 10. Mechanism of Selenocysteine incorporation.....	17
Figure 11. General model of NMD in yeast.....	19
Figure 12. General model of EJC dependent NMD in mammalian cells.....	21
Figure 13. Faux 3'UTR model of NMD.....	22
Figure 14. The distribution of length of -1 PRF signal encoded peptides in Homo sapiens.....	23
Figure 15. Model of -1 PRF dependence on NMD.....	24
Figure 16. Predicted -1 PRF signals in ORFs involved in yeast telomere maintenance.	34
Figure 17. -1 PRF signals in the yeast EST1, EST2, STN1 and CDC13 mRNAs respond to cellular mutants (panels A and B) and a drug (panel C) that were previously found to promote changes in -1 PRF promoted by viral -1 PRF signals.....	38

Figure 18. Delineation mathematical relationships between -1 PRF and mRNA abundance in wild-type (Panel A), and NMD-deficient cells (Panel B).....	41
Figure 19. Steady-state abundances of native EST1, EST2, STN1 and CDC13 mRNAs in mutant and drug treated cells.....	42
Figure 20. Ablation of -1 PRF in EST2, or of NMD affects telomere length and promotes G2/M cell cycle arrest.....	44
Figure 21. Sequences of -1 PRF signals in three human messages encoding proteins required for telomere maintenance.....	47
Figure 22. Model: telomerase recruitment to uncapped telomeres is controlled by the relative stoichiometries of telomerase components in yeast.....	51
Figure 23. Causative mutations in X-DC and SCA26.....	59
Figure 24. Dual Luciferase reporter assays to monitor -1 PRF and +1 PRF in yeast and human cells.....	61
Figure 25. Dual luciferase reporter assays to monitor in-frame stop codon readthrough in yeast and human cells.....	62
Figure 26. Yeast based studies of the effects of the cbf5-D95A and eEF2 mutants on mRNA abundance.....	64
Figure 27. Increased rates of -1 PRF and enhanced NMD lead to shortened telomeres.	65
Figure 28. General Model of Ribosomopathies.....	68
Figure 29. -1 PRF in human mRNA IL-2RG is regulated by miRNAs.....	75

List of Abbreviations

ATP	Adenosine Triphosphate
dsRNA	Double stranded RNA
CCR5	Chemokine receptor 5
CDS	Coding sequence
CrPV	Cricket paralysis virus
DLR	Dual luciferase assay system
DMEM	Dulbecco's modified eagle medium
EDTA	Ethylenediaminetetraacetic acid
GTP	Guanine triphosphate
HIV	Human immunodeficiency virus (usually type 1)
IRES	Internal ribosome entry site
LB	Luria bertani broth
LSU	Large subunit of the ribosome
MFE	Minimum Free Energy
M ⁷ G	7-methylguanosine
mRNA	Messenger RNA
miRNA	MicoRNA
ncRNA	Non-coding RNA
NMD	Nonsense mediated decay
PABP	Poly-adenosine binding protein
PCR	Polymerase chain reaction
PPCC	Probability plot correlation coefficient
pol	Polymerase
poly A	Poly-adenosine
PRF	Programmed ribosomal frameshifting
PTC	Premature termination codon
PTR	Programed translational Readthrough
qPCR	Quantitative (real time) PCR
RF	Release Factor
RSV	Rous sarcoma virus
RT	Read through (control)
rPTC	Peptidyl transferase center (ribosomal)
SARS	Severe acute respiratory syndrome
siRNA	Short interfering RNA
ssRNA	Single stranded RNA
SSU	Small subunit of the ribosome
tRNA	Transfer RNA
UTR	Untranslated region

Chapter 1

Introduction

Gene regulation is achieved by myriad cellular processes. In the ‘Central Dogma’ of molecular biology mRNA is centrally placed in the flow of information in biological systems and the regulation of mRNA abundance is extremely important. The rates of mRNA transcription and degradation, silencing and storage of mRNA are the parameters that affect mRNA abundance. Post-transcriptional control mechanisms of gene regulation have the strongest effects on mRNA abundance and hence on protein levels. These mechanisms are mainly attributed to *cis*-acting elements in the 5’ and 3’ untranslated regions of mRNAs and to the trans-acting factors that they interact with. The role of protein coding regions in translational control remains largely unexplored. *Cis*-acting elements in protein coding regions are generically classified as “recoding” elements. Recoding phenomena denote exemptions to the rules of the genetic code. These include, but are not limited to -1 and +1 Programmed Ribosomal Frameshifting, termination suppression, stop-start elements and incorporation of selenocysteine or pyrrolysine. These non-canonical mechanisms were first described in viruses and later identified in prokaryotic and eukaryotic genomes (1). Viruses use translational recoding mechanisms for their proteomic expansion, while most recoding events in eukaryotes serve to fine-tune gene expression during posttranscriptional regulation (2)(3).

Speed and accuracy of translation are important attributes that help maintain cellular homeostasis (4). Defects in translation, e.g. mis-incorporation of amino acids into

polypeptides, can result in protein misfolding, aggregation and disruption of cellular fitness. Dysfunctional translational machinery has deleterious effects on global gene expression and such defects are associated with a growing number of human diseases collectively known as ‘ribosomopathies’. Although each ribosomopathy is associated with specific pathologies, all are generally first typified by the appearance of anemias and, later in life, by cancers (5). The heart of this thesis is to explore how defects in the interplay between mRNAs and ribosomes affect gene expression and contribute to disease pathogenesis.

The Translation cycle

The abundance of the mRNA is tightly regulated from transcription to degradation. Eukaryotic mRNA is synthesized by RNA polymerase II as a primary transcript from the transcriptional unit. The transcriptional unit is a region on the genome that contains appropriate signals for transcriptional initiation and termination. The *cis*-elements that flank the transcriptional unit and the proteins that interact with them regulate the levels of the nascent mRNA. Maturation of the nascent mRNA involves 5’ end capping methylation, pre-mRNA splicing, and poly (A) addition to the 3’ end (6). Once the mature fully processed mRNA is synthesized in the nucleus it is transported to cytoplasm and translated by the ribosome. The actively translating ribosome co-ordinates the intricately series of individual activities required to complete the cycle of initiation, elongation and termination.

Initiation

Translation initiation in eukaryotes is the multistep process that first recruits the ribosomal 40S subunit (small subunit or SSU) to the mRNA, translocates it to the appropriate initiation codon, and then recruits the 60S subunit (large subunit, or LSU). In cap-dependent translation, translation initiation begins with two parallel processes: 1) recruitment of initiator tRNA to the 40S subunit in complex with eukaryotic initiation factors (eIF) 1, 1A, 5 and 5 to make the 43S pre-initiation complex, and 2) recruitment of the eIF4-complex of proteins to 5' (7mGpppN) cap of the mRNA (7). The cap binding proteins eIF4E and eIF4G in turn can bind to the poly (A) binding protein (PABP) associated with the 3' untranslated region (UTR) to “circularize” the mRNA, stabilizing it against exonucleolytic attack. Once circularized, the 43S pre-initiation complex is recruited to the mRNA, where it subsequently scans in the 5' to 3' direction in the 5' UTR until it recognizes an AUG start codon in an appropriate context (8). After the recognition of initiation codon and 48S complex formation (43S complex and eIF3, eIF1, eIF1A), eIF5 and eIF5B promote the hydrolysis of eIF2-bound GTP. Clearance of these factor enables 60S subunit joining to make the translationally competent 80S ribosome (9) (**Figure 1**).

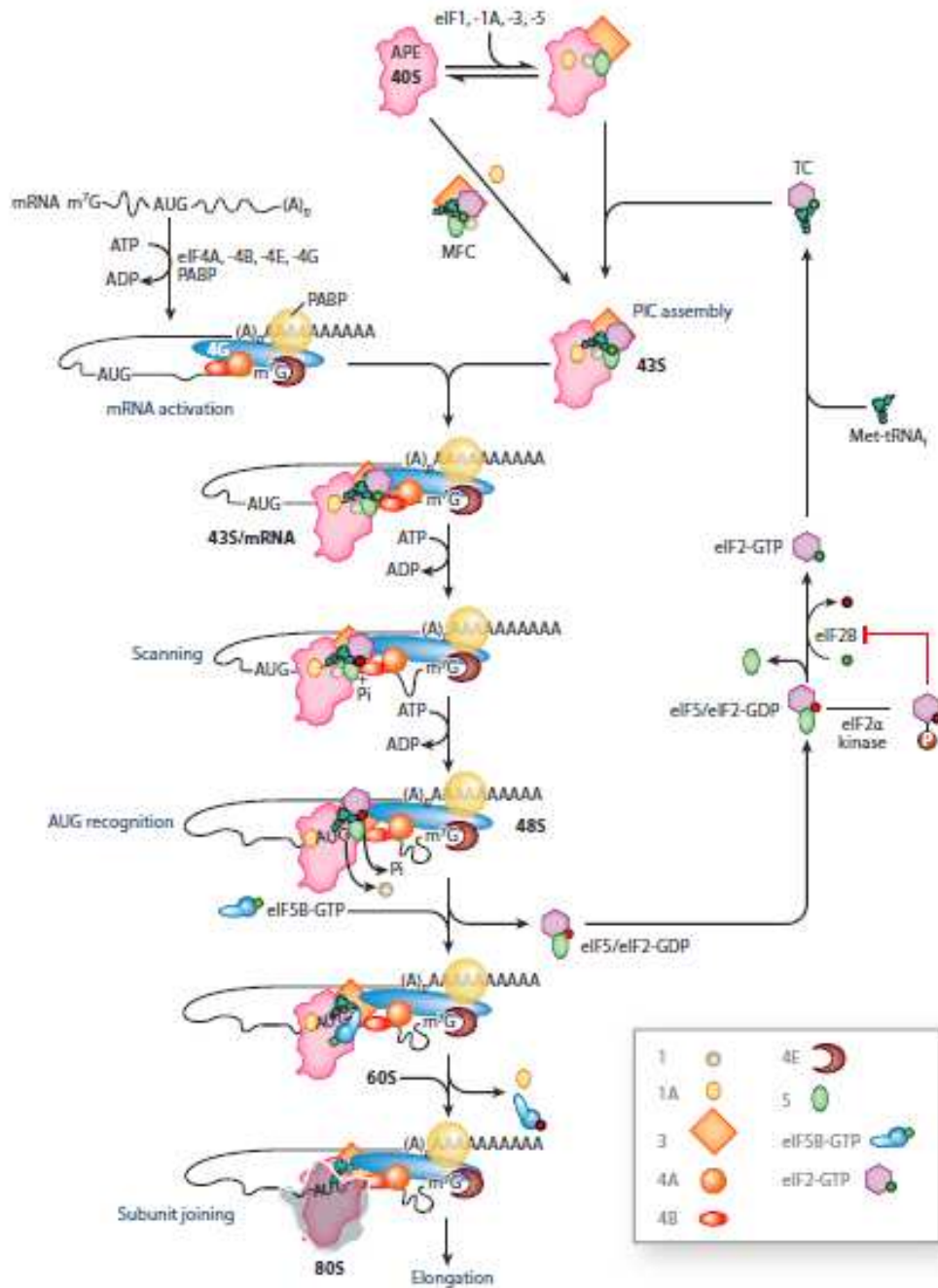


Figure 1. Model of canonical eukaryotic translation initiation pathway.

Translation initiation in eukaryotes begins by the recruitment of the 43S pre-initiation complex on the mRNA through the cap binding complex. Once recruited the 43S pre-initiation complex scans for the initiation codon to form the 48S initiation complex. Post recognition of the initiation codon the structural rearrangements in the 48S initiation complex promote GTP hydrolysis of eIF5 and eIF5B, recruiting the 60S subunit to form the translationally competent 80S ribosome. This figure is adapted from Hinnebusch (8).

Elongation

Once the two subunits join, base pairing interactions between the initiator tRNA and the AUG start codon in the ribosomal P-site function to define translational reading frame. In canonical translation, reading frame must be maintained throughout the process. During each translation elongation cycle, an aminoacyl tRNA is delivered to the A-site by in complex with eEF1A and GTP – this is called the Ternary Complex (TC). Properly charged aa-tRNAs delivered by the TC and the complementary base pairing between anticodon on aminoacyl tRNA and mRNA codon results in the acceptance of the tRNA, a process called accommodation(10),(11). Accommodation of the aa-tRNA prompts a conformational change in ribosome that triggers GTP hydrolysis by eEF1A, releasing eEF1A. During the elongation process, this also results in release of deacylated tRNA from the E-site (**Figures 2 and 3**)(12)(13)(14).

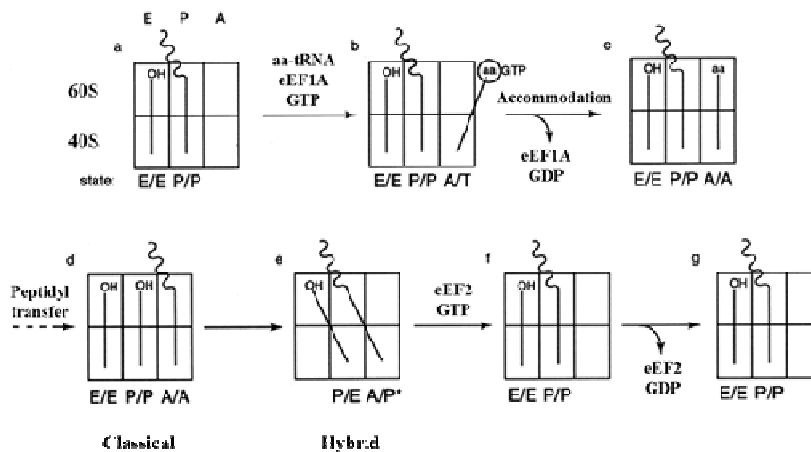


Figure 2 The positions of the tRNAs during the elongation cycle: the Hybrid States model.

The relative positions of the tRNAs during the 'classical' (unrotated) and the 'hybrid' (rotated) states during translational elongation. The figure is modified from (15).

After accommodation, the 3' end of the aa-tRNA is positioned directly at the peptidyltransferase center (PTC) of the LSU resulting in immediate transfer of the

nascent peptide from the incoming aminoacyl-tRNA in a trans-esterification reaction called peptidyltransfer (16). Post peptidyltransfer the tRNAs that were previously in the ‘classical’ (unrotated) state of P/P and A/A adopt the ‘hybrid’ (rotated) P/E and A/P conformation(17)(18). The hybrid state permits the binding of the ternary complex mimic eEF2 and GTP. Binding of eEF2-GTP drives the small subunit to rotate back to the unrotated (classical) state, moving the ribosome along the mRNA in the 3’ direction by three nucleotides in a process called translocation. Subsequently, GTP hydrolysis enables eEF2 dissociation, completing the translation elongation cycle (**Figure 3**). (19)(20).

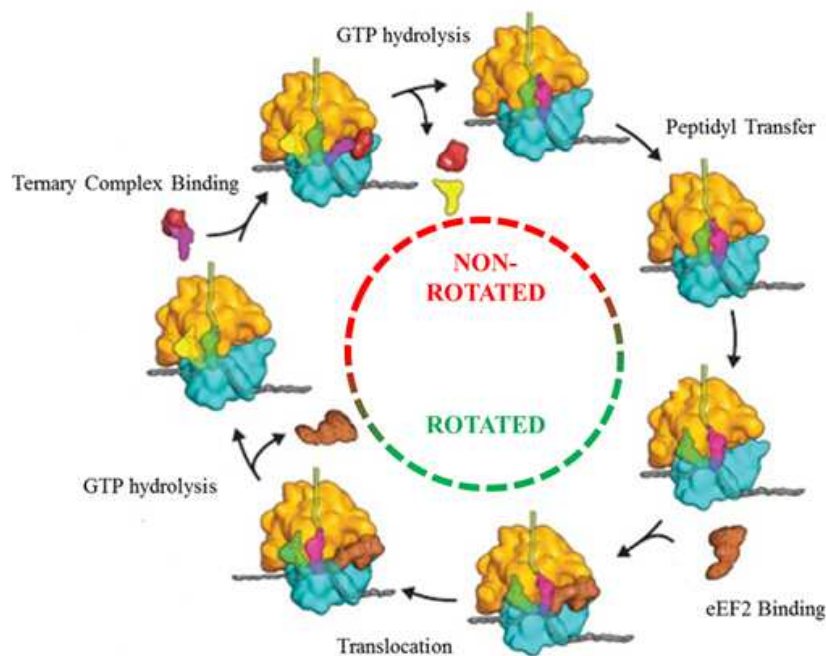


Figure 3 Overview of the eukaryotic translational elongation.

Eukaryotic translation elongation is a multi-step process, where the ribosome is either in the ‘classical’ (unrotated) and the ‘hybrid’ (rotated) state. Elongation factors eEF1A and eEF2 bring new tRNAs and promote translocation through GTP hydrolysis. The figure is modified from (21).

Termination

Three codons, UAA, UAG and UGA do not code for any amino acid. They do not have any cognate tRNAs(22), and are called “stop” or “nonsense” codons. When these codons are enter the A-site during elongation protein factors called release factors (RFs) bind to the ribosome. In eukaryotes, a single release factor eRF1 (eukaryotic release factor 1) decodes all the three stop codons in association with eRF3 (a G-protein) and GTP. The eRF1:eRF3:GTP complex is a molecular mimic of the aminoacyl tRNA TC(23). The binding of this complex promotes a hydrolysis reaction resulting in release of the peptide from ribosome-associated tRNA (24)(14).

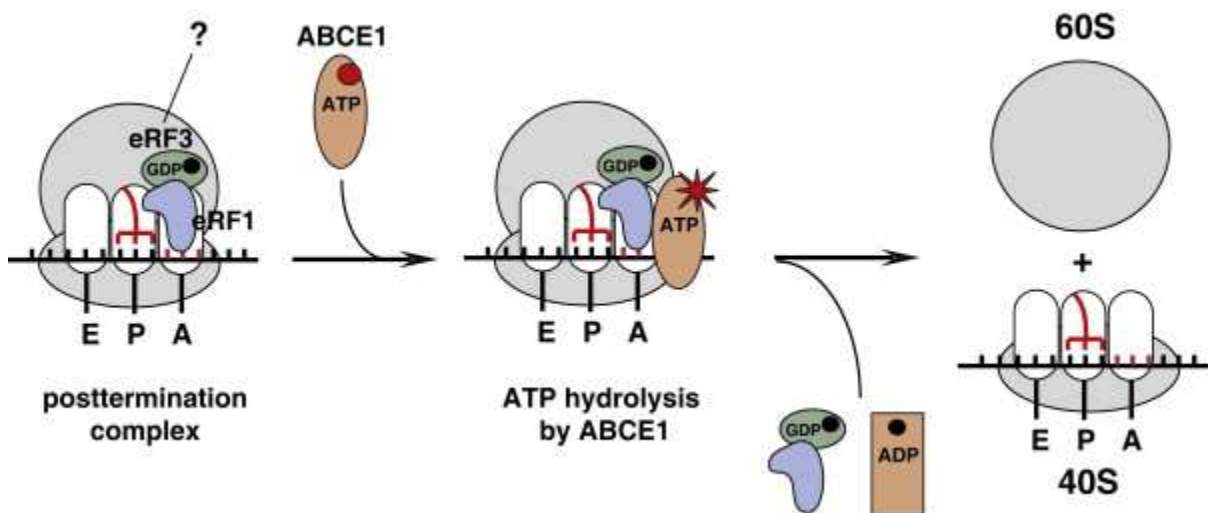


Figure 4. The model of eukaryotic translation termination

Recognition of the stop codon recruits the eRF1:eRF3:GTP complex to the ribosomal A-site. eRF3 is a G-protein. This is followed by the binding of ABCE-ATP to the release factor complex. Subsequent GTP and ATP hydrolysis results in release of the ribosomal subunits from the mRNA and the consequent recycling. This figure is from (25).

Post peptide release the 80S ribosomal subunits along with the deacylated tRNA (at the P-site) and the eRF1 (at the A-site) are still bound to the mRNA (**Figure 4**).

Recent data suggests that the protein ABCE1 (an ATPase) promotes ribosomal subunits release and subsequent recycling. According to another model the release of ribosomal subunits and recycling is achieved via eIF3 (eukaryotic initiation factor 3) to the small subunit (SSU) which induces a conformational change.

Translational Recoding

In canonical translation, the ribosome initiates at a 'start' codon, maintains reading frame during elongation, and terminates at a canonical 'stop' codon. The directed or programmed alteration to this canonical process is usually referred to as 'translational recoding'. These recoding events are mRNA specific and the mRNA sequences that direct them are known as 'recoding signals'. While undirected recoding events are very rare, the presence of specific cis-acting elements on mRNAs can increase their frequencies by up to 2 – 3 orders of magnitude (26). The most common translational recoding events involve either repositioning of the ribosome on an mRNA (programmed ribosomal frameshifting, or PRF), or decoding of stop codons with a tRNA (termination suppression). Common variations within these two general categories include directing the ribosome to slip by one base in the 5' direction (+1 PRF), one base in the 3' direction (-1 PRF), or utilizing various suppressor tRNAs at defined stop codons (1)(3).

Programmed -1 Ribosomal Frameshifting

Programmed -1 frameshifting (-1 PRF) was first described in retroviruses(27)(28). In viruses -1 PRF uses a single mRNA transcript to encode two peptides and maintain them at a specific ratio. The majority of the translated product consists of the shorter, unshifted protein. A -1 PRF event causes the ribosome to bypass the 0-frame termination codon, resulting in a C-terminally extended fusion protein. -1 PRF has been identified in plus stranded RNA viruses, dsRNA viruses, and retroviruses (29)(30) (**Figure 5**). The L-A virus of yeast uses -1 PRF to regulate its ratio of structural capsid protein (gag) and gag-pol fusion protein to incorporate the RNA-dependent RNA polymerase (pol) into the viral particle (31). Changing the rate of -1 PRF negatively impacts the process of viral particle assembly by altering the gag/gag-pol ratios (32).

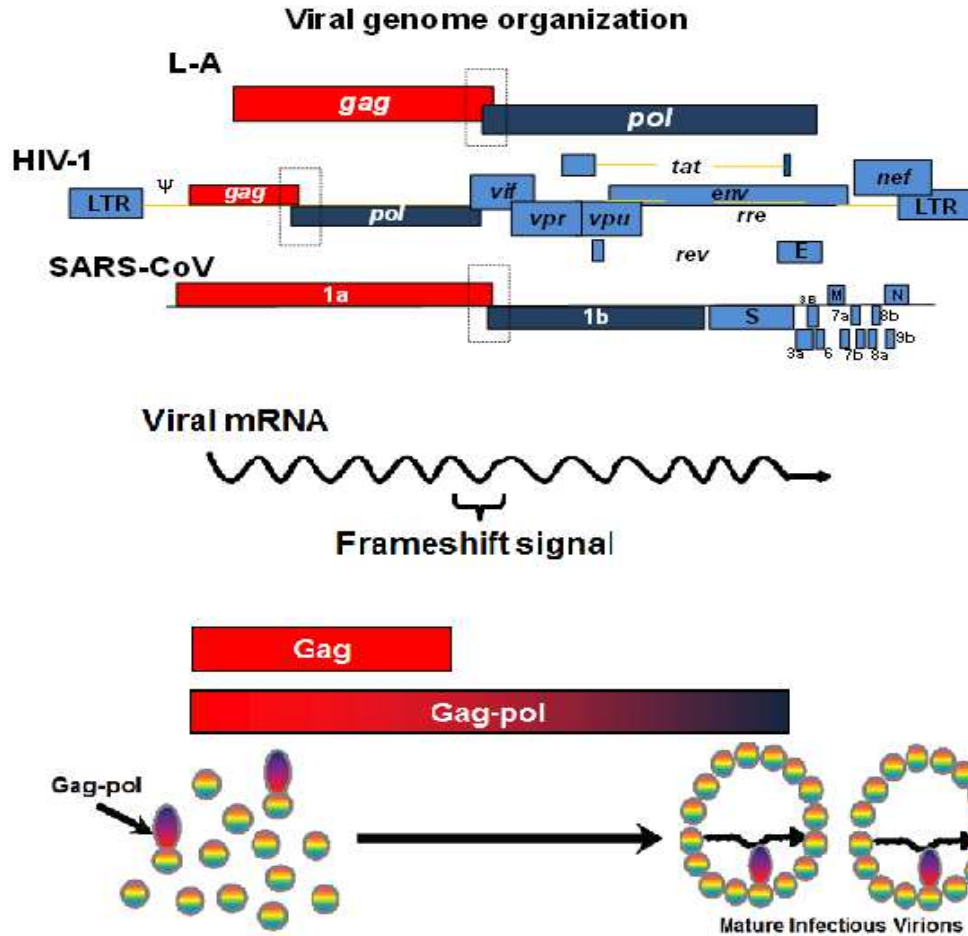


Figure 5. Viral -1 PRF: Organization and regulation of gene expression

The figure shows a schematic of -1 PRF signals in L-A, HIV-1 and SARS genomes. The overlap regions highlighted by the rectangles harbors the -1 PRF signals. These sequences on the mRNA stochastically shift reading frame of the elongating ribosome and translate a fusion protein. Thus we have a scenario where the virus is able to coopt the host's translational machinery to get a specific ratio of two protein products from a single transcript.

A typical -1 PRF signal as shown in (Figure 6). It consists of following components: a 'slippery' heptameric sequence of seven nucleotides where the actual slippage of A- and P- site tRNAs takes place; a short spacer region of zero to 14 nucleotides and a downstream stimulatory mRNA secondary structure (33). The IUPAC notation of the slippery heptameric sequence is denoted by N NNW WWH (spaces denote reading frame); where N is any three identical bases, W is any three identical weak bases and H is any base except guanine (2). In the 'simultaneous slippage model' of -1 PRF, the

elongating ribosome pauses due to the mechanical barrier presented by the downstream mRNA structure. At this point the peptidyl and aminoacyl-tRNAs are placed at the heptameric slippery site. While the ribosome resolves the downstream secondary structure the tRNAs break codon:anti-codon interactions and re-basepair one nucleotide upstream, causing the translational reading frame to shift one nucleotide in the 5' direction (28).

Additionally the 'integrated model of -1 PRF' hypothesizes that the tRNA slippage occurs post-delivery of the aa-tRNA and before peptidyltransfer and translocation(33). According to this model the downstream RNA secondary structure obstructs the movement of the ribosome resulting in the tension at the mRNA entry tunnel(34). This tension can be relieved by breaking codon:anti-codon base pairing and re-base pairing one nucleotide backwards(35). According to another model, the -1 PRF event occurs due to incomplete translocation. The downstream element impedes the ribosome movement resulting in a 2 nucleotide translocation (instead of 3) post eEF2 binding and GTP hydrolysis (36).

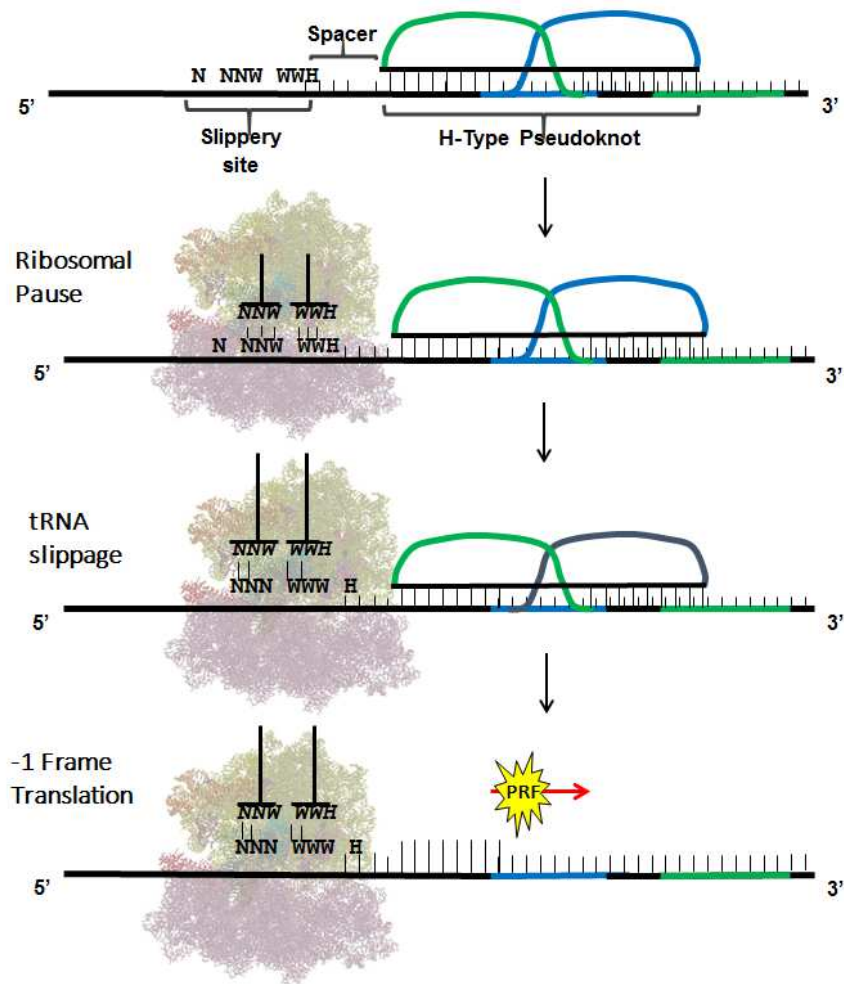


Figure 6. Structure and mechanism of -1 PRF.

The elements of a -1 PRF signal include a slippery heptamer of the form NNNWWWH (IUPAC notation), a spacer and a downstream mRNA secondary structure which is usually an H-type pseudoknot. A frameshift event occurs during the ribosomal pause when a translating ribosome encounters downstream secondary structure, usually a pseudoknot. This creates tension along the spacer which is relieved by a shift of one base, where by the P- and A- site codons at the slippery site repair in the -1 frame and translation continues. The figure is modified from (37).

A separate model posits that the tRNAs in the E- and P-sites are located over the NNW WWH nucleotides of the heptameric slippery site are forced to move one nucleotide backwards due to the downstream stimulatory structure, such that the incoming aa-tRNA in the A-site base pairs in the -1 frame, whereby the -1 frameshift

occurs during the subsequent translocation post peptidyltransfer. All the above discussed models are supported by empirical data, hence the mechanism of -1 PRF can be described as a series of ‘kinetic partitioning’ events occurring during elongation(38)(39). (Figure 7).

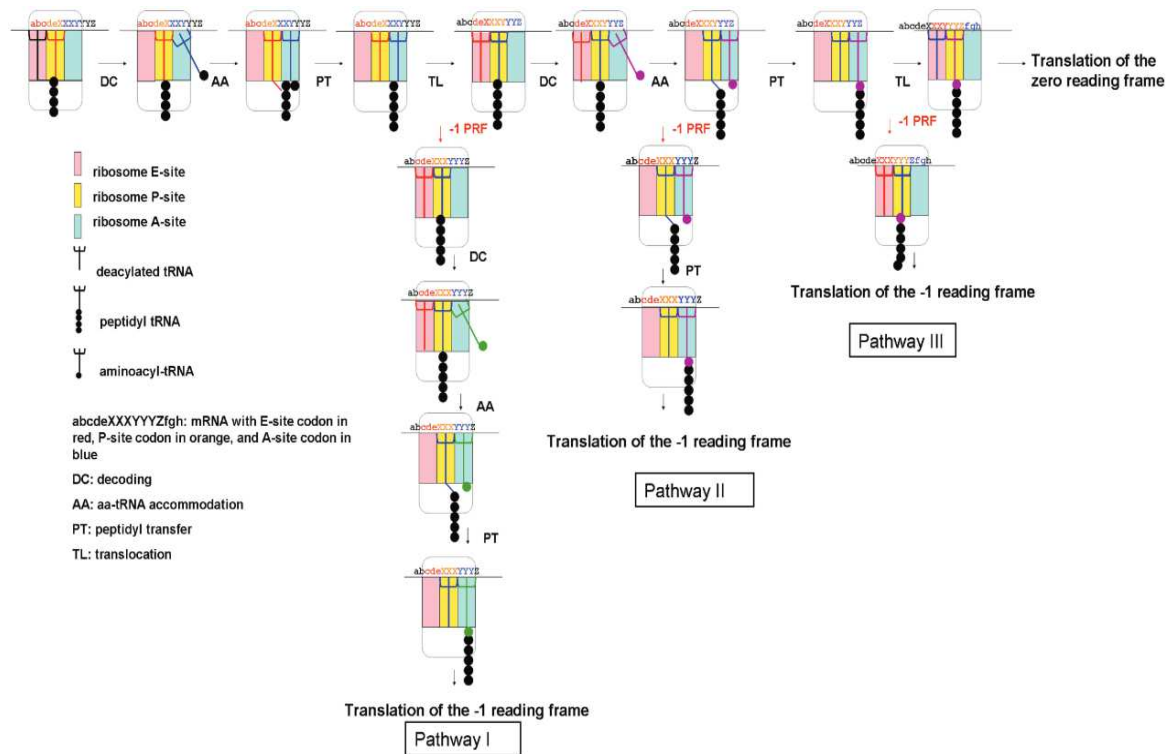


Figure 7. Kinetic partitioning of mechanisms of -1 PRF.

Two elongation cycles are diagrammed showing the on-product 0-frame translation and three separate pathways which result in the ribosome reading in the -1 frame. Thus the aminoacyl-tRNA mechanically wedges into the A-site during the first translocation event (Pathway I); tension of the mRNA caused by the mRNA secondary structure is relieved by slippage during the second accommodation event (Pathway II); or the second elongation cycle is frustrated by the mRNA secondary structure (Pathway III). This figure is from (39).

“Genomic” Frameshifting

Historically most molecular mechanisms are first discovered in viruses and later described in more complex organisms. This paradigm led to the hypothesis that ‘-1

PRF is used to regulate cellular mRNAs'. Thus the Dinman laboratory queried the prevalence of -1 PRF signals in eukaryotic genomes and found suitable frameshift sites at much higher frequencies than random (40). The publically available databases of +1 and -1 PRF signals are incomplete and do not provide a user friendly interface to search for recoding signals of one kind (41)(42)(43). The Programmed Ribosomal Frameshifting database (PRFdb) serves this need of providing a user friendly interface to search predicted -1 PRF signals over 20 eukaryotic genomes(44). The PRFdb computational pipeline is shown in **Figure 8**.

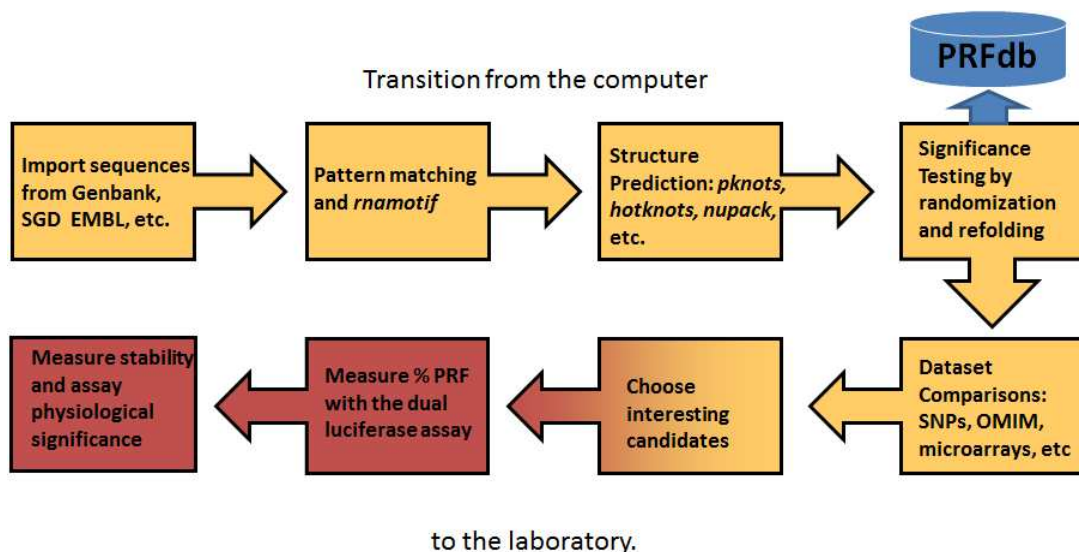


Figure 8. Pipeline for predicting and validating genomic -1 PRF signals.

Mature mRNA sequences to be analyzed are imported from the available databases. These sequences are filtered by RNAmotif and structure prediction algorithms for correctly placed slippery sites and downstream stimulatory secondary structure. The predicted sequences are randomized and refolded to calculate randomized MFEs (minimum free energies) and Z scores and stored in the database. Interesting candidates that are both biologically and statistically significant are taken to bench for validation and characterization.

A general observation from analysis of the PRFdB is that, unlike viral PRF signals, there are very few coding regions in the -1 frame immediately following a PRF signal. Instead, -1 frame termination codons were found closely downstream from the examined PRF signals. This engendered the hypothesis that ribosomes which

shift reading frame in response to these cis-acting PRF signals would terminate translation prematurely. As a result, messages containing PRF signals would be regulated similarly to messages containing a premature termination codon (PTC) (45).

Programed + 1 Ribosomal Frameshifting

Examples of +1 PRF signals have been described in viruses (46)(47), *E. coli* (48), yeast (49) (50) and mammalian cells (51). In a +1 PRF event the slippage of the tRNAs also occurs at the heptameric slippery site. The requirement of a downstream RNA secondary structure is optional. A well-studied example of +1 PRF is the yeast *TyI* retrotransposon of yeast. The 0-frame translation results in synthesis of the gag structural protein and a +1 PRF event results in production of a C-terminally extended gag-pol fusion protein (52) (53). The frameshift occurs at the heptameric sequence ‘CCU AGG C’. The AGG codon is called a ‘hungry codon’ (its cognate tRNA is in low abundance in the cell), which causes the ribosome to pause. The ribosomal pause causes the P-site tRNA to slip one nucleotide in the 3’ direction, such that the next codon is ‘GGC’. There is no RNA secondary structure downstream of the slippery sequence. The yeast gene *EST3*, encoding a component of the telomerase holoenzyme complex, harbors a +1 PRF signal between ORF1 and ORF2 (54). The +1 PRF event occurs over the slippery site of ‘CUU AGU U’ (**Figure 9**). This allows the translation of full-length Est3p (55).

A +1 PRF signal is also found in the yeast gene of *OAZ1*, encoding ornithine decarboxylase antizyme that regulates polyamine biosynthesis by degrading ornithine

decarboxylase. A +1 PRF event, which is induced by high levels of polyamines, results in synthesis of full-length antizyme (56)(57). OAZ1 +1 PRF requires the heptameric slippery site ‘UCC UGA U’ and a downstream pseudoknot that induces a ribosomal pause and the consequent +1 frameshift (58).

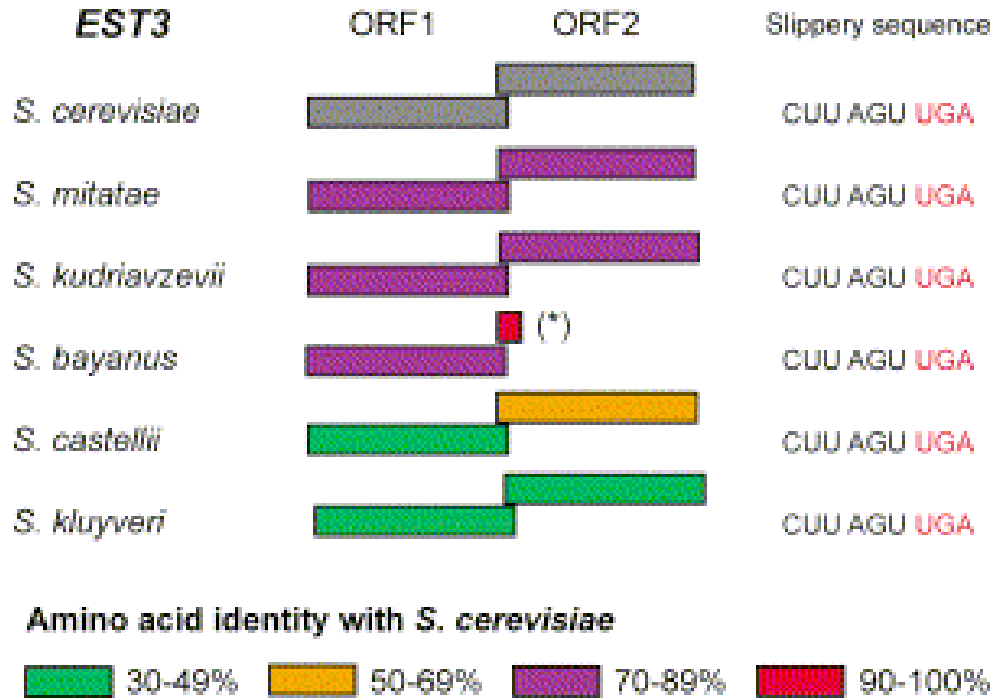


Figure 9. Programed +1 ribosomal frameshift signal in yeast *EST3* gene.

The +1 PRF signal in the *EST3* gene is conserved in many yeast species. The overlap sequence between ORF1 and ORF2 harbors the slippery sequence ‘CUU AGU UGA’. The P-site tRNA slips one nucleotide in the 3’ direction. This results in bypass of the 0-frame termination codon and synthesis of full length Est3p. This figure is from (55).

Nonsense Suppression

Accurate stop codon recognition is an important aspect of translational fidelity. Nonsense suppression (also called stop codon readthrough) refers to the rate at which the stop codons are translated by suppressor tRNAs. Selenocysteine incorporation at a

UGA codon, as a mechanism of nonsense suppression is well studied. This requires a selenocysteine incorporation signals (SECIS) 3' of the UGA (59). The SECIS is recognized by a specialized elongation factor SelB that delivers the tRNA^{sec} to the A-site. In eukaryotes the SECIS is located in the 3' UTR and requires an adaptor protein SBP2 (60)(61) (**Figure 10.**).

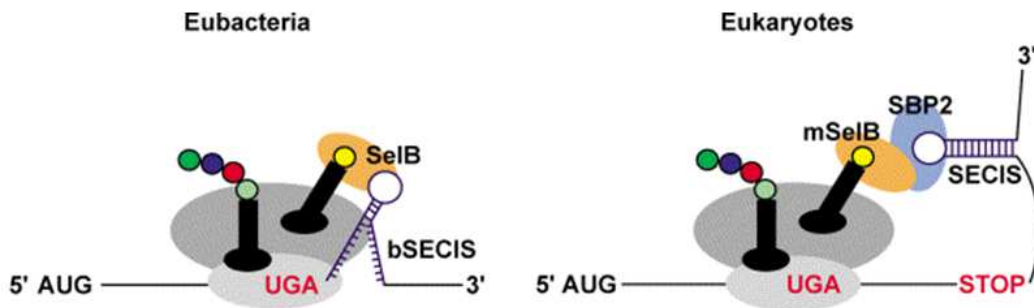


Figure 10. Mechanism of Selenocysteine incorporation.

The diagram shows the general mechanism of selenocysteine incorporation at UGA in both prokaryotes and eukaryotes. Selenocysteine incorporation in prokaryotes requires specialized elongation factor SelB and selenocysteine incorporation signals (SECIS) immediately after the stop codon. In eukaryotes the SECIS is located in the 3' UTR and the selenocysteine incorporation requires an additional accessory protein SBP2. This figure is from (55).

Programmed stop codon readthrough is also employed by many RNA viruses as a strategy for proteomic expansion. In the Murine leukemia virus (MuLV), it is achieved through a ribosomal pause induced by a strong pseudoknot (62)(63). The ribosomal pause enables the reverse transcriptase to interact with the eRF1 that enhances the efficiency of stop codon readthrough via depletion of the release factor (64). Recent published work has shown that the expression a cellular gene, the anti-angiogenic factor VEGF-Ax is regulated through programmed translational (stop codon) readthrough in human endothelial cells (65).

Nonsense Mediated (mRNA) Decay Pathway

The NMD pathway evolved to maintain transcriptome fidelity primarily by disposing of mRNAs with premature termination codons (PTC) (66)(67)(68)(69). Such transcripts can arise defects in a gene sequence itself, aberrant transcription and through splicing errors. Alternatively spliced and selenoprotein encoding mRNAs are also substrates of NMD (70)(71)(72). Recent work also suggests selective degradation of certain mRNAs is also dependent on the nature of the 3' UTR (73)(74)(75).

General model of NMD in *Saccharomyces cerevisiae*

The NMD surveillance complex in yeast requires the three Upf proteins Upf1-3 (76). The Upf1:Upf2:Upf3 complex works by interacting with the release factors upon decoding of a stop codon that is not located close to the polyA tail. In this context, the association of release factors occurs in the absence of Pab1, enhancing recruitment of the Upf1 to the eRF1-eRF3 complex (77). Upf1 activation happens after its association with Upf2 and Upf3. The Upf1:Upf2:Upf3 complex binds the ribosome through interactions between Upf1 and rpS26 (78). Activation of Upf1 causes release and degradation of the peptide and subsequent dissociation of eRF3 from the termination complex (**Figure 11**). The large subunit dissociates from the mRNA while the small subunit is still bound. Upf1 also recruits the decapping enzyme complex that destabilizes the closed loop structure, initiating mRNA decay

(79)(80). Transcripts with 3'UTRs, that sequester the Pab1 from the bonafide stop codon, are good substrates for NMD (75).

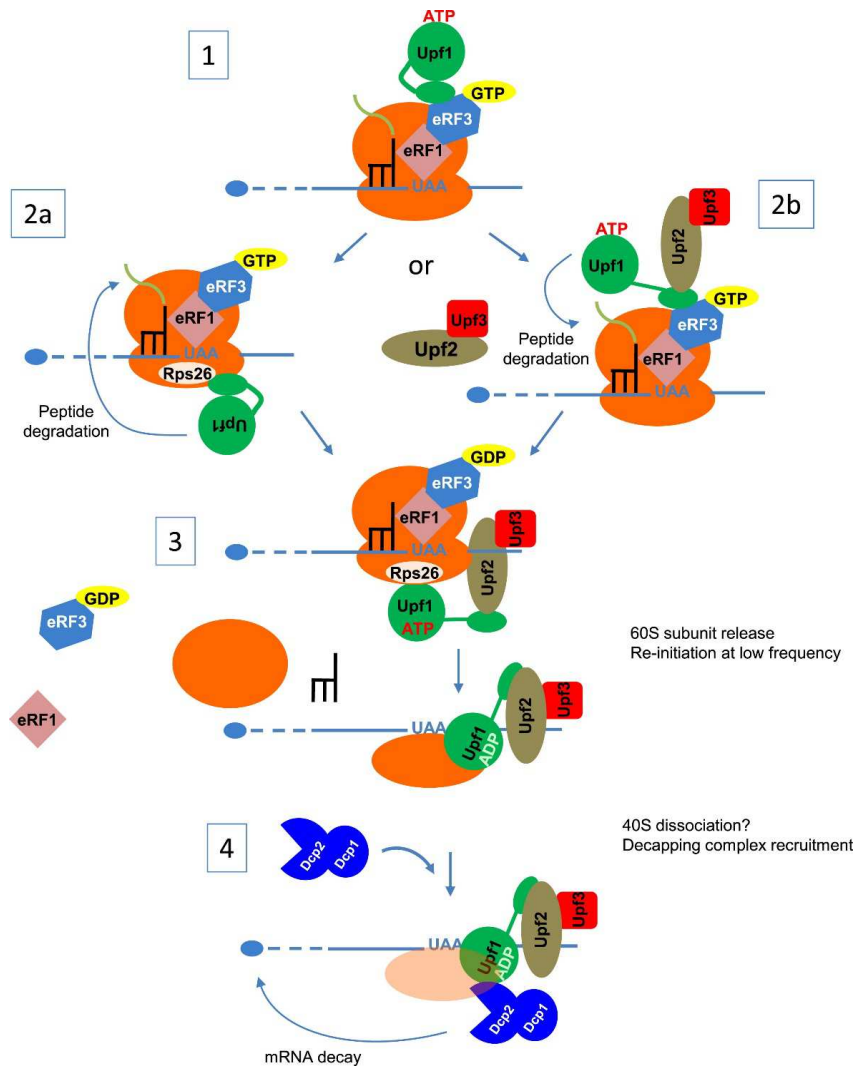


Figure 11. General model of NMD in yeast.

NMD is triggered by the recognition of the premature termination codon by the termination complex in yeast and binding of Upf1. In context of PTC the absence of Pab1p in the vicinity promotes the association of Upf1 with the termination complex. Subsequent activation of Upf1 causes peptide release, ribosomal subunit dissociation and activation of downstream mRNA decay complexes. This figure is from (79).

General model of NMD in Mammalian cells.

The exon junction complex dependent (EJC) dependent model of NMD is well studied in mammals. Post splicing the EJCs remain bound to the mRNA 20-24 nucleotides upstream of the exon-exon junctions. The NMD protein Upf2 associates with the EJCs. Since the actual stop codons are located in the final exon, the presence of an EJC 5' of the stop codon is unusual. Termination complex assembly at such a stop codon, where the EJC is located $\geq 50-55$ nucleotides upstream of an EJC, triggers NMD through UPF2. The UPF1 recruits UPF2 which in turn recruits UPF1 to the termination complex at the PTC (81). This is followed by the association of SMG1 with UPF1 (82)(83). The UPF1, SMG1 along with the release factors form the SURF complex (84). Phosphorylation of UPF1 by SMG1 results in the recruitment of SMG6 and SMG5-7 complex. SMG6 performs the endonucleolytic cleavage between the PTC and the EJC and SMG5-7 complex recruits the decapping and polydeadenylating complexes at 5' and 3' ends respectively (85)(86) (**Figure 12**).

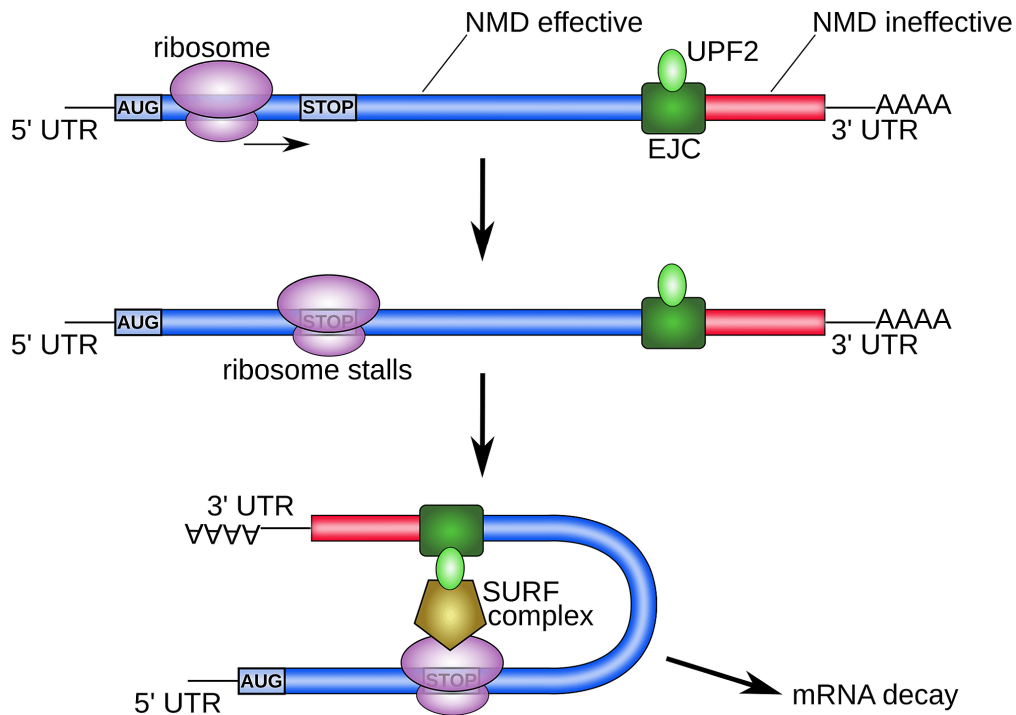


Figure 12. General model of EJC dependent NMD in mammalian cells.

The premature termination codon is recognized when the termination complex 3' of the EJC. The UPF2 protein associated with the EJC recruits the SURF complex. This triggers NMD by recruiting decapping and polyadenylating complexes at the 5' and 3' end of the mRNA. The figure is from (87).

Alternative models of NMD

Other less characterized models of the surveillance pathway have been discovered in other eukaryotes. The faux 3' UTR model of NMD has been studied in drosophila and yeast (88) (74). In normal termination the recruitment of the termination complex happens in the vicinity of Pabp1 followed by subsequent release and recycling of ribosomal subunits (89). According to the faux 3' UTR model the interaction between the ribosome and mRNPs in the 3'UTR is necessary for the appropriate termination and normal rates of mRNA decay (**Figure 13**). Absence of these mRNPs in the vicinity of the stop codon triggers NMD. Studies have also shown that introns located upstream of the PTC can also enhance mRNA decay, suggesting a role of additional trans-acting factors that are involved in NMD (90). An

alternative branch of NMD that relies on the less characterized factor of UPF3a has been studied in T cells (91).

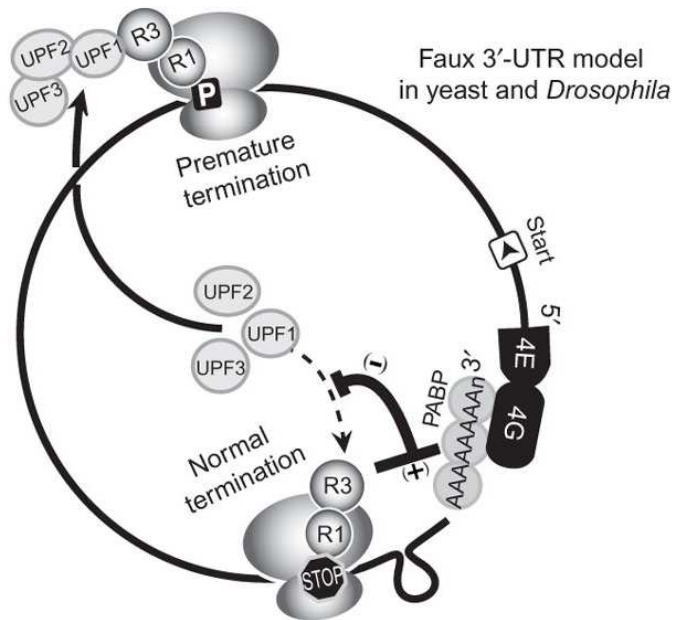


Figure 13. Faux 3'UTR model of NMD.

The translation termination at the PTC is inefficient due to the lack of interaction between termination complex with the Pabp1. This activates NMD by recruitment of UPFs at the termination complex thereby enhancing rapid mRNA decay. The figure is from (88).

Most mammalian genes have introns and splicing defects can generate aberrant PTC-containing transcripts. These deleterious mRNAs are largely degraded via NMD. In yeast, microarray data suggests that approximately 12% of the genes are regulated through NMD (92). Thus NMD is a major post-transcriptional surveillance pathway and defects in NMD have severe implications on global gene expression. The deletion of NMD factors UPF1 and UPF2 causes embryonic lethality in drosophila, mice and zebrafish (93)(94). Recent studies have shown that, this surveillance pathway serves as a moderator in the manifestation of hereditary and acquired genetic diseases (reviewed in (95)).

The relationship between -1 PRF and NMD in cellular gene expression.

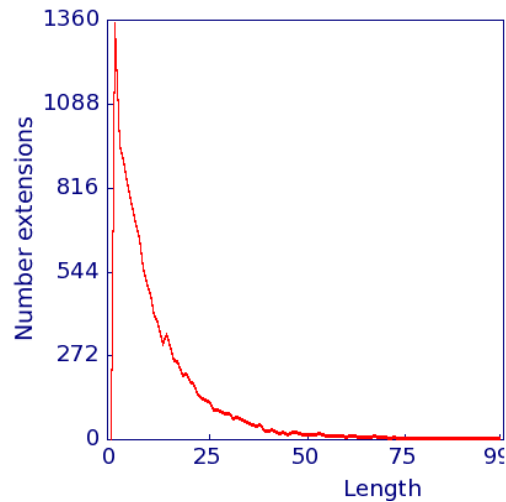


Figure 14. The distribution of length of -1 PRF signal encoded peptides in Homo sapiens.

The graph shows the length of peptide encoded post -1 PRF event on X-axis and the number extension on Y-axis for all predicted -1 PRF signals in the humans.

In viruses, -1 frameshift events typically cause elongating ribosomes to bypass the 0-frame stop codon enabling the synthesis of C-terminally extended fusion proteins. In contrast the vast majority of cellular -1 frameshift event redirect elongating ribosomes to premature termination codons. This is demonstrated in **Figure 14**, which shows the distribution of peptide lengths encoded after -1 PRF events for all predicted -1 frameshift signals in the human genome: only 0.07% of candidate -1 PRF containing sequences extend more than 30 codons beyond the frameshift event (37). This led to the hypothesis that ‘-1 PRF signals function as mRNA destabilizing element via the NMD pathway’. When an elongating ribosome is directed to a premature termination codon after a -1 frameshift event, it recruits the components of NMD pathway causing rapid degradation of the message (**Figure 15**). This hypothesis was first

tested using example of -1 PRF signal in yeast L-A virus (96) and later validated using the -1 PRF signal in the *EST2* mRNA (97). The yeast *EST2* gene encodes the reverse transcriptase subunit of the telomerase complex (98). The open reading frames of *EST2* has five functional -1 PRF signals. It was shown that the full length native *EST2* mRNA is a substrate of NMD due to -1 PRF and ablation of all five -1 PRF signals resulted in stabilization of *EST2* mRNA (97). Similarly the -1 PRF signal containing human CCR5 mRNA was stabilized upon ablation of -1 PRF (99). Thus, NMD is downstream to -1 PRF.

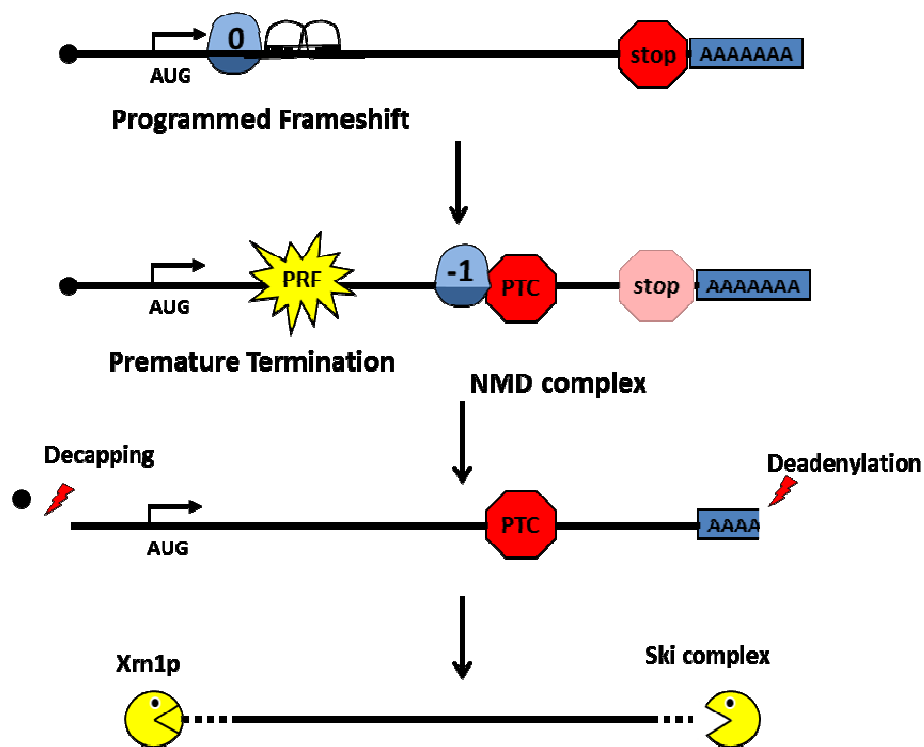


Figure 15. Model of -1 PRF dependence on NMD.

For genomic frameshift signals an elongating ribosome is directed to a -1 frame premature termination codon after as frameshift event. The recognition of the PTC by the ribosome results in activation of NMD and subsequent degradation of the frameshift signal containing mRNA.

Ribosome Biogenesis and Ribosomopathies.

Ribosome biogenesis is a complex multistep process involving over 200 accessory proteins and transacting factors (100)(101). In yeast the ribosomal RNA (rRNA) is transcribed by RNA polymerase I, except 5S rRNA which is transcribed by RNA polymerase III. The pre-rRNA undergoes exonucleolytic and endonucleolytic cleavages followed by base modifications to form mature 18S, 25S and 5.8S rRNA (102). The most common base modifications include pseudouridylation and methylation (103). Pseudouridylation is the largest single base modification in rRNA. The ribosomal proteins are transported to the nucleolus, where they are processed and assembled with the rRNA to form 43S and 66S preribosomal particles that are transported to the cytoplasm (104). These preribosomal subunit are transported with some non-ribosomal proteins that prevent the premature association of the ribosomal subunits.

Ribosomopathies are a class of congenital diseases caused by structural and functional defects of the ribosomal components. Ribosomopathies are rare and are characterized by hypo-proliferative phenotype characterized by bone marrow failure, anemias, dystosis and recently have been associated with the tumor suppressor protein p53 (105). **Table. 1** shows the list of currently accepted ribosomopathies and their causative gene defects. In general ribosome dysfunction results in defects in protein synthesis and the ensuing disease pathogenesis. In chapter 3, we use X-DC as a model for ribosomopathies to investigate the effects of translational fidelity defects on cellular gene expression.

DISEASE	GENE DEFECT	CLINICAL FEATURES	TREATMENT
Diamond-Blackfan anemia (DBA)	10–15 ribosomal proteins (esp. S19, S26, L5, L11)	Anemia Growth retardation Congenital (esp. craniofacial and thumb) abnormalities	Corticosteroids Blood transfusions Hematopoietic stem cell transplantation (HSCT) Leucine (?)
5q-syndrome	RPS14	Anemia	Lenalidomide
Schwachman-Diamond syndrome (SDS)	SBDS	Exocrine pancreatic insufficiency Hematologic abnormalities (esp. neutropenia) Neurocognitive impairment GI (esp. liver) abnormalities	Pancreatic enzyme supplementation HSCT
X-linked dyskeratosis congenita (DC)	DKC1	Mucocutaneous abnormalities (e.g. skin pigmentation and nail changes) Pulmonary fibrosis Bone marrow failure	Oxymetholone HSCT
Cartilage-hair hypoplasia (CHH)	RMRP	Short stature Bone deformities Hair growth abnormalities	Symptomatic
Treacher-Collins syndrome (TCS)	TCOF1	Craniofacial abnormalities	Symptomatic
Bowen-Conradi syndrome	EMG1	Severe growth retardation	None
North American Indian childhood cirrhosis	hUTP4/Cirhin	Biliary cirrhosis Portal hypertension	Liver transplantation

Table 1. Clinical characteristics of different ribosomopathies.

This table is adapted from (105).

Scope of work and Thesis Summary

The heart of the work described in this thesis is to understand how defects in the interplay between mRNAs and ribosomes can affect gene expression and thus contribute to disease pathogenesis. Emerging research shows that exceptions to the rules of translation play critical roles in regulating gene expression. Structured segments of RNA can ‘program’ ribosome to slip on mRNAs to either produce different proteins or promote rapid mRNA degradation. Programmed -1 Ribosomal

Frameshifting, having recently been identified as molecular mechanism for regulating gene expression in eukaryotes, has emerged as the paradigm in this line of research has. Published work has increased our understanding of the molecular and biophysical mechanisms underlying -1 PRF and computational analysis predicts that approximately 10% of the genes in both yeast and humans are regulated via this mechanism (44). The observations that global dysregulation of -1 PRF has deleterious effects on gene expression leads us to hypothesize that ‘-1 PRF plays an important role in regulating cellular gene expression’. The most important aspect of this thesis work is to explore the biological and biomedical significance of -1 PRF. There is growing evidence that defects in the structure and function of the ribosome and its trans-acting factors which compromise translational fidelity, including altered rates of -1 PRF, plays an important role in class of diseases called ribosomopathies. Recent observations have shown that mutations associated with the ribosomopathy X-linked Dyskerotosis Congenita (X-DC) and Spinocerebellar ataxia type 26 (SCA26) promote increased rates of -1 PRF along with the other defects in translational fidelity (106)(107). This work uses this preliminary data as a foundation to characterize how defects in the aspects of translation contribute to disease pathogenesis.

The work presented in the following chapter explores the role of -1 PRF in the yeast telomere maintenance and cell cycle control. Preliminary data also suggests that this may be also applicable to human cells. Regulation of telomere length is biologically important because of its association with ageing and cancer. In Chapter 3, we discuss X-DC and SCA26 as models to understand how inherited defects in translational machinery may contribute disease pathogenesis. We have validated operational -1

PRF signals in additional human genes that are associated with other human disease. These studies establish a paradigm for understanding the linkage between translational fidelity and human disease.

Chapter 2

Telomere maintenance is globally controlled by programmed ribosomal frameshifting and the nonsense-mediated mRNA decay pathway

Introduction

Programmed ribosomal frameshift (PRF) signals are *cis*-acting elements located inside of open reading frames in mRNAs that are able to stochastically redirect translating ribosomes to shift into alternative reading frames. In the typical viral context, these elements allow the translational apparatus to bypass a 0-frame encoded in-frame stop codon and continue synthesis of a C-terminally extended fusion protein. The use of programmed -1 ribosomal frameshifting (-1 PRF) by a wide variety of RNA viruses has enabled definition of some broad rules for at least one class of these elements (2). A typical -1 PRF promoting mRNA sequence motif contains three elements: a heptameric “slippery site” where the translational shift in reading frame actually takes place; a short spacer sequence of usually less than 12 nucleotides; and a downstream stimulatory structure (usually an mRNA pseudoknot). In eukaryotic RNA viruses, the slippery site has the heptameric motif $N NNW WWW$, where the incoming reading frame is indicated (33). Current models posit that aminoacyl- (aa-) and peptidyl-tRNAs are positioned on this sequence while the ribosome pauses at the downstream secondary structure, which is thought to provide an energetic barrier to elongating ribosomes, positioning them at the slippery site (108)(109)(34)(39). The

nature of the slippery sequence enables re-pairing of the non-wobble bases of both the aa- and peptidyl-tRNAs with the -1 frame codons. mRNA pseudoknots are the most common stimulatory structures but stem-loops and other structures are also capable of stimulating -1 PRF (110)(111) .

There are a growing number of examples of functional PRF signals in expressed eukaryotic gene (112)(54)(113)(114)(115)(116)(45). The existence of these PRF signals in a wide variety of viral and prokaryotic genomes suggests an ancient and possibly universal mechanism for controlling the expression of actively translated mRNAs. The past few years have seen the publication of several reports describing *in silico* identification of “recoding signals” using a wide variety of computational approaches(40)(117)(118)(119)(120). While many different bioinformatics methodologies have been used, these tend to fall into two general and complementary strategies. The first, based on the observation that viral frameshifting events direct ribosomes into new ORFs, is to first find out-of-frame ORFs followed by the identification of sequences that may function as PRF signals. The strength of this approach is that it can identify new classes of *cis*-acting signals capable of directing efficient PRF; its weakness is that it cannot identify new functional outcomes of frameshifting. The second strategy involves searching for mRNA motifs known to promote efficient PRF. While this approach cannot identify new classes of frameshift signals, it can enable an expansion of our understanding of functional uses for PRF. Using this strategy and a package of bioinformatics and statistical tools, we previously demonstrated that approximately 10% of genes in all eukaryotic genome

contain high confidence -1 PRF signals(45)(40)(44). Interestingly, like many *cis*-acting elements, -1 PRF signals appear to rapidly evolve, and wet lab studies demonstrated that 9 (out of 9 selected) high confidence putative -1 PRF signals from a variety of *S. cerevisiae* genes promoted efficient recoding *in vivo* (97). A searchable database of predicted -1 PRF signals in these genomes is available in the Predicted Ribosomal Frameshift Database (PRFdb) at <http://prfdb.umd.edu/>.

One key finding of our research is that the outcome and function of -1 PRF differs significantly between viruses and eukaryotic genomic frameshifting. While viral -1 PRF events direct ribosomes into new ORFs, resulting in synthesis of C-terminally extended proteins, the vast majority of -1 PRF events on eukaryotic cellular mRNAs are predicted to direct elongating ribosomes to premature termination signals, suggesting that -1 PRF is used to control mRNA abundance and stability through the nonsense-mediated mRNA decay (NMD) pathway. This hypothesis was supported by the demonstration that a well characterized viral -1 PRF signal can act as a *cis*-acting, NMD-dependent mRNA destabilizing element (96). A more recent study revealed that functional -1 PRF signals derived from naturally occurring yeast mRNAs can promote rapid degradation of a reporter mRNA by -1 PRF through NMD and, to a lesser extent, the no-go decay (NGD) pathway (97). That work began to explore the biological significance of -1 PRF by using the yeast EST2 mRNA, which encodes the catalytic subunit of telomerase. There, we showed that the EST2 mRNA is destabilized by -1 PRF, that ablation of all of its predicted -1 PRF signals resulted in

its stabilization, and that global increases or decreases in -1 PRF resulted in decreased or increased steady-state abundance EST2 mRNA respectively (97).

During the course of that study, additional putative -1 PRF signals were computationally identified in the EST2 mRNA and in the mRNAs encoding other components and regulators of telomerase: Est1p, Stn1p, and Cdc13p. Importantly, all of these mRNAs are stabilized in NMD⁻ cells (121), and we speculated that yeast cells may use -1 PRF to limit the expression of these proteins in order to maintain the correct stoichiometric balance among telomere associated components. Here, we have empirically characterized the computationally predicted -1 PRF signals in these mRNAs, demonstrating that each contains at least one operational -1 PRF signal. That the same underlying molecular mechanism is operational is suggested by experiments showing that mutated slippery sites ablate -1 PRF, and by the demonstration that all are responsive to mutants and drugs that were previously shown to alter rates of -1 PRF as directed by a virus derived signal. In general, the ability to function as mRNA destabilizing elements correlated with the extent to which any particular element promoted -1 PRF, and in these cases, ablation of NMD resulted in partial stabilization of a reporter mRNA. Importantly, altering rates of EST2 mRNA -1 PRF, either by ablation of EST2 slippery sites, through the activity of extragenic mutants, or by the use of -1 PRF altering drugs mimicked the effects on NMD ablation of yeast telomere length. These findings suggest that -1 PRF is utilized to control the abundance of telomerase components, and thus telomere length in yeast cells. Preliminary data also suggests functional -1 PRF signals in three human

messages encoding proteins required for telomere maintenance. This suggests that -1 PRF may also play important role in human telomere maintenance and ageing.

Results

The mRNAs encoding at least 4 proteins involved in yeast telomere maintenance contain operational -1 PRF signals.

A search for -1 PRF signals in the yeast EST2 mRNA revealed 10 slippery sites in the correct reading frames, and further examination of the computationally predicted structures and statistical analyses suggested that 5 of these had the potential to encode operational -1 PRF signals (**Table 2** and **Figure 16**). Note that, while the signal beginning at position 72 appeared to lack significant mRNA structure, the presence of a “double slippery-site” A AAU UUA AAA made it an attractive candidate nonetheless. Similarly, searches for -1 PRF signals in the mRNAs encoding other proteins involved in telomere maintenance revealed three candidates in EST1, two in STN1 and one in CDC13. Synthetic oligonucleotides containing these sequences were used to clone the predicted -1 PRF signals into standard yeast high copy dual-luciferase reporter plasmids (122). Note that in order for frameshifted ribosomes to bypass -1 frame termination codons present in the native sequences, either 1 base was deleted from, or 2 bases were added to the spacer regions immediately 3' of the slippery sites, thus directing shifted ribosomes back into the original reading frame and enabling synthesis of the downstream firefly luciferase reporter.

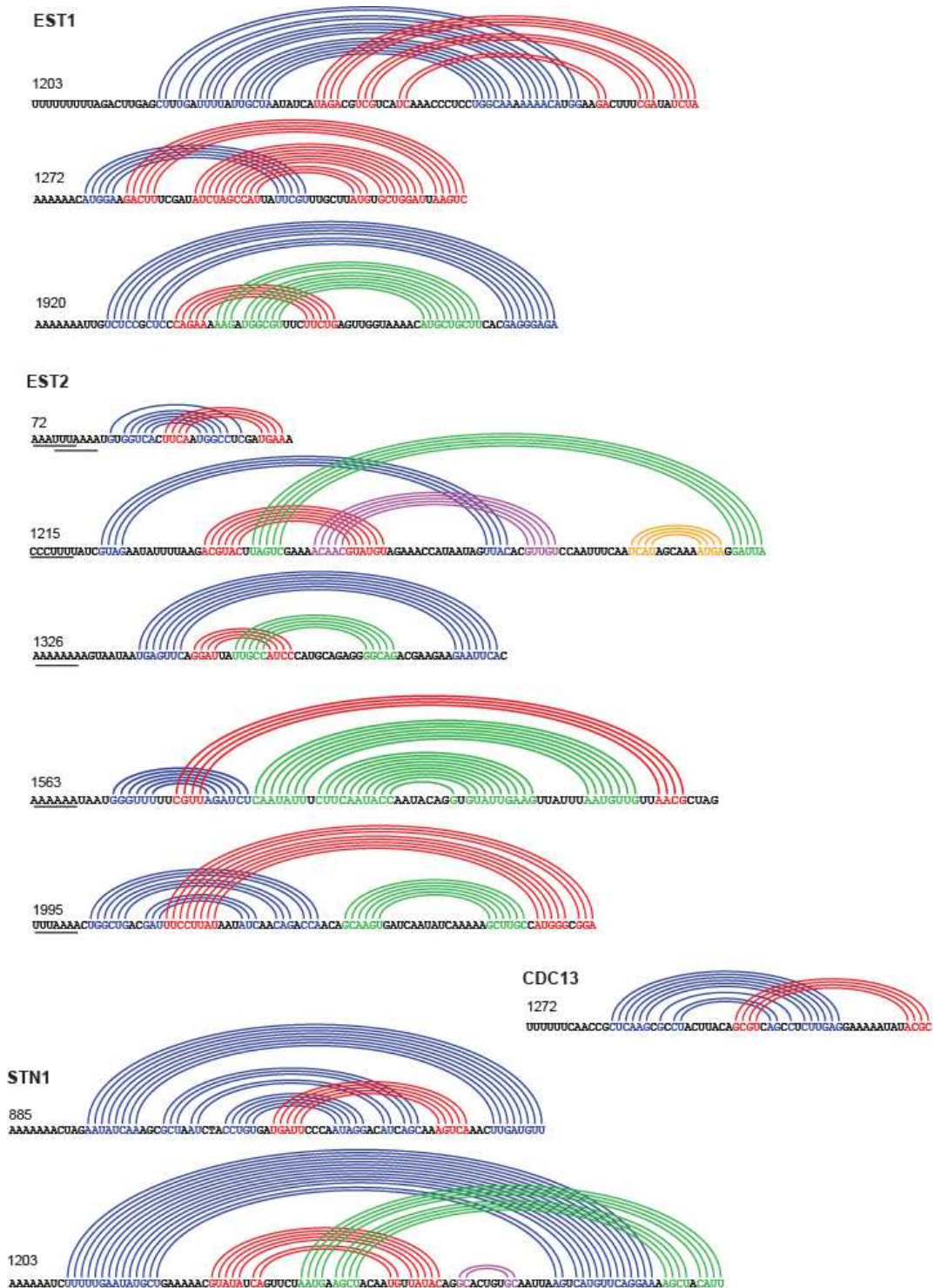


Figure 16. Predicted -1 PRF signals in ORFs involved in yeast telomere maintenance. Sequences of potential -1 PRF signals in EST1, EST2, STN1 and CDC13 ORFs assayed in this study. The number represents the tandem slippery site beginning within the ORF. The predicted mRNA secondary structure is shown as a linear Feynman diagram.

While these modifications may change actual rates of -1 PRF, the resulting plasmids nonetheless remain useful for determining whether or not the sequences in question are fundamentally capable of promoting efficient rates of -1 PRF. Employing a cutoff of 1% (i.e. approximately 20-fold above non-programmed frameshifting (122)), the EST2 mRNA was found to harbor three functional -1 PRF signals, EST1 contains two, and STN1 and CDC13 each have one (**Table 2**). To ascertain whether -1 PRF promoted by these sequences adhered to canonical simultaneous slippage mechanism (123), the slippery sites were silently mutagenized so that they would disrupt the slippery sequences while still encoding the same peptide sequences. While none of these slippery site mutations completely abrogated -1 PRF, they all reduced rates of frameshifting 3 to 6 fold. The residual -1 PRF promoting activities can be accounted for by the fact that the constraints imposed by silent mutagenesis retained considerable potentials for non-base-pairing between shifted tRNAs and the -1 frame codons.

^a ORF	^b Position	^c Slippery site Silent slip site Mut (ssM)	^d % -1 PRF efficiency % -1 PRF ssM
L-A virus gag/pol	1969	G GGU UUA ND	6.5% ± 0.62
EST1	1203	U UUU UUU ND	0.10 ± 0.08
	1272	A AAA AAC G AAG AAC	6.33 ± 0.71 1.29 ± 0.18
	1920	A AAA AAA G AAG AAC	1.73 ± 0.03 0.83 ± 0.15
EST2	72/75	A AAU UUA AAA ND	0.58 ± 0.04
	1215	C CCU UUU U CCA UUC	10.65 ± 0.10 1.44 ± 0.14
	1326	A AAA AAA G AAG AAC	1.40 ± 0.04 0.66 ± 0.03
	1653	A AAA AAU G AAG AAC	67.15 ± 2.86 13.12 ± 1.79
	1995	U UUA AAA ND	0.54 ± 0.04
STN1	885	U UUU UUU ND	0.04 ± 0.07
	1203	A AAA AAU G AAG AAC	24.36 ± 1.19 3.23 ± 0.16
CDC13	1272	U UUU UUC	4.20 ± 0.04
		C UCU UUC	2.94 ± 0.03

Table 2. Most predicted -1 PRF signals in ORFs involved in yeast telomere maintenance promote efficient -1 PRF in yeast cells.

^a Yeast gene. ^bPosition in the ORF of the first nucleotide of the predicted -1 PRF signal. Note that 72/75 represents a tandem slippery site beginning at nt 72 of the EST2 ORF. ^cSlippery site sequence of the predicted -1 PRF signal. Below these are shown silent protein coding slippery site mutants (ssM). ND indicates slippery site mutants that were not assayed because the wild-type sequence was determined to not promote efficient -1 PRF. ^dPredicted frameshift signals were cloned in dual luciferase reporters, and -1 PRF efficiencies were monitored in yeast cells. Upper lines show mean and standard deviations of % -1 PRF promoted by wild-type sequences. Lower lines show this data for the ssM constructs. ND: not determined.

The -1 PRF signals in the EST1, EST2, STN1 and CDC13 mRNAs respond to cellular mutations and drugs that globally affect -1 PRF.

We have previously characterized a large number of yeast mutants that globally alter rates of -1 PRF (124). To independently test whether these sequences promote -1 PRF by the canonical mechanism, rates of -1 PRF were assayed in isogenic cells expressing alleles of *RPL3* or *RPL10* or *NMD3* that had previously been shown to stimulate or inhibit -1 PRF as directed by the L-A virus derived sequence (125)(126)(127). As shown in **Figure 17A**, rates of -1 PRF directed by all of the sequences were stimulated in cells expressing the *rpl3-mak8* allele while it was uniformly inhibited in cells expressing the *rpl3-R247A* allele of *RPL3*. Similarly, the yeast strains expressing *rpl10-R98S* and *rpl10-R98S+NMD3-Y379D* alleles of *RPL10* and *NMD3* enhanced rates of -1 PRF directed by all of the sequences in question (**Figure 17B**). Previous studies have demonstrated that rates of -1 PRF can also be affected by the peptidyltransferase inhibitor anisomycin (128). Consistent with the hypothesis that these are canonical -1 PRF signals, anisomycin uniformly inhibited -1 PRF directed by all of the sequences, and the extent of -1 PRF inhibition was dose-dependent (**Figure 17C**). In sum, these data support the hypothesis that these sequences all promote -1 PRF through the canonical mechanism.

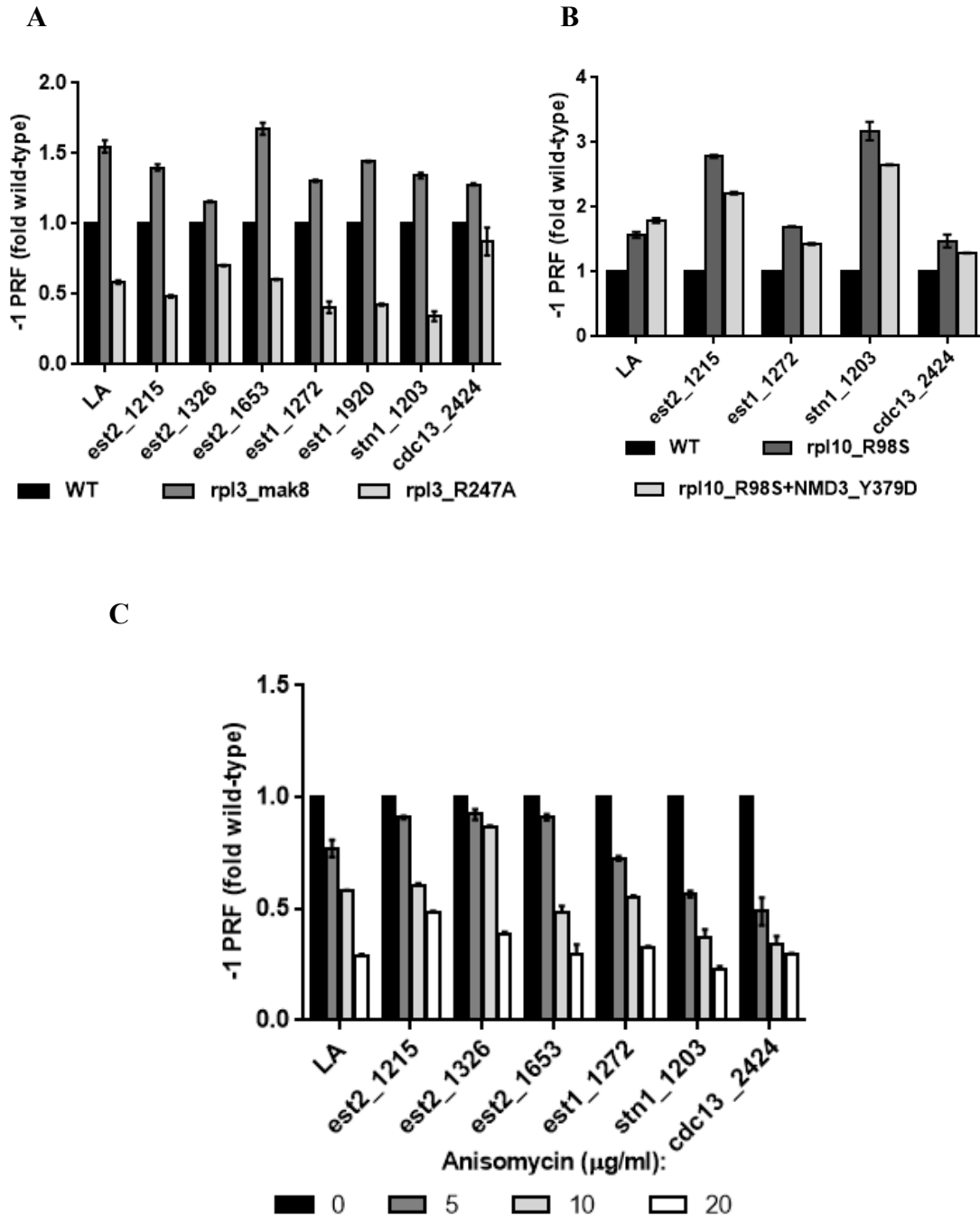


Figure 17. -1 PRF signals in the yeast EST1, EST2, STN1 and CDC13 mRNAs respond to cellular mutants (panels A and B) and a drug (panel C) that were previously found to promote changes in -1 PRF promoted by viral -1 PRF signals.

-1 PRF was monitored using dual luciferase reporters ^[26] in isogenic cells expressing *RPL3* alleles or (panel B) isogenic cells expressing *RPL10* alleles. All assays were performed enough times to generate meaningful statistical data ^[52]. Error bars represent standard error. Note that the following the gene name denotes the specific mRNA and first nucleotide of the -1 PRF signal. This nomenclature is used throughout.

mRNA destabilization activity is inversely correlated with the strength of individual -1 PRF signals.

Analysis of the predicted outcomes of -1 PRF events suggests that >95% of the genomic -1 PRF signals should direct translating ribosomes to premature termination codons suggesting that -1 PRF could be used to post-transcriptionally regulate gene expression through the nonsense-mediated mRNA decay (NMD) pathway (129)(130). In a series of proof-of-principle experiments using the well-defined -1 PRF signal from the yeast dsRNA L-A virus we demonstrated that: 1) this signal can function as an mRNA destabilizing element; 2) mRNA destabilization requires the presence of a functional -1 PRF signal; 3) mRNA destabilization requires an intact NMD pathway, and; 4) mRNA half-life is inversely proportional to the frequency of -1 PRF (i.e. the greater the rate of -1 PRF, the greater the frequency of ribosomes being directed to a nonsense codon and vice versa) (96). These principles were subsequently shown to apply to -1 PRF signals identified in 4 endogenous yeast mRNAs (97). To test whether the -1 PRF signals examined in the current study were also capable of functioning as NMD-dependent mRNA degradation signals, they were cloned into a yeast *PGK1*-reporter and their effects on *PGK1* mRNA steady state abundances were assayed in isogenic *UPF1* and *upf1Δ* cells as previously described (97). The presence of an in-frame PTC reduced *PGK1* reporter mRNA abundance to $6.0\% \pm 0.3\%$ of the readthrough control levels, and this was 14.8 ± 0.6 -fold more abundant in an isogenic *upf1Δ* strain. The strong EST3_1653 -1 PRF signal also significantly decreased the *PGK1* reporter mRNA steady-state abundance (0.04 ± 0.01 -fold of

readthrough levels), and was stabilized 21.8 ± 2.8 -fold in the *upf1Δ* strain background. As rates of -1 PRF decreased, the effects of these elements on mRNA abundance also decreased. The STN1_1203 and EST2_1215 -1 PRF signals (~24% and ~11% -1 PRF efficiency respectively) resulted in ~60% and ~40% reductions of PGK1 mRNA reporter abundance in wild-type cells (0.32 ± 0.01 and 0.49 ± 0.03 -fold readthrough), and were stabilized 3.22 ± 0.01 and 2.44 ± 0.03 and ~ 1.74 fold in *upf1Δ* cells. The EST1_1272 element (~6% -1 PRF) promoted an ~40% decrease in reporter mRNA abundance (0.61 ± 0.02 -fold readthrough), which was stabilized 1.42 ± 0.06 -fold in *upf1Δ* cells, and the CDC13 -1 PRF signal (~4% -1 PRF) promoted an ~20% reduction in PGK1 reporter mRNA abundance (0.81 ± 0.13 -fold readthrough), while deletion of *UPF1* resulted in a 1.19 ± 0.02 - fold stabilization of this mRNA. Finally, as -1 PRF rates approached 1% (EST1_1920), the reductions in PGK1 reporter mRNA abundance were in the range of only 10% (0.91 ± 0.02 -fold readthrough), and NMD did not appear to be a significant factor (0.94 ± 0.11). Graphic analyses of these data reveal exponential relationships between -1 PRF efficiency and mRNA abundance (**Figure 18A**) which is mirrored by increased abundance of the reporter upon ablation of NMD (**Figure 18B**).

Steady-state abundance of the cellular EST1, EST2, STN1 and CDC13 mRNAs is inversely affected by changes in global rates of -1 PRF.

Consistent with the hypothesis that the presence of operational -1 PRF signals renders these mRNAs substrates for NMD, all four have been previously shown to be stabilized upon ablation of NMD (131)(132). Here, these findings were recapitulated

by applying qRT PCR methods to total mRNAs isolated from isogenic wild-type and *upf1Δ upf2Δ upf3Δ* cells (**Figure 18A**).

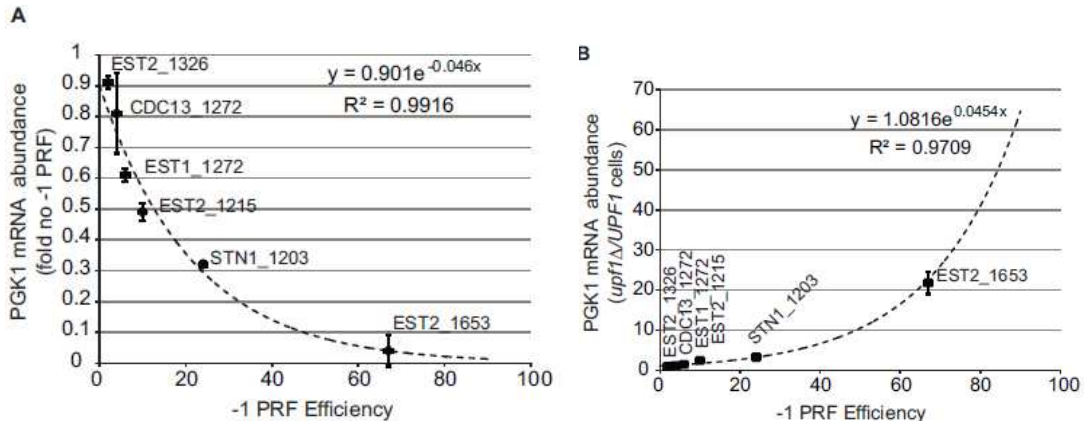


Figure 18. Delineation mathematical relationships between -1 PRF and mRNA abundance in wild-type (Panel A), and NMD-deficient cells (Panel B).

The -1 PRF signals from the yeast EST1, EST2, STN1 and CDC13 mRNAs were cloned into yeast PGK1 reporters in their native orientations so that frameshift events would direct elongating ribosomes to premature termination codons (PTC). A PGK1 vector without inserted sequences was used as a control. These reporters were transformed and expressed in isogenic wild-type (A), or *upf1Δ* cells (B), and mRNA steady-state abundances were determined by qRT-PCR using the endogenous yeast U3 snoRNA as an internal standard. (A) Steady-state abundances of -1 PRF signal containing PGK1 reporter mRNAs/PGK1 control mRNA (i.e. no -1 PRF) in wild-type cells, fit to a logarithmic function. (B) Steady-state abundances of -1 PRF signal containing PGK1 reporter mRNAs in isogenic *upf1Δ* versus *UPF1* cells fit to a logarithmic function. Error bars denote standard deviation.

Given the ability of -1 PRF signals to affect the abundance of the PGK1 reporter mRNA, we tested the hypothesis that global changes in -1 PRF rates would similarly affect the steady-state abundance of these mRNAs. qRT-PCR analysis of total RNAs isolated from isogenic cells expressing *rpl3-mak8*, *rpl3-R247A*, or *rpl10-R98S* and *rpl10-R98S+NMD3-Y379D* mutants revealed an inverse correlation between changes in -1 PRF and the steady-state abundances of the EST1, EST2, STN1 and CDC13 mRNAs (**Figure 19B**). Specifically, the steady-state abundances of these mRNAs were decreased when -1 PRF was globally increased (*rpl3-mak8*, *rpl10-R98S* and *rpl10-R98S+NMD3-Y379D*), and increased in *rpl3-R247A*, where -1 PRF is globally

inhibited. The steady-state abundances of these mRNAs were also assayed in the presence of increasing concentrations of anisomycin. Similarly, their steady-state abundances were increased in a dose dependent manner, i.e. as -1 PRF rates decreased, the mRNA abundances increased (**Figure 19C**)

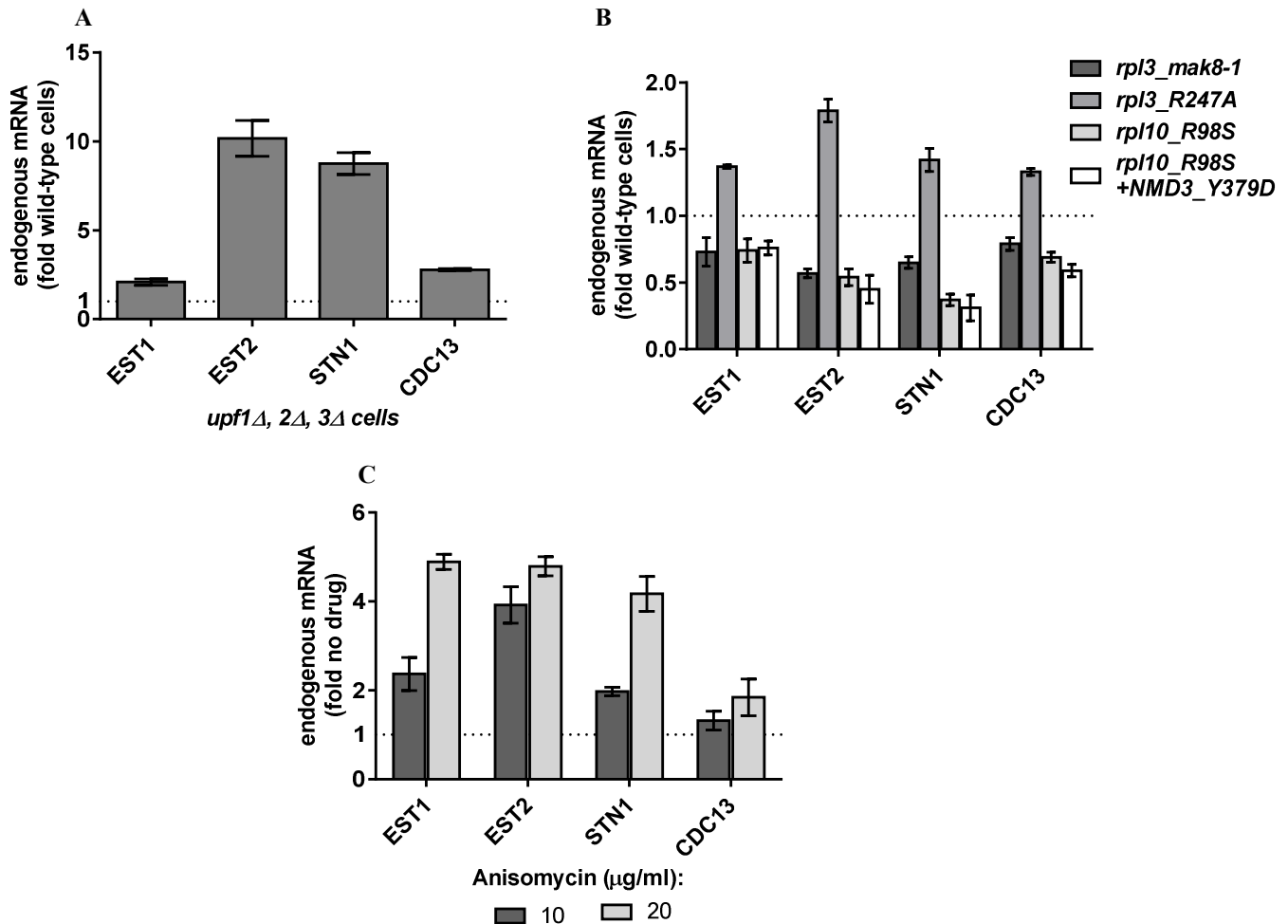


Figure 19. Steady-state abundances of native EST1, EST2, STN1 and CDC13 mRNAs in mutant and drug treated cells.

qRT PCR was used to determine steady state abundances of the native mRNAs using the G3PD mRNA as an internal standard. **(A)** mRNA abundances were monitored in isogenic *UPF1* and *upf1Δ upf2Δ upf3Δ* cells. **(B)** mRNA abundances in isogenic wild-type and *rpl3-mak8-1*, *rpl3-R247* (compared to wild-type *RPL3*), and *rpl10-R98S* and *rpl10-R98S+NMD3-Y379D* (compared to *RPL10-NMD3*) cells. **(C)** mRNA abundances were monitored in wild-type cells treated with the indicated concentrations of anisomycin. Error bars denote standard error.

Alteration of -1 PRF in the EST2 mRNA results in telomeres of intermediate length and accumulation of large, multiply budded cells.

One would expect that overexpression of telomerase would lead to longer telomeres. However, previous studies made the intriguing finding that telomeres are very short in NMD-deficient cells, and that overexpression of *EST2*, *STN1* or *CDC13* resulted in telomeres of intermediate length (133)(134)(135). To test if this is linked to -1 PRF and mRNA stability, isogenic *est2Δ*, *upf2Δ* and *est2Δ /upf2Δ* cells were transformed with low copy (*CEN6*) vectors expressing full-length *EST2* (pEST2), or one containing silent protein coding slippery site mutants (ssM). The mRNA produced from this mutant was previously shown to be ~8.5-fold more abundant than that transcribed from pEST2 (136). Genomic DNAs were harvested, digested with *Pst* I, and a Southern blot was probed for yeast telomeric sequences as previously described (133). Consistent with previous reports, complementation with the wild-type *EST2* clone restored long telomeres (L) in *est2Δ* cells, and ablation of NMD uniformly resulted in short telomeres (S) (**Figure 20A**). Importantly, expression of pEST2ssM as the sole source of Est2p promoted intermediate length telomeres (indicated by “I”), recapitulating the *EST2*, *STN1* and *CDC13* overexpression observations. These findings establish a linkage between -1 PRF and telomere length homeostasis through NMD in yeast.

Short telomeres create a “crisis” for dividing cells, triggering a series of signals that result in a delay in mitosis, specifically arrest at the G2/M boundary, as cells attempt

to restore their telomeres before committing to division (reviewed in (137)). Cells arrested at this “checkpoint” can continue to grow, increasing in volume, and eventually they can bypass mitosis, producing multiply budded yeast cells.

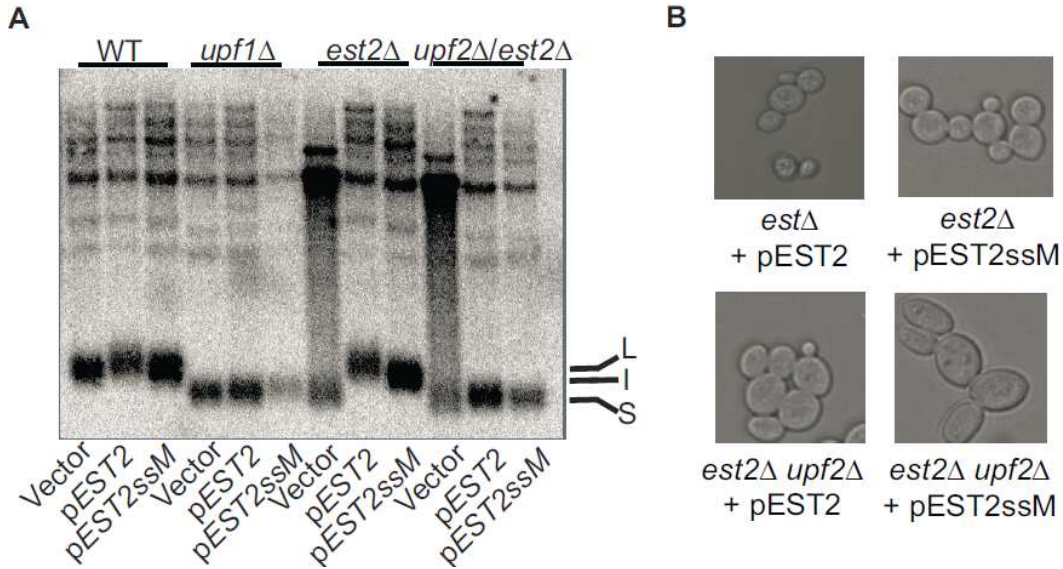


Figure 20. Ablation of -1 PRF in *EST2*, or of NMD affects telomere length and promotes G2/M cell cycle arrest.

(A) Southern blot of Pst I digested DNAs isolated from isogenic wild-type, *upf1Δ*, *est2Δ*, or *upf1Δ est2Δ* cells were transformed with either an empty *CEN6* low copy vector (vector), the same vector expressing the wild-type *EST2* gene (p*EST2*), or one in which the slippery sites of all 5 tested -1 PRF signals had been silently mutated (see Table 1). The blot was probed using DNA oligonucleotides complementary to telomeric repeat sequences as described [33]. Letters along the right hand side indicate **L**ong, **I**ntermediate, and **S**hort telomeres respectively. (B) Phase contrast microscopy (100x) of cells used in panel A harvested from logarithmically growing cultures.

In unpublished observations, we had noted that NMD-deficient cells tend to be unusually large and accumulate with large daughter buds suggestive of a G2/M mitotic delay. In combination with the results presented above, this led to the hypothesis that NMD-dependent defects in telomerase expression might affect the cell cycle. If true, then overexpression of Est2p by the p*EST2*ssM construct should confer a similar phenotype. This is indeed what we observed: *est2Δ* cells expressing p*EST2*ssM tended to be somewhat larger than isogenic cells expressing p*EST2* and

also displayed the large daughter bud phenotype. This phenotype was exaggerated in *est2Δ upf1Δ* cells expressing either pEST2 or pEST2ssM (**Figure 20B**). These findings suggest that -1 PRF may play an important role in controlling the cell cycle through telomerase expression.

-1 PRF signals as classic, rapidly evolving *cis*-acting elements.

A prior analysis of -1 PRF signals from BUB3, EST2, SPR6 and TBF1 orthologs the closely related yeast species *S. paradoxus*, *S. mikatae*, *S. bayanus*, *S. castellii*, *S. kudriavzevii* and *S. kluyveri* suggested that while no specific -1 PRF signals appeared to be conserved among these orthologs, the presence of high probability predicted -1 PRF signals in the orthologs of all of these genes (although not in every species) suggested that the mechanism itself may be conserved in these families of mRNAs, an observation that was supported by the finding that no -1 PRF signals were found in any of the orthologs of six genes that were found to lack predicted -1 PRF signals in *S. cerevisiae* (*PGK1*, *HHT1*, *TEF2*, *MIC14*, *CMD1* and *GRX1*) [24]. To address whether -1 PRF may be a conserved mechanism in yeast telomere maintenance, the orthologous genes for EST1, STN1, and CDC13 were queried. These data are presented in Appendix 7. One potential -1 PRF signal was found in the EST1 orthologs from *S. paradoxus*, *S. bayanus*, and *S. mikatae*, but the EST1 mRNAs from *S. castellii*, *S. kluyveri* and *S. kudriavzevii* lacked predicted -1 PRF signals. Potential -1 PRF signals were found in the STN1 orthologs from *S. paradoxus*, *S. bayanus*, *S. castellii* and *S. kluyveri* but not in *S. mikatae* or *S. kudriavzevii*. Similarly, orthologous CDC13 mRNAs from *S. paradoxus*, *S. castellii*, *S. kluyveri* and *S. mikatae*

were found to harbor potential -1 PRF signals, but those from *S. bayanus* and *S. kudriavzevii* did not. The potential evolutionary significance of these observations are discussed below.

Functional -1 PRF signals in three human messages encoding proteins required for telomere maintenance.

A search for -1 PRF signals in mRNAs encoding proteins involved in the human telomere maintenance revealed candidate frameshift signals in the TERF2, TERF2IP and SMG6 open reading frames (**Figure 21**). TERF2 protein is a component of the telomere nucleoprotein complex called the shelterin complex (telosome) (138). It is present at the telomere repeats and plays a protective role by preventing telomere shortening and end-to-end fusions of the chromosomes (139)(140). TERF2IP is also a component of the shelterin complex and binds to the telomere ends through TERF2(140). It plays a major role in telomere capping (141)(142). SMG6 is the human homolog of the yeast EST1 (143). Besides its involvement in telomere end capping, SMG6 also serves as an endonuclease in the process of NMD at the premature termination codons (PTC) (143)(144).

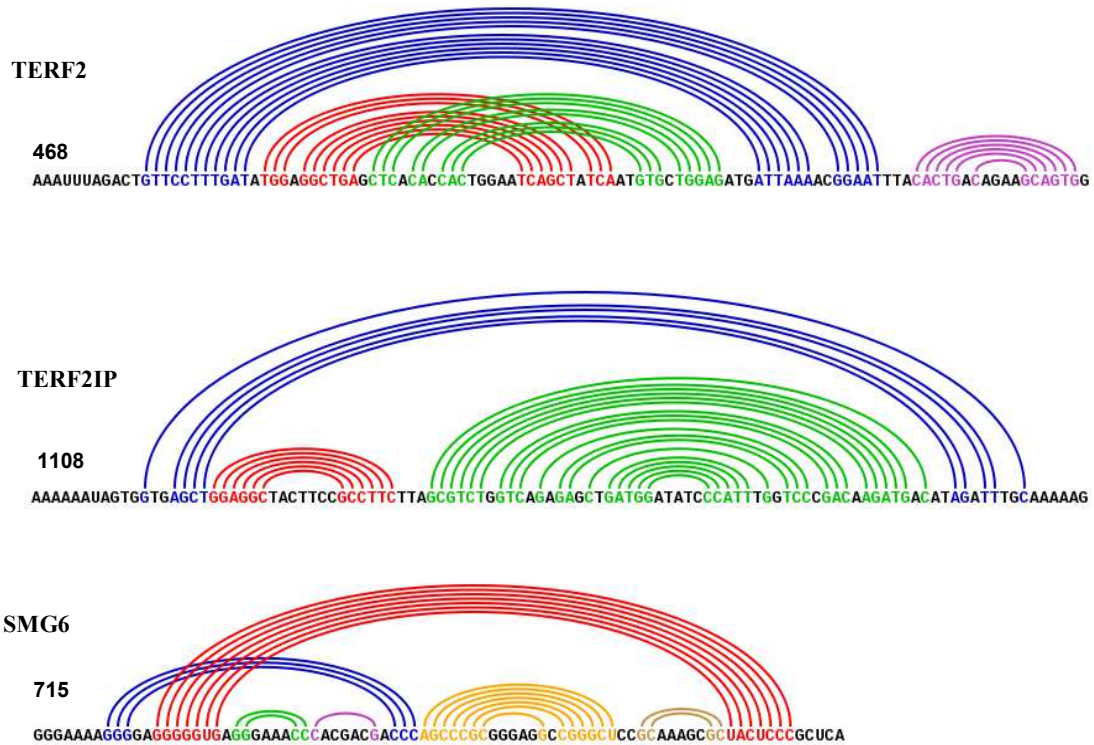


Figure 21. Sequences of -1 PRF signals in three human messages encoding proteins required for telomere maintenance.

The figure shows the predicted -1 PRF signals in human mRNAs encoding TERF2, TERFIP and SMG6 protein involved in human telomere maintenance. The numbers indicate the position in the ORF of the first nucleotide of the frameshift signal.

These candidate -1 PRF signals were cloned in mammalian dual luciferase reporter and -1 PRF efficiencies were monitored in HeLa cells. Again, employing cutoff of 1%, we observe that all the three candidate frameshift signals promote significant rates of -1 PRF ranging from ~1.73% for SMG6 to ~10.34% for TERF2 (**Table 3**). These findings suggest that -1 PRF may also play important role in human telomere maintenance.

^a ORF	^b Position	^c Slippery site	^d % -1 PRF efficiency
TERF2	468	A AAU UUA	10.34% \pm 1.19%
TERF2IP	1108	A AAA AAU	7.45% \pm 0.72
SMG6	715	C CCA AAC	1.73% \pm 0.17

Table 3. Predicted -1 PRF signals in ORFs involved in human telomere maintenance promote efficient -1 PRF in yeast cells.

^a Human gene. ^bPosition in the ORF of the first nucleotide of the predicted -1 PRF signal. ^cSlippery site sequence of the predicted -1 PRF signal. ^dPredicted frameshift signals were cloned in dual luciferase reporters, and -1 PRF efficiencies were monitored in HeLa cells.

Discussion

It is now clear that the canonical -1 PRF signals consisting of a heptameric slippery site closely followed by an mRNA pseudoknot that were first characterized in RNA viruses are also widely utilized in eukaryotic cellular mRNAs. Furthermore, it is also well established that, by shifting translating ribosomes to premature termination codons, these elements have mRNA destabilizing activities through the NMD pathway. Here, we have investigated the potential biological relevance of such frameshifting by identifying and characterizing -1 PRF signals in mRNAs encoding yeast proteins involved in telomere maintenance. The active -1 PRF signals in the mRNAs encoding Est1p, Est2p, Stn1p and CDC13p function as mRNA destabilizing elements through NMD. Interestingly, the wide range of -1 PRF efficiencies promoted by the seven different -1 PRF signals enabled a mathematical analysis of the relationship between -1 PRF and mRNA steady-state abundances (**Figure 19**). The inverse-exponential correlation between -1 PRF and mRNA abundance suggests that there are limits to changes in -1 PRF above or below which biological effects may be seen. In addition, a phylogenetic analysis revealed that -1 PRF signals in general, but not any specific -1 PRF signals, appear to be utilized in these telomere-

associated mRNAs in the yeasts. This is consistent with our previous analyses of -1 PRF signals in other yeast genes (136).

How chromosome ends are stably maintained is one of the central questions of modern biology (reviewed in (121)). Telomeres are thought exist in a range of states, from fully capped full-length, to uncapped and short (see model, **Figure 22**, adapted from models proposed in(137)(145)). As telomeres age, they progressively shorten, and at some point reach an intermediate, uncapped status. In yeast, telomere shortening promotes recruitment of the MRX+Tel1p and CST complexes (where C = Cdc13p, Stn1p, Ten1p), inducing checkpoint arrest at the G2/M boundary. Phosphorylation of Cdc13p by Tel1p enables recruitment of telomerase through Est1p, stimulating telomere repair, and releasing cells from checkpoint arrest. Failure to recruit telomerase leads to further telomere shortening, where they eventually resemble double-stranded breaks (DSB). These short telomeres recruit the DSB repair machinery, resulting in strong checkpoint arrest. Eventually, these short telomeres are maintained by this machinery, resulting in telomere end joining, and bypass of checkpoint arrest. The net effect is to “immortalize” telomeres, resulting in longer lifespans, but at the cost of genome integrity. Previous studies have shown that telomerase is limited in yeast, presumably as a means to ensure its recruitment to uncapped telomeres (146)(147). Importantly, defective expression of individual components of yeast telomerase or telomerase recruiting proteins affects telomere length. For example, overexpression of *TLC1* resulted in very short telomeres (148), while overexpression of *STN1*, *CDC13* (134), or *EST2* (148) all promoted the

intermediate telomere length phenotype. Furthermore, ablation of NMD resulted in short telomeres (128)(134)(149), suggesting that the NMD pathway is downstream to the activities of individual protein components of the telomere repair machinery. Here, we have demonstrated the presence of operational -1 PRF signals in the EST1, EST2, STN1 and CDC13 mRNAs. One result of -1 PRF events on these mRNAs is to direct elongating ribosomes to premature termination codons, consistent with the fact that they are substrates for NMD (**Figure 20A**). We have shown that these -1 PRF signals function as mRNA destabilizing elements in an NMD-dependent manner, and that this follows an inverse logarithmic relationship (**Figure 18A**).

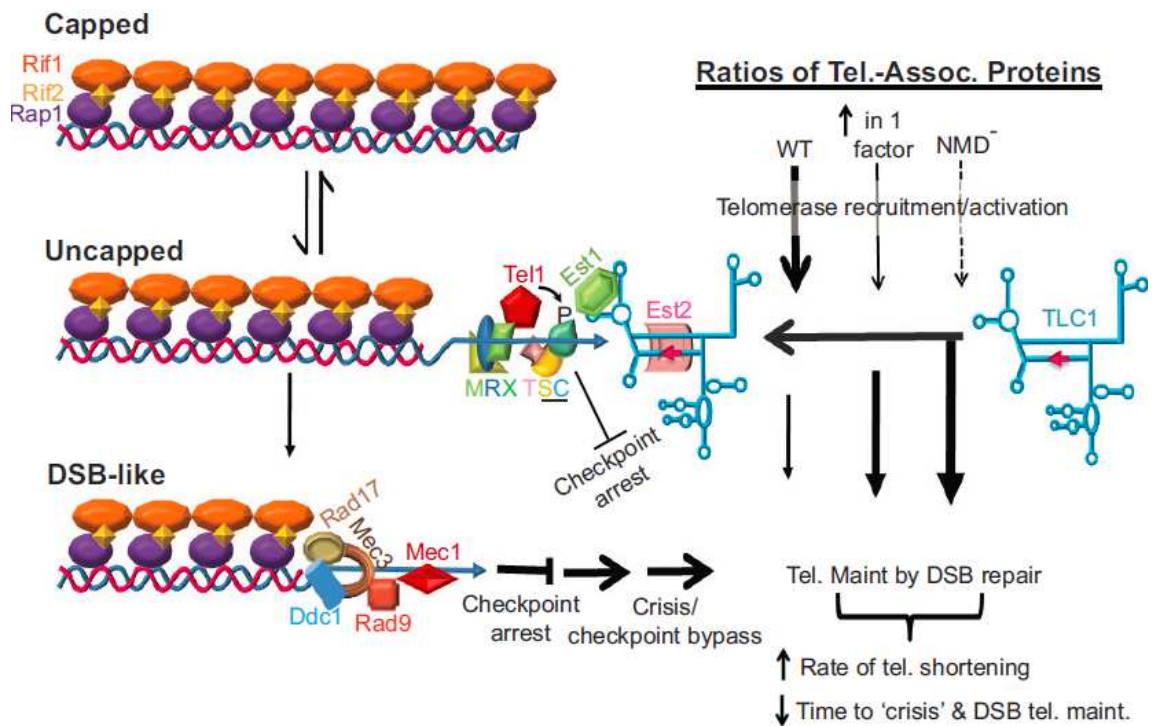


Figure 22. Model: telomerase recruitment to uncapped telomeres is controlled by the relative stoichiometries of telomerase components in yeast.

Yeast telomeres exist in a range of states, from fully capped and full length to uncapped and short. As telomeres age, they progressively shorten, and at some point reach an intermediate, uncapped status, recruiting the MRX+Tel1p complex. Tel1p phosphorylates Cdc13p (part of the Cdc13, Stn1, Ten1 complexes shown as TSC), promoting telomerase recruitment through Est1p, and inducing checkpoint arrest at the G2/M boundary. Telomerase recruitment stimulates telomere repair (up arrow on left), and releases cells from checkpoint arrest. Failure to recruit telomerase leads to further telomere shortening (down arrow on right), where they eventually resemble double-stranded breaks (DSB-like). These short telomeres also promote checkpoint arrest, but since they cannot recruit telomerase they enter crisis. Recruitment of the DSB repair machinery promotes chromosome end joining in some cells, where homologous recombination is used to amplify telomere sequences enabling checkpoint bypass. We propose that maintaining the correct stoichiometric ratios of telomerase components is critical for telomerase recruitment and telomere length homeostasis. Alteration in the expression of one of these factors, e.g. overexpression of Est2p by ablation of -1 PRF, weakly inhibits telomerase recruitment resulting in accumulation of shorter, intermediate length telomeres and accumulation of cells arrested at G2/M. Overexpression of all of these factors by inactivation of NMD has strong dominant-negative effects on telomerase recruitment, increasing the proportion of cells with short telomeres with similarly strong cell cycle effects.

Consistent with these observations, the steady-state abundances of the native EST1, EST2, STN1 and CDC13 mRNAs are inversely correlated with changes in -1 PRF (**Figures 19B, 19C**). Intriguingly, the mRNA encoding the third protein component of yeast telomerase, Est3p, harbors a +1 PRF signal (150) and is stabilized in NMD-deficient cells (133)(132). We propose that -1 PRF plays a role in maintaining the correct stoichiometric ratios of telomerase components critical for telomerase recruitment. Overexpression of any one of these components, e.g. by ablation of -1 PRF in the EST2 mRNA, has dominant-negative effects on telomerase recruitment, resulting in accumulation of intermediate length telomeres (see pEST2ssM expressed in *est2Δ* cells, **Figure 20A**). Furthermore, we suggest that global overexpression of all of these components by inactivation of NMD further increases the rate of telomere shortening, hastening the formation of DSB-like, i.e. short telomeres. This model also accounts for the observation that that ablation of -1 PRF in the EST2 mRNA, or ablation of NMD resulted in accumulation of large budded cells, a hallmark of checkpoint arrest at the G2/M boundary (**Figure 20B**).

We are not unaware that these studies pose more questions than they answer. In particular, we hope that this report inspires deeper research into the impact of -1 PRF in yeast telomere maintenance by laboratories better equipped for such inquiry. More broadly, our studies suggest that -1 PRF is a fundamental molecular mechanism that is used to fine tune a myriad of physiological processes. The big questions in the field that need to be addressed in the future include: 1) which mRNAs are actively engaged in -1 PRF in which cell types? 2) Where along these mRNAs are ribosomes actively shifting? 3) Are there thresholds above or below which changes in -1 PRF

have meaningful biological effects? And 4) how and in response to what stimuli can -1 PRF be regulated? The answers will have broad impact over the next decade.

Methods Summary

Strains, genetic manipulations, and media. *Escherichia coli DH5 α* was used to amplify plasmid DNA. Transformations of *E. coli* were performed as described previously using the calcium chloride method (151). Yeast cells were transformed using the alkali cation method (152). Yeast strains used in this study are shown in Appendix 1. Yeast were grown on YPAD and synthetic complete media (H-) (153).

Plasmids and assays of -1 PRF and mRNA steady state abundance. *URA3*-based high copy dual luciferase and mRNA stability plasmids were previously described (129). Oligonucleotide primers were purchased from IDT (Coralville, IA). Computationally identified putative -1 PRF signals shown in (Figure 15) were amplified from yeast genomic DNA by PCR using oligonucleotide primers which terminated in a *Sal* I restriction site at the 5' and *Bam* HI at the 3'. The zero-frame dual-luciferase reporter plasmid (pJD375) along with the -1 PRF signal containing dsDNA fragments were digested using these restriction enzymes and ligated together to generate endogenous -1 PRF signal containing dual-luciferase vectors. The wobble bases of slippery heptamers were mutagenized to synonymous codons in dual luciferase reporters by oligonucleotide site-directed mutagenesis using the QuickChange[®] Lightning Site-Directed Mutagenesis Kit (Agilent). *PGK1* reporter constructs for individual -1 PRFs were made as previously described (136). Read through *PGK1* plasmid pJD753 and premature termination codon vector (pJD828)

were used as controls for *PGK1* reporter steady state assays. Oligonucleotide primers were chosen to terminate in *Kpn* I restriction sites and amplify 41 and 30 bases of *Renilla* and firefly luciferase derived sequences respectively. The resulting amplicons were cloned into the *Kpn* I site 492 bases into the *PGK1* open reading frame of the unmodified *PGK1* containing vector (pJD741). A premature termination codon vector (pJD828) was generated by cutting the readthrough (pJD753) with *Bam*HI and backfilling with Klenow fragment. Plasmids expressing full length *EST2* and the *EST2*ssM mutant were previously described (136). Assays to determine rates of -1 PRF and mRNA steady-state abundances were performed as previously described. Plasmids used in this study are listed in Appendix 2.

Southern Blot analyses of *est2* mutants. Full length *EST2* expression vectors (pJD641), *EST2* mutant vectors (pJD796), and null plasmids (pJD315) were transformed into WT (JD1281), *EST2* deletion (JD1287), *UPF2* (JD1288) and *EST2/UPF2* (JD1276) deletion strains. Southern analyses were performed as described previously (134)(154) Genomic DNA was extracted from mid-logarithmic cell cultures and *Pst* I was used to digest DNA in 10 μ g aliquots. The resulting fragments were separated on a 1% agarose gel and transferred to a Hybond-N-membranes (Amersham) and hybridized to a probe derived from yeast telomeric DNA. This probe was prepared from pBC6 (a gift from the Berman lab) by PCR amplifying the telomeric region using M13 oligos. The resulting linear amplicon was used as template to create α [³²P] internally labeled telomeric TG repeat sequence using the “Decalabel random priming kit” from Stratagene. Signals were detected

using a GeneStorm phosphoimager (Bio-Rad) and quantified using QuantifyOne (Bio-Rad).

Microscopic methods. Yeast cells were visualized using a Zeiss Axiophot microscope at 100x magnification.

Phylogenetic analyses

The EST1, STN1 and CDC13 orthologs from the genomes of *S. paradoxus*, *S. mikatae*, *S. bayanus*, *S. castellii*, *S. kudriavzevii* and *S. kluyveri* were extracted from the Yeast Gene Order Browser (<http://wolfe.gen.tcd.ie/ygob/>)(155). Orthologs were identified for all genes and nucleotide sequences were analyzed for the presence of potential -1 PRF signals as previously described^[16;23]. Results are compiled in Appendix 7.

Mammalian Dual-luciferase assays.

The dual-luciferase reporters containing the TERF2, TERF2IP and SMG6 -1 PRF signals were made using the modified DNA fragment assembly protocol of In-Fusion HD cloning kit from Clontech. Mammalian dual-luciferase reporters were transfected into HeLa cells using FuGene HD transfection reagent. Translational recoding was measured as described in (156).

Chapter 3

When Translation Goes Bad.

Introduction

Ribosome is a large and complex molecular machine that decodes the information in the mRNA to make proteins from amino acids during the process of translation. Translational control is the most important aspect of post-transcriptional gene regulation and has strongest the effects on the mRNA abundance and hence protein levels. A yeast cell contains more than 200,000 ribosomes in the cytoplasm and the cell produces up to 2000 ribosomes per minute to meet the protein synthesis demand of the cell (157). The yeast 80S ribosome consists of approximately 5500 nucleotides of rRNA and 79 ribosomal proteins (158,159). Over 200 accessory proteins and transacting factors are involved in ribosome biogenesis and over 35 proteins interact with the ribosome during canonical translation process (100)(104). Many proto-oncogenes and tumor suppressors are direct regulators of the translational apparatus (160)(161). Defects in the translational apparatus have been associated with a class of human diseases collectively called ribosomopathies. Ribosomopathies are typified as congenital diseases caused by structural and functional defects of the ribosomal components. The ribosomopathies are characterized by a spectrum of abnormalities including anemias, ataxias, mental retardation, connective tissues disorders and elevated risk of developing cancer (162)(163) Ribosomopathies are linked to mutations in genes associated with ribosomal proteins, rRNA processing, ribosome assembly and transport (105)(5)(164). For example, Diamond-Blackfan Anemia

syndrome (DBA) is associated with mutations in the genes encoding ribosomal proteins S19, S26, S24, L5 and L11 (165)(166). DBA is characterized by normochromic macrocytic anemia, growth retardation and other congenital disorders. DBA patients have an elevated risk of hematopoietic neoplasms and osteogenic sarcomas (167).

Relevant to this study is X-linked Dyskeratosis Congenita (X-DC), a ribosomopathy caused by mutations in *DKC1*, the mammalian gene encoding dyskerin (168). The homolog in yeast is named *CBF5*. X-DC is characterized by several mucocutaneous abnormalities (skin pigmentation, nail changes etc.), pulmonary fibrosis, bone marrow failure, increased susceptibility to cancer and rapid ageing (105)(169)(170). Pursuant to the aging phenotype, X-DC patients have radically reduced telomere lengths (171)(172). Dyskerin (and Cbf5p in yeast) is the pseudouridine synthase and forms the catalytic core of the larger H/ACA ribonucleoprotein complex that catalyzes the isomerization of uridine to pseudouridine (ψ) in rRNA (173)(174). Pseudouridylation is the most common single nucleotide modification of the ribosomal rRNA and is conserved from bacteria to humans (173)(175)(176)(177). The yeast rRNA contains 44 pseudouridine (ψ) residues (**Figure 23**) that are important for proper assembly and function of the ribosome (178). The pseudouridine bases are clustered around functionally important regions of the ribosome, including the peptidyl transferase center, the decoding center, A-, P- and E-sites of the large and small subunits, and the mRNA platform (103)(179). In yeast, substitution of aspartic acid at position 95 in the catalytic domain of Cbf5p (*cbf5-D95A*) abolishes *in vivo* pseudouridylation of rRNA with no effects on the pre-rRNA synthesis (180)(181).

The hypo-pseudouridylated ribosomes in *cbf5-D95A* mutant have decreased affinity for both A- and P-site tRNAs and CrPV IGR IRES (106)(182). It has been shown that ψ defects in *cbf5-D95A* mutant in yeast, *DKC1^m* cells in mice and siRNA knockdown of DKC1 in human cells promote translational fidelity defects. These include increased rates of -1 PRF and decreased UAA (stop codon) readthrough (106).

Spinocerebellar ataxia type 26 (SCA26) is an autosomal dominant neurodegenerative disorder (183). It is one of the 31 subtypes of SCAs characterized by late onset Purkinje cell death and atrophy of the cerebellum (184)(185). The single variant that co-segregated with SCA26 defect was identified as C->A transversion in the ubiquitously expressed elongation factor 2 (eEF2) open reading frame. This transversion generates proline to histidine substitution at position 596. The yeast equivalent mutation in eEF2 is P580H (107). The yeast P580 lies in domain IV adjacent to H699 which is the diphthamide-bearing moiety that interacts with the 40S ribosomal subunit (**Figure 23**). The P596H variant of eEF2 in human cells does not cause destabilization or mislocalization of the protein. However, the P580H mutant in yeast promoted increased rates of -1 PRF as directed by the yeast L-A viral -1 frameshift signal.

An outstanding question is how ‘defective’ translation can produce specific pathological features. Preliminary findings suggest these genetically inherited defects result translational fidelity defects (i.e. changes in rates of -1 PRF, +1 PRF, and stop codon recognition), with attendant effects on mRNA abundance, gene expression and

telomere maintenance. These studies establish a paradigm for understanding the linkage between translational fidelity and human disease.

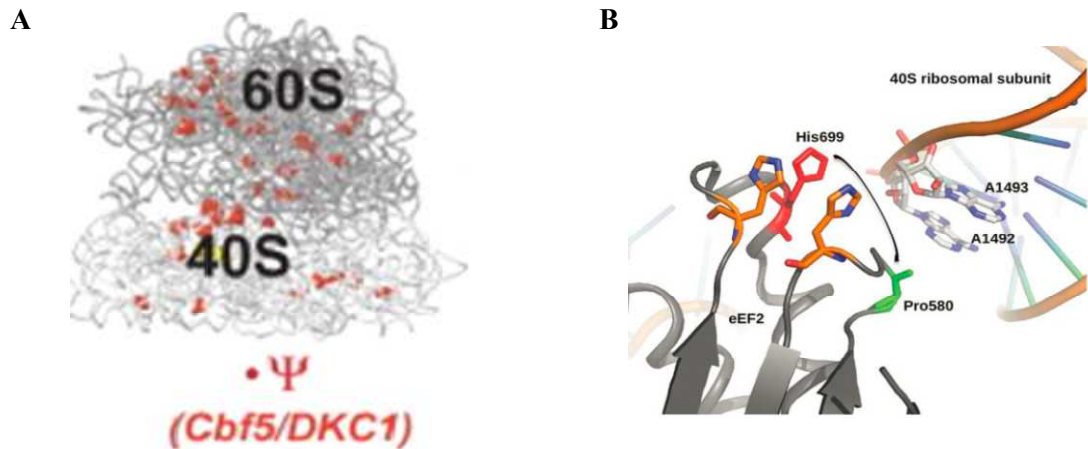


Figure 23. Causative mutations in X-DC and SCA26.

(A) Shows the locations of 44 pseudouridine bases on the rRNA as red dots. Pseudouridylation is the single most common modification of rRNA and is conserved from yeast to humans. X-DC is a ribosomopathy caused by various mutations in the DKC1 gene (CBF5 is the yeast homolog) encoding pseudouridine synthase. These mutations result in hypopseudouridylation of the rRNA. This figure is from (106) (B) Diagram of the crystal structure of EF2 in complex with the yeast 40S ribosomal subunit. SCA26 is caused by the eEF2-P596H mutation. The yeast equivalent mutation is P580H. The P580 amino acid is located in domain IV, very close to diphthamide-bearing moiety H699. This figure is from (107).

Results

Mutations associated with X-DC and SCA26 promote increased rates of -1 PRF and decreased rates of +1 PRF.

Maintenance of the translational reading frame is an important aspect of the translational fidelity. As described in Chapter 2, functional -1 PRF signals were identified in the mRNAs encoding Est1p, Est2p, Stn1p and Cdc13p involved in yeast telomere maintenance (186). The *cbf5*-D95A, *eEF2*-P580H and *eEF2*-H699Q mutants had been previously shown to stimulate -1 PRF directed by L-A virus derived sequence using bicistronic reporter assay (106)(107). As shown in (**Figure 24A**) these mutants also enhanced rates of -1 PRF directed by frameshift signals in yeast telomere maintenance genes *EST1* (beginning at nucleotide 1272), *EST2* (beginning at nucleotide 1215), *STN1* (beginning at nucleotide 1203) and *CDC13* (beginning at nucleotide 1272). Previous studies have shown that -1 PRF as directed by frameshift sequences derived from HIV-1 and human CCR5 and IL-7RA genes is enhanced in HeLa cells with siRNA-mediated knockdown of DKC1. Consistent with this, we show that siRNA-mediated knockdown of DKC1 in human cells increased IL-2RG promoted -1 PRF by 1.8-fold (**Figure 24B**). Moreover, -1 PRF was also enhanced ~1.8 fold for HIV-1 and ~2.2 fold for CCR5 frameshift signals in SC26 patient derived LCL cells (**Figure 24C**). The +1 PRF directed by the yeast *Ty1* retrotransposable element is inhibited in *cbf5*-D95A and *eEF2*-P580H cells (**Figure 24D**). Altogether, these results suggests that frame maintenance defects associated with the X-DC and SCA26 mutations are conserved in yeast and humans.

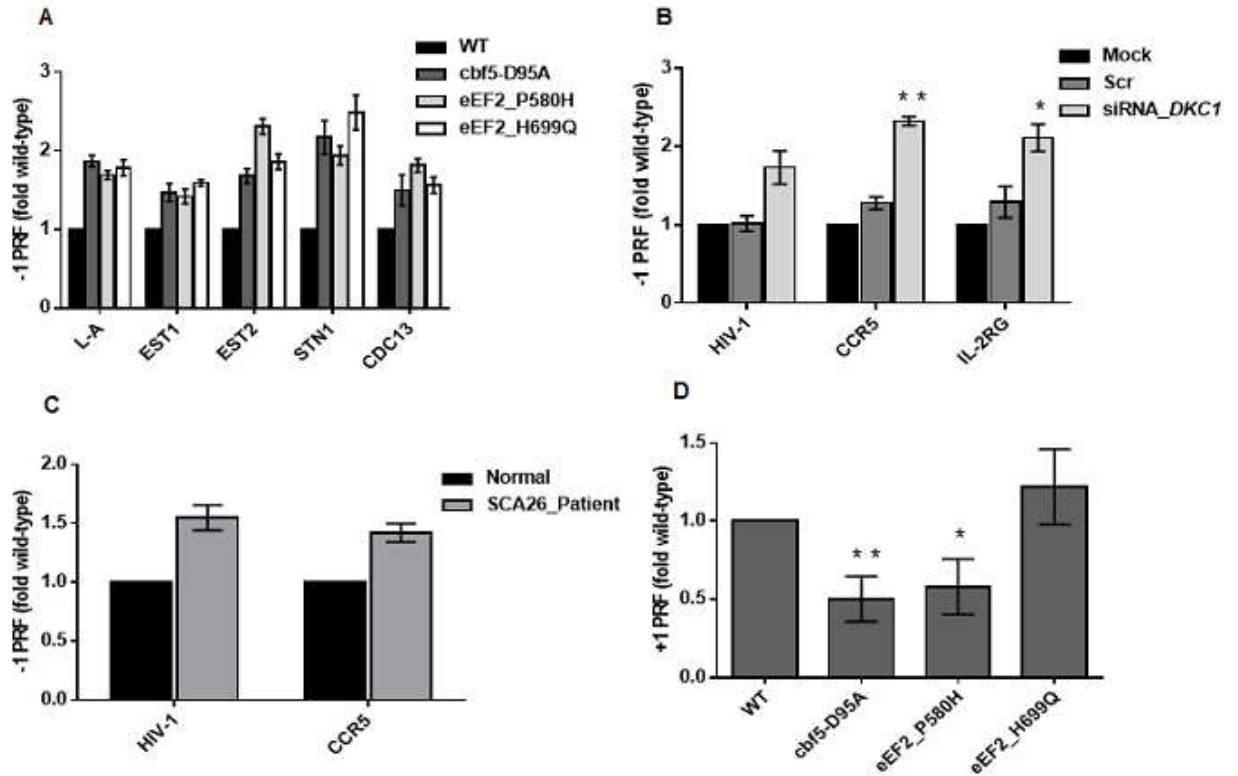


Figure 24. Dual Luciferase reporter assays to monitor -1 PRF and +1 PRF in yeast and human cells.

-1 PRF rates were measured in yeast strains (A) expressing *cbf5*-D95A allele of CBF5 or *eEF2*-P580H and *eEF2*-H699Q alleles of eEF2 using frameshift signals in yeast telomere maintenance genes *EST1*, *EST2*, *STN1* and *CDC13*. (B) and (C) -1 PRF efficiency was monitored in HeLa cells transfected mock, scrambled or *DKC1* siRNA or normal and SCA26 patient derived LCL cells using frameshift signals in HIV-1, human CCR5 and IL-2RG. (D) +1 PRF rates were measured in yeast strains using frameshift signal derived from yeast *Ty1* retrotransposable element. Error bars denote standard error. All results are expressed as fold WT. *P < 0.05, **P < 0.01.

Mutations associated with X-DC and SCA26 promote enhanced recognition of stop codon.

In vivo dual luciferase assays were also used to monitor the in-frame stop codon readthrough in both yeast and human cells. In general, all the yeast mutants under consideration promoted increased fidelity at the three termination codons as compared to their respective isogenic wild type. The *cbf5*-D95A mutant recognized the UAA and UAG stop codons with ~2-fold greater efficiency than isogenic wild-

type cells, consistent with the earlier work performed by Jack *et. al.* (106) (**Figure 25A**). The SCA26 associated P580H mutation promoted ~30% and ~25% increased fidelity at UAA and UAG codons respectively (**Figure 25A**). Similarly, human cells with siRNA knockdown of DKC1 also exhibited enhanced recognition at the stop codons (**Figure 25B**). Hence, the defects in reading frame maintenance and stop codon recognition associated with X-DC and SCA26 mutations are conserved in both yeast and human cells.

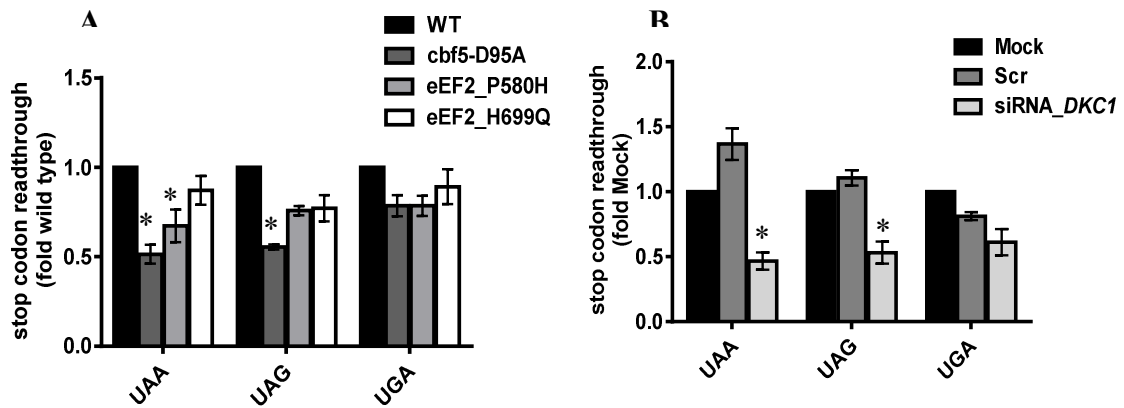


Figure 25. Dual luciferase reporter assays to monitor in-frame stop codon readthrough in yeast and human cells.

Stop codon readthrough rates were measured in (A) yeast expressing *cbf5*-D95A allele of CBF5 or *eEF2*-P580H and *eEF2*-H699Q alleles of eEF2 and (B) in HeLa cells transfected with *DKC1* siRNA. All results are expressed as fold WT (or mock). Error bars denote standard error. *P < 0.05, **P < 0.01.

Increased fidelity at stop codons results in more efficient clearance of NMD substrates.

Nonsense mediated mRNA decay pathway (NMD) maintains transcriptome fidelity by rapidly clearing cells of mRNAs containing premature termination codons (PTC). The components of NMD interact with the release factors to enhance termination and degrade aberrant mRNAs (187). Transcripts with uORFs and long 3'UTRs are also substrates of NMD and their abundances are controlled by this surveillance pathway.

The efficiency of NMD is dependent on the fidelity of the translation termination (188)(189). Therefore, enhanced recognition of the termination codons in D95A, P580H and H699Q mutants are expected to cause increased clearance of substrates of NMD. To test this hypothesis we used the yeast PGK1 reporter system, where the readthrough PGK1 reporter encodes a continuous transcript that is highly stable (97), while introduction of an in-frame UAA termination codon results in rapid destabilization of the message via NMD (**Figure 26A**). Presence of sequences from *Renilla* and firefly luciferase genes allows for specific detection of the reporter transcripts. These reporters were introduced into isogenic sets of yeast cells and the steady state mRNA abundances were determined by qRT-PCR with U3 snoRNA as the loading control. The steady state mRNA abundances of PGK1 nonsense transcripts (normalized to the readthrough control for respective strains) were reduced in *cbf5-D95A*, *eEF2-P580H* and *eEF2-H699Q* cells (**Figure 26B**). Additionally known yeast endogenous NMD substrates *GCN4* (a transcriptional activator) (190) and *CCR4* (a dominant polydeadenylase) (191) were also destabilized in the mutant cells (**Figure 26C**). The mRNAs of *GCN4* and *CCR4* have uORFs and their abundances are regulated via NMD (192)(72). Thus efficient decoding of the stop codons causes efficient clearance of NMD substrates probably due to efficient recruitment of termination factor and hence the components of NMD.

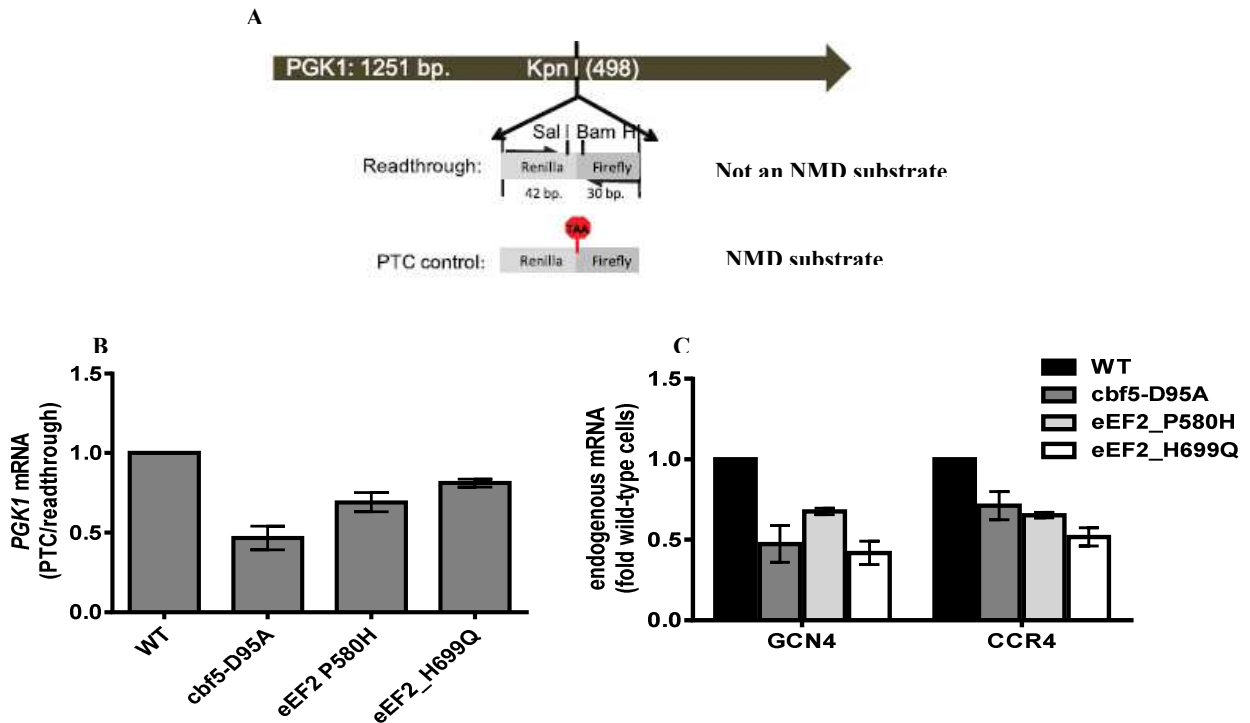


Figure 26. Yeast based studies of the effects of the *cbf5-D95A* and *eEF2* mutants on mRNA abundance.

(A) Schematic of *PGK1* reporters used to monitor effects of mutations on steady-state abundance of PTC containing mRNAs. (B) Steady-state mRNA abundance of the PTC/readthrough control reporter mRNAs shown in panel A (as fold wild type cells). (C) Steady-state abundances of two endogenous mRNAs known to be NMD substrates (shown as fold wild-type cells). Error bars denote standard error.

Increased rates of -1 PRF and enhanced NMD lead to shortened telomeres.

Recent studies have shown that the steady state abundances of the -1 PRF signal containing cellular *EST1*, *EST2*, *STN1* and *CDC13* mRNAs is inversely affected by global changes in -1 PRF rates (186). Similarly, the steady state mRNA abundances of the endogenous *EST1*, *EST2*, *STN1* and *CDC13* mRNAs were reduced in *cbf5-D95A*, *eEF2-P580H* and *eEF2-H699Q* cells as monitored by qRT-PCR (Figure 27A). A qPCR analysis of the genomic DNA revealed reduced abundance of the telomere repeat sequence in *cbf5-D95A*, *eEF2-P580H* and *eEF2-H699Q* cells indicative of defects in telomere maintenance (Figure 27B). Functional -1 PRF

signals were recently identified in human TERF2, TERF2IP and SMG6 mRNAs involved in telomere maintenance (**Chapter 2**). Consistent with the earlier findings siRNA-mediated knockdown of DKC1 in HeLa cells promote increased rates of -1 PRF directed by sequences located in TERF2, TERF2IP and SMG6 mRNAs (**Figure 27C**). The altered rates of -1 PRF may result into decreased abundances of the respective mRNAs and proteins contributing to the progeria like symptoms of this disease.

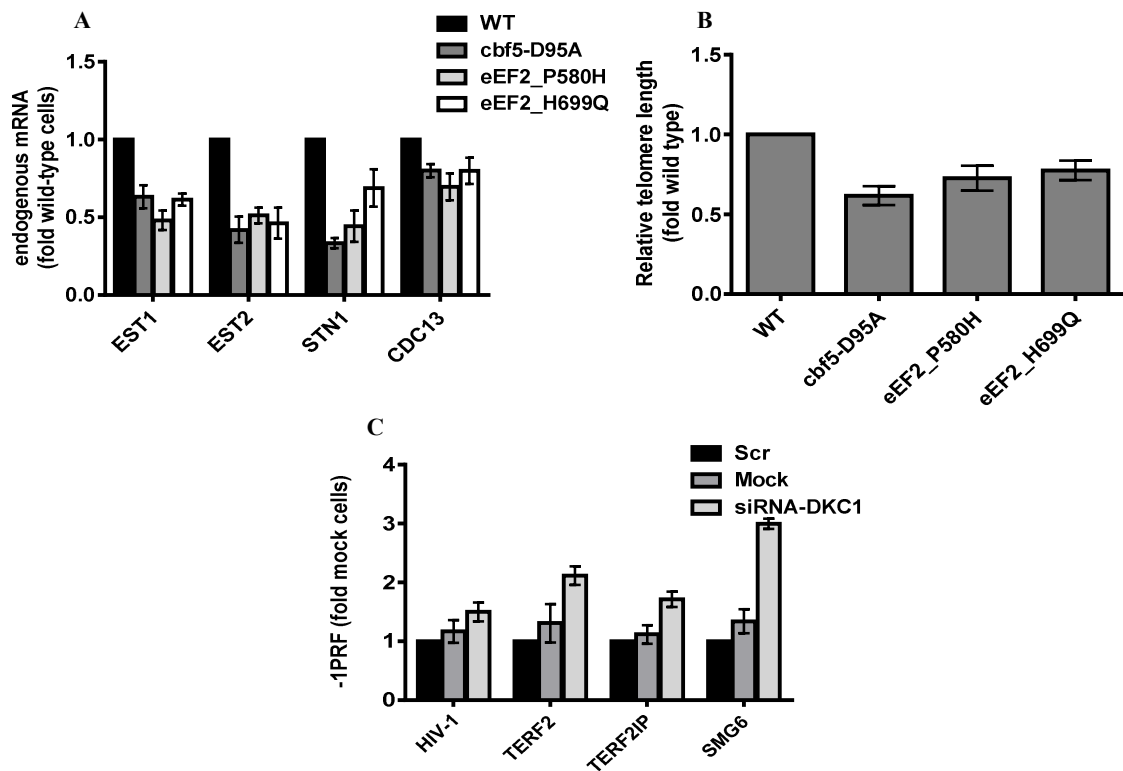


Figure 27. Increased rates of -1 PRF and enhanced NMD lead to shortened telomeres.

(A). Steady-state endogenous abundances of EST1, EST2, STN1 and CDC13 mRNAs were monitored using quantitative RT-PCR in yeast strains. (B). Relative telomere length measured as abundance of telomere repeat sequence quantified by RT-PCR, with the single-copy reference gene *SGS1* as the loading control. (C) -1 PRF efficiency was monitored in HeLa cells transfected mock, scrambled or *DKC1* siRNA using frameshift signals in human TERF2, TERF2IP and SMG6 mRNAs. All results are expressed as fold WT or mock. Error bars denote standard error.

Discussion

There is a growing body of evidence connecting translational fidelity defects and human disease (127)(106)(163). Here we use X-DC and SCA26 as models to understand how mutations in genes associated with translational machinery may contribute to distinct pathological features of these lethal diseases.

Previous studies have shown that impairment rRNA pseudouridylation in *cbf5-D95A* cells decreases ribosomal affinity for tRNAs at both the A- and P- site (106). Both A- and P- site tRNAs are the substrates for -1 PRF and increased rates of -1 PRF is consistent with the increased slippage of both tRNAs. The P580 residue of yeast eEF2 (and P596 in mammalian eEF2) is located very close to the diphthamide moiety. The proline to histidine substitution likely hinders the interaction of the eEF2 with the ribosome thereby disrupting translocation. Consistent with recent kinetics studies (193) impairments in translocation would be expected to result in increased rates of -1 PRF, consistent with the observations in yeast *eft2-P580H* and *eft2-H699Q* cells can be attributed to hindered translocation of the ribosome during elongation. Similarly, impaired translocation in these cells may result in slowed ribosomal transit time at termination codons, enhancing the probability of their recognition by eRF1, resulting in the observed increased fidelity at the stop codons in these mutants.

Increased rates of -1 PRF in the *cbf5-D95A*, *eft2-P580H* and *eft2-H699Q* cells results in decreased steady state abundances of the endogenous EST1, EST2, STN1 and CDC13 mRNAs, which encode proteins involved in telomere length maintenance. Consequently these yeast cells have short telomeres. Additionally ψ defects also promote increased rates of -1 PRF promoted by the functional frameshift signals

located in the human mRNAs encoding TERF2, TERF2IP and SMG6 proteins. Interestingly, preliminary data from the Ruggero laboratory suggests that TERF2 protein expression is decreased in X-DC patient cells (Davide Ruggero, personal communication). These observations suggest a novel link between ribosome function and telomere maintenance. Computational analyses suggest that ~10% of eukaryotic cellular mRNAs harbor functional -1 PRF signals (44). In the human transcriptome, 99.93% of these are predicted to direct elongating ribosomes to a -1 frame premature termination codon, triggering rapid degradation of the mRNA via NMD. Thus, we suggest that the roots of the pathological features associated with X-DC and SCA26 can be traced to the intrinsic translational defects that cause decreased abundance of -1 PRF signal containing mRNAs via NMD.

Programmed translational readthrough (PTR) is of physiological significances in *Drosophila* and human fibroblast cells (194)(195). PTR in the mRNA encoding the human vascular endothelial growth factor A (VEGFA) generates a 22 amino acid C-terminally extended isoform VEGF-Ax. VEGF-Ax exhibits antiangiogenic activity (65). Increased fidelity at the stop codons due to rRNA ψ defects may result in decreased rates of PTR on this mRNA, and hence decreased VEGF-Ax synthesis contributing to increased susceptibility to cancer.

NMD depends on translation efficiency (196). It plays an important role in the differentiation of neural and hematopoietic progenitor cells (197)(198)(199). Several pro-hematopoietic factors have been identified as targets of NMD and their dysregulation due to aberrant activation or inactivation of NMD inhibits hematopoiesis (199). Genetic perturbations associated with X-DC and SCA26 result

in enhanced clearance of mRNAs NMD targets (**Figure 26 and 27A**). These also include mRNAs harboring -1 PRF signals. Unpublished data demonstrates decreased expression of proteins involved in hematopoietic stem cell differentiation that contribute to bone marrow failure in X-DC patients. In sum, these findings lay a general framework for a proposed mechanism for X-DC, SCA26 and ribosomopathies. This is modeled in (**Figure 28**).

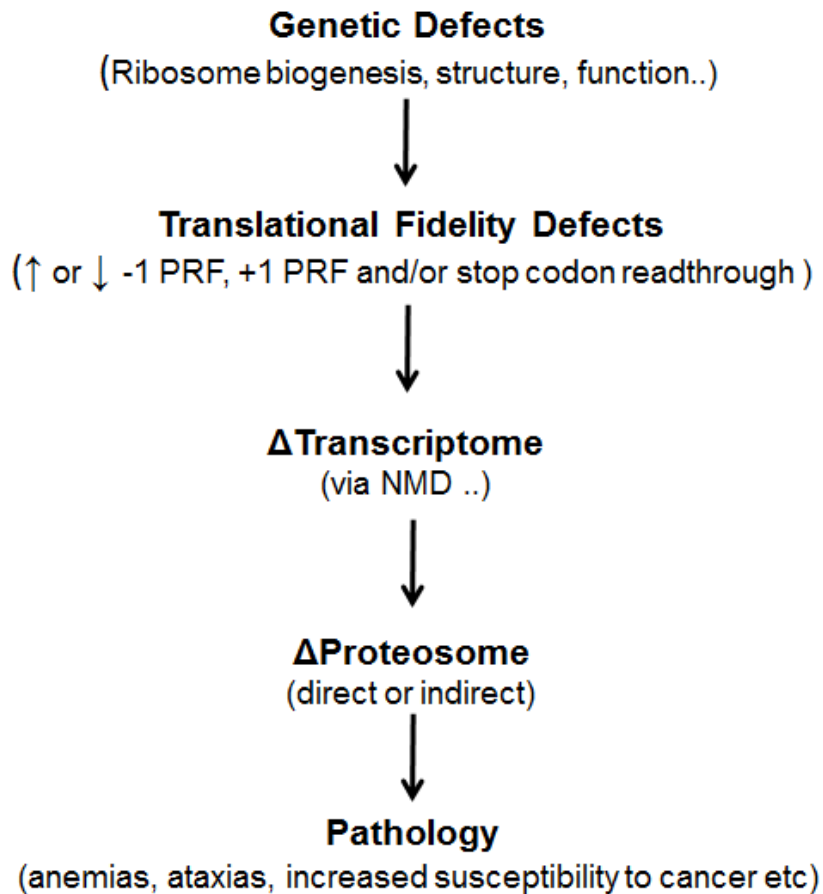


Figure 28. General Model of Translationopathy.

Mutations in genes that participate in translation confer translational fidelity defects. The translational fidelity defects include but are not limited to +1 PRF, -1 PRF and/or stop codon readthrough. The type and the magnitude of translational fidelity defects elicit downstream post-transcriptional surveillance pathways like NMD. This leads to altered gene expression and progression to disease like anemia, ataxia etc.

Methods Summary

Strains, genetic manipulations, and media. *Escherichia coli DH5 α* was used to amplify plasmid DNA. Transformations of *E. coli* were performed as described previously using the calcium chloride method (151). Yeast cells were transformed using the alkali cation method (152). Yeast strains used in this study are shown in Appendix 1. Yeast were grown on YPAD and synthetic complete media (H-) (153).

Translational Fidelity assays

Yeast dual Luciferase reporters harboring the yeast L-A virus -1 PRF signal, the Ty1-derived +1 PRF signal, or in-frame UAA, UAG or UGA codon were previously described (122). Yeast cells were transformed using the alkali cation method (152). Mammalian dual-luciferase reporter containing the HIV-1, CCR5, IL-2RG, TERF2, TERF@IP and SMG6 -1 PRF signals or in-frame UAA, UAG or UGA codon were used. The mammalian dual-luciferase reporters were transfected into HeLa cells using FuGene HD transfection reagent. siRNA knockdown experiments in HeLa cells employed either mock, DKC1 or control scramble siRNA oligos. Translational recoding was measured as described (200).

Plasmids and assays of -1 PRF and mRNA steady state abundance. *URA3*-based high copy mRNA stability plasmids were as previously described in (136). Oligonucleotide primers were purchased from IDT (Coralville, IA). Read through *PGK1* plasmid pJD753 and premature termination codon vector (pJD828) were used for *PGK1* reporter steady state assays. Oligos used for the steady state qRT-PCR for

endogenous messages are described in Appendix 6. Assays to determine mRNA steady-state abundances were performed as previously described (136). Plasmids used in this study are listed in Appendix 2.

Telomere Length Assays

Genomic DNA was isolated from cells in mid-logarithmic using the “smash and grab” DNA preparation method (201). qPCR was used to determine yeast telomere repeat content (T) relative to the single-copy reference gene *SGS1* (S) with the Bio-Rad iTaq Universal SYBR Green. The T/S ratios were calculated from three experimental replicates at each of three DNA concentrations (100, 200, and 400 ng). The Student *t*- test for two-tailed *P* value calculations was used throughout.

Chapter 4

Conclusion and Future Directions

In Central Dogma of molecular biology, the mRNA ensures precise propagation of genetic information and functions as an effector of the cellular phenotype. Post-transcriptional regulation of mRNA quality and quantity governs the cellular homeostasis. Translational recoding, first described in viruses, has recently emerged as an important mechanism of post-transcriptional gene regulation (1)(3)(55). The focus of this thesis work has been to investigate the physiological relevance of translational recoding in human disease, with a primary focus on -1 PRF. Analysis of predicted -1 PRF signals across 20 genomes suggests that it is a universal mechanism (130). Thus the focus of this project has been to increase our knowledge of cellular gene regulation by -1 PRF.

The involvement of -1 PRF in telomere maintenance is one of the major findings of this work. How chromosome ends are stably maintained is one of the central questions of modern biology. Regulation of telomere length is also medically important because of its association with ageing and cancer. Proteins involved in yeast telomere maintenance are expressed in limited quantities and their defective expression leads to shorter telomeres (145). Operational -1 frameshift signals in messages involved in yeast telomere length maintenance are capable of affecting mRNA stability via NMD (186)(97). Here, we showed that rates of -1 PRF and the activity of NMD govern the abundances of these messages and hence the

stoichiometries of these proteins. We found that global changes in the -1 PRF rates affects the abundances of these messages with attendant effects on stoichiometry and hence telomere length. In addition, these studies capitalized on the fact that the -1 PRF signals in the telomere maintenance protein coding mRNAs are operational along a wide range of -1 PRF efficiencies. We capitalized on these to define a mathematical relationship between -1 PRF efficiency and mRNA abundance as shown below (37).

$$f(x) = e^{-0.05x}$$

i.e. mRNA abundance is a function of -1 PRF efficiency 'x'. The exponential relationship also suggests that there are limits to changes in -1 PRF above or below which effects may be seen. Another interesting observation is that the -1 PRF signals in these messages are not fully conserved in other yeasts (Appendix 6).

In the course of this work, we also developed a novel qPCR based assay to analyze relative telomere length in yeast cells. This simple, rapid and scalable assay represents a significant improvement over conventional *in-situ* hybridization and Southern blot assays that had been the norm until now. Toward the end of this work we also began the process of expanding our studies of -1 PRF and telomere maintenance to human biology. Identification of functional -1 PRF signals in human telomere maintenance genes suggests that -1 PRF is widely used to control telomere length. Importantly, X-DC is characterized by progeria and telomere shortening. While the accepted dogma in this field is that mutations in XDC1 directly affect telomerase through the direct association of its encoded protein, there is actually no

direct evidence supporting this. Our findings suggest an alternative explanation for the telomere shortening and progeria phenotype of these patients. Indeed, our findings in yeast and in human cells lead us to the hypothesis that global dysregulation of -1 PRF may contribute to disease pathogenesis. Here, we have used X-DC and SCA26 as model systems to understand other ribosomopathies, and to understand the normal aging process. Abnormalities in ribosome function that are implicated in both congenital and acquired syndromes have been broadly classified as ‘ribosomopathies’. However, the precise molecular mechanisms that contribute to these pathologies are unknown. In Chapter 3, we used X-DC and SCA26 as model systems to investigate how mutations associated with the components of translational machinery affects gene expression. These mutations promote increased rates of -1 PRF and increased fidelity at stop codons. These defects trigger enhanced rates of NMD-directed degradation on -1 PRF signal containing mRNAs. Preliminary data from our lab suggests that other pathologies associated with different ribosomopathies may also be due to specific defects in translational fidelity. We have found that the magnitude and type of translational fidelity defects can elicit enhanced NMD. However, the true contribution of dysregulation of -1 PRF and NMD to disease pathogenesis remains unknown. One avenue of future inquiry utilizes X-DC and SCA26 as the disease models to identify the repertoire of translationally regulated mRNAs associated with specific dysfunction in the translational apparatus. Such a course of inquiry would identify novel diagnostic and prognostic markers associated with X-DC and SCA26.

Sequence specific regulation of -1 PRF by ncRNAs as demonstrated with human CCR5 mRNA, the first in which -1 PRF is stimulated by miR-1224 (99), has potentially profound impact on our understanding of post-transcriptional gene regulation. Additionally an operational -1 PRF signal was also identified in the mRNA encoding human interleukin 2 receptor γ -chain (IL-2RG) encoding mRNA (**Figure 29A**). Defects in the expression of IL-2RG can result in Severe Combined Immunodeficiency Syndrome (SCID) (202). siRNA knockdowns of Argonaut 1 (AGO1) stimulated IL-2RG mediated -1 PRF (**Figure 29B**). Additionally, single nucleotide polymorphisms (SNPs) identified within the IL-2RG -1 PRF sequence have the potential to alter -1 PRF efficiency, and thus may account for a SCID disease phenotype. This further broadens our hypothesis to include ‘dysregulation of miRNA expression as it affects -1 PRF may in part contribute to human disease phenotypes’. One possible way to identify miRNAs associated with cellular -1 PRF signals may be to perform *in vivo* pull-down experiments using specific -1 PRF signals as “bait”.

Operational frameshift signals are also found in the genomes of alphaviruses: WEEV (Western equine encephalitis virus), EEEV (Eastern equine encephalitis virus) and VEEV (Venezuelan equine encephalitis virus) (203). Alphaviruses belong to Togaviridae family and have +ssRNA genomes. The frameshift product is a structural component of the virion called TF (transframe). Alphaviruses are significant human pathogens and are classified as Category B select agents by the CDC based on a number of criteria including a history of being developed as bioweapons (204). Their -1 PRF sequences may also be regulated by miRNAs.

Identification and characterization of regulation of PRF by miRNAs may suggest novel approaches for the design of anti-viral therapeutics.

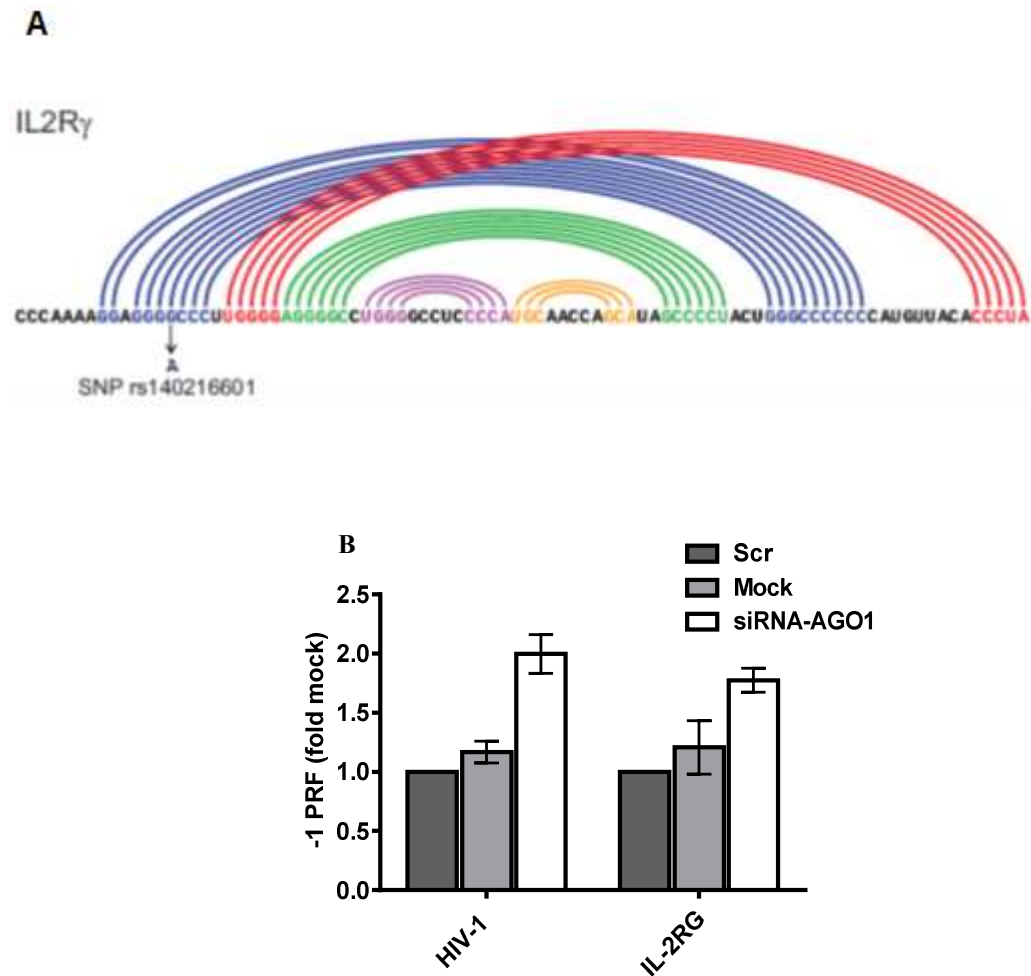


Figure 29. -1 PRF in human mRNA IL-2RG is regulated by miRNAs.

(A) Predicted -1 PRF signal in human IL-2RG mRNA shown as Feynman diagram. Identified SNP is shown below the diagram. (B) -1 PRF efficiency was monitored using dual luciferase assay in cells transfected with mock, scrambled or *AGO1* siRNA. Error bars denote standard error.

The PRFdb predicted ~10% of the genes in humans have at least one functional -1 PRF signal. This translates to 1,943 high probability -1 PRF signals in the human genome. We have cloned and validated -1 PRF signals in 13 human genes associated with different diseases. These are shown in Appendix 9 and their description is included in Appendix 10. However, at this juncture, additional high probability -1

PRF signals need to be cloned and validated. In my postdoctoral work I will capitalize on the First-year Innovative and Research Experiences (FIRE) - Found in Translation (FIT) Research stream as a multiplier of labor and time. The FIRE-FIT research stream involves 30 undergraduate students that work in a laboratory setting to clone and validate predicted -1 PRF signals. Beginning this spring semester the students are being trained to clone and test selected human mRNA sequences. This will generate empirical for validating and identifying functional -1 PRF in the human genome. The list of -1 PRF sequences that are being cloned and tested are shown in appendix 11. We intend to follow up with questions regarding the biological and biomedical significance of -1 PRF.

Next-generation sequencing of RNA and ribosome protected messages provide valuable information that can relate the observations of mRNA structure and function to individual molecules. The data generated using these techniques is increasing at an exponential rate. The genome wide predictions in PRFdb can be sieved through the available RNA-seq and ribosome profiling datasets to relate the individual predictions with mRNA abundance and ribosome pausing. Additionally the empirical data generated through the FIRE program will help us identify bonafide -1 PRF signals across the human genome. This will increase our understanding of how defects in the interplay between mRNA and ribosomes contribute to human disease.

Chapter 5

Experimental Procedures

Cell Culture

The HeLa and LCL cell lines were cultured as per the ATCC guidelines. HeLa cell lines were cultured at 37° with 5% CO₂ using Dulbecco's Modified Eagle's Medium (DMEM) supplemented with 10% irradiated fetal bovine serum (FBS), 1x non-essential amino acids (NEAA), 4 mM glutamine and 1% Penicillin/Streptomycin. The LCL cell lines (both normal and patient derived cells) were cultured in RPMI media supplemented with 10% FBS and 1% Penicillin/Streptomycin. The cells were passaged (HeLa cells using trypsin) when growing exponentially. The LCL cells were cultured in drug free RPMI medium for 6 hours post plasmid transfections.

Dual Luciferase Assays

Dual luciferase assays were performed using a Turner Biosystems GloMax-Multi Microplate Multimode Reader and Dual Luciferase Reagent Kit from Promega. Data analysis were performed as described in (156).

Yeast cells were to mid-log phase before analysis. The cells were lysed using glass beads (instead of the recommended lysis buffer in the Promega kit) in PBS buffered lysis solution containing protease inhibitor cocktail. The lysates were diluted 1:2 – 1:10 depending on the cell culture volume. The lysates were aliquoted in 96 well plates and analyzed in the luminometer using the 50 µl (as compared to suggested 100 µl) of each Renilla and Firefly luciferase substrates. The dual luciferase assays

for the mammalian cells were performed as per the guidelines of the Promega protocol.

Quantitative Real Time Reverse transcriptase PCR

Yeast cells

Yeast cells were grown to mid-log phase and RNA was isolated using Trizol Reagent with no modifications. DNase digestion was done using the RNA Microaqueous kit from Ambion (Life Technologies). cDNA was made using the iScript cDNA synthesis kit from Bio-Rad. cDNA was diluted 1:100 – 1:10,000 depending the RNA concentration. Reactions were performed using the iTaq Universal SYBR green mix from Bio-Rad. Reactions were amplified using the Bio-Rad CFX 96 thermocycler as follows: 25⁰C for 10 seconds, 95⁰C for 5 min, followed by 45-60 cycles of 95⁰C for 10 seconds, 48⁰C for 15 seconds, and 72⁰C for 15 seconds. Melting curves were monitored by taking readings every 0.5⁰C from 55-95⁰C. U3 snoRNA was used as loading control.

Mammalian cells

RNA was isolated from mammalian cells using the Microaqueous kit from Ambion (Life Technologies).. cDNA was made using the iScript cDNA synthesis kit from Bio-Rad and diluted 1:10 – 1:100 depending the RNA concentration. Reactions were performed using the iTaq Universal SYBR green mix from Bio-Rad. Reactions were amplified using the Bio-Rad CFX 96 thermocycler as follows: 25⁰C for 10 seconds, 95⁰C for 5 min, followed by 45-60 cycles of 95⁰C for 10 seconds, 50⁰C for 15

seconds, and 72⁰C for 15 seconds. Melting curves were monitored by taking readings every 0.5⁰C from 55-95⁰C. GAPDH mRNA was used as loading control.

Transfections

Plasmid

Plasmid transfections were performed using modified FuGene HD transfection protocol from Promega. Efficient transfections were achieved using 3:1 ratio of plasmid to transfection reagent. The plasmid transfection reagent complexes prior adding to the cells were incubated in drug and serum free DMEM or RPMI media at room temperature. Transfections for LCL cells were performed using modified Nucleofector transfection kit V protocol from Lonza. Efficient transfection were achieved using double the amount pf plasmid as recommended in the protocol. Dual luciferase assays were performed 24-48 hours post transfections.

siRNA

Cells were transfected with synthetic RNA oligonucleotides specific to the mRNA of interest (hDKC1, hAGO1) or scrambled oligonucleotides using the HiPerFect transfection reagent from Qiagen. Initial transfections were performed at 5, 10 and 20 nM of siRNA for optimization. Most final transfections were performed at 10 and 20 nM. The siRNA-transfection reagent complexes were incubated in serum and drug free DMEM media prior adding to the cells. The media was replaced 6-8 hours after transfections. Assays were performed 12-24 hours post siRNA transfections. When other plasmids were also transfected, the assays were performed 24-48 hours post siRNA transfection.

Transformations

Bacteria

Transformations using the bacterial strain DH5 α were performed as described in (153) . For site-directed mutagenesis experiments (for larger plasmids and SDM products) a modified protocol as described in Quick Change Lightning Site-Directed mutagenesis was used. Stellar Competent cell (Clontech Laboratories Inc.) transformation protocol was used for DNA fragment assembly method used for -1 PRF signal cloning.

Yeast

Yeast strains were transformed using modified alkali cation method as described in (205) . Yeast cells were grown in mid-log phase in YPAD or appropriate selective media. Transformations were performed using 0.1 M LiOAc/TE and excess (600 μ l) PEG/LiOAc/TE buffers. Approximately double amount of ssDNA was used. The sample were incubated at 30°C for 30-90 minutes (approximately double time recommended incubation time). The cells were heat shocked at 42°C for 15 minutes before plating on appropriate selective media. For the CBF5 strains the transformations were performed at room temperature without heats shock.

Appendix 1: Yeast Strains Used

Strain number	Genotype	Purpose
JD1361	yRP1674 <i>MATa his3Δ leu2Δ met15Δ ura3Δ</i>	Wild-type strain for steady state assays and frameshifting.
JD1367	yRP2077 <i>MATa upf1::KanMX4 his3Δ leu2Δ met15Δ ura3Δ</i>	NMD deficient strain isogenic to JD1361 for steady state.
JD1228	<i>MATa ura3-52 lys2-801 trp1Δ leu2Δ hisΔ RPL3::HIS3</i> pJD166_WT.trp	Strain expressing wild-type ribosomal protein L3 on a plasmid(pJD166) for frameshifting and steady state assays
JD1229	<i>MATa ura3-52 lys2-801 trp1Δ leu2Δ his3Δ RPL3::HIS3</i> pJD166_mak8.trp	Strain isogenic to JD1228 expressing up-frameshifting <i>rpl3-W255C/P257S</i> (i.e. <i>mak8</i>) allele, for frameshifting and steady state assays
JD1560	<i>MATa ura3-52 lys2-801 trp1Δ leu2Δ his3Δ RPL3::HIS3</i> pJD166(R247A).trp	Strain isogenic to JD1228 expressing down-frameshifting <i>rpl3-R247A</i> allele, for frameshifting and steady state assays
JD1524	<i>MATa ade2-1 can1-100 his3-11 leu2-3, 112 trp1-1 ura3-1 cbf5::TRP1</i> with <i>CBF5</i> on pRS313	Strain expressing wild-type <i>CBF5</i> gene on a plasmid, for frameshifting and steady state assays
JD1525	<i>MATa ade2-1 can1-100 his3-11 leu2-3, 112 trp1-1 ura3-1 cbf5::TRP1</i> D95A allele on pRS313	Strain isogenic to JD1524 expressing <i>cbf5-D95A</i> allele on a plasmid, for frameshifting and steady state assays
JD960	<i>MATa ade2-1 his3-11,15 leu2-3, 112 trp1-1 ura3-1 can1-100 UPF1 UPF2 UPF3</i>	Wild-type strain for steady state assays.
JD961	<i>MATa ade2-1 his3-11,15 leu2-3, 112 trp1-1 ura3-1 can1-100 upf1::HIS3 UPF2 UPF3</i>	NMD deficient strain isogenic to wild-type JD960 for steady states assays.
JD967	<i>MATa ade2-1 his3-11,15 leu2-3, 112 trp1-1 ura3-1 can1-100 upf1::LEU2 upf2::URA3 upf3::his3</i>	NMD deficient strain isogenic to wild-type JD960 for steady states assays.
JD1263	<i>MATa/a trp1Δ /trp1Δ leu2Δ/leu2Δ can1-100/can1-100 ade2-1/ade2-1 est2Δ::URA3/EST2 upf2Δ::HIS3/UPF2 VR-ADE2-TEL/VR-TEL</i> (YJB2659)	Parental diploi dstrain of <i>est2</i> mutant strains used in this study, Berman lab

JD1281	<i>MATa trp1Δ leu2Δ can1-100 ade2-1 ura3-1 his3-11 VR-ADE2-TEL</i>	Wild-type strain for assaying telomere length
JD1287	<i>MATa trp1Δ leu2Δ can1-100 ade2-1 est2Δ::URA3 his3-11 VR-ADE2-TEL</i>	Telomerase deficient strain to assay telomere length
JD1288	<i>MATa trp1Δ leu2Δ can1-100 ade2-1 ura3-1 upf2Δ::HIS3 VR-ADE2-TEL</i>	NMD deficient strain to assay telomere length
JD1276	<i>MATa trp1Δ leu2Δ can1-100 ade2-1 est2Δ::URA3 upf2Δ::HIS3 VR-ADE2-TEL</i>	Telomerase and NMD deficient strain to assay telomere length
JD1693	<i>MATa rpl10::KanMX lysΔ0 met15Δ leu2Δ ura3Δ his3Δ</i>	Strain expressing wild-type ribosomal protein L10 on a plasmid for frameshifting and steady state assays
JD1694	<i>MATa rpl10-R98S::KanMX lysΔ met15Δ leu2Δ ura3Δ his3Δ</i>	Strain isogenic to JD1693 expressing <i>rpl10-R98S</i> allele on a plasmid, for frameshifting and steady state assays
JD1695	<i>MATa rpl10::KanMX lysΔ met15Δ leu2Δ ura3 Δ NMD3Δ -Y379D his3Δ pURA3- NMD3Δ -Y379D</i>	Strain isogenic to JD1693 expressing <i>NMD3-Y379D</i> allele on a plasmid, for frameshifting and steady state assays
JD1696	<i>MATa ade2 Δ lys2 Δ ura3 Δ his3 Δ leu2 Δ trp1 Δ eft1Δ:HIS3 eft2 Δ:TRP1 pURA3-EFT1</i>	Strain expressing wild-type ribosomal protein eEF2 on a plasmid for frameshifting and steady state assays
JD1697	<i>MATa ade2 Δ lys2 Δ ura3 Δ his3 Δ leu2 Δ trp1 Δ eft1Δ:HIS3 eft2 Δ:TRP1 pURA3-<i>eft1-P580H</i></i>	Strain isogenic to JD1696 expressing <i>eEF2-P580H</i> allele on a plasmid, for frameshifting and steady state assays
JD1698	<i>MATa ade2 Δ lys2 Δ ura3 Δ his3 Δ leu2 Δ trp1 Δ eft1Δ:HIS3 eft2 Δ:TRP1 pURA3-<i>eft1-H699Q</i></i>	Strain isogenic to JD1696 expressing <i>eEF2-H699Q</i> allele on a plasmid, for frameshifting and steady state assays

Table 4. Yeast strains used in chapters 2 and 3.

Appendix 2: Yeast based plasmids

Plasmid Name	Backbone Plasmid	Description
pJD375	pRS316	Dual luciferase cassette in pRS316, genomic context
pJD376	pJD375	LA frameshift signal sequence inserted in dual luciferase reporter, viral context
pJD521	pJD375	EST2 PRF sequence at 1653 inserted in dual luciferase reporter, viral context
pJD1017	pJD375	EST2 PRF sequence at 72 inserted in dual luciferase reporter, viral context
pJD1018	pJD375	EST2 PRF sequence at 1215 inserted in dual luciferase reporter, viral context
pJD1019	pJD375	EST2 PRF sequence at 1326 inserted in dual luciferase reporter, viral context
pJD1020	pJD375	EST2 PRF sequence at 1920 inserted in dual luciferase reporter, viral context
pJD1038	pJD375	STN1 PRF sequence at 885 inserted in dual luciferase reporter, viral context
pJD1039	pJD375	STN1 PRF sequence at 1203 inserted in dual luciferase reporter, viral context
pJD1040	pJD375	EST1 PRF sequence at 885 inserted in dual luciferase reporter, viral context
pJD1042	pJD375	EST1 PRF sequence at 1272 inserted in dual luciferase reporter, viral context
pJD1043	pJD375	EST1 PRF sequence at 1920 inserted in dual luciferase reporter, viral context
pJD1803	pJD375	CDC13 PRF sequence at 1272 inserted in dual luciferase reporter, viral context
pJD753	pJD0741	Readthrough containing small amounts of Renilla and Firefly in PGK1 reporter
pJD828	pJD753	Premature termination codon in PGK1 reporter
pJD754	pJD753	EST2 PRF sequence at 1653 inserted in PGK1 reporter
pJD766	pJD753	EST2 PRF sequence at 1215 inserted in PGK1 reporter
pJD1071	pJD753	EST2 PRF sequence at 1326 inserted in PGK1 reporter
pJD1074	pJD753	STN1 PRF sequence at 1203 inserted in PGK1 reporter
pJD1076	pJD753	EST1 PRF sequence at 1272 inserted in PGK1 reporter
pJD1804	pJD753	CDC13PRF sequence at 1272 inserted in PGK1 reporter
pJD0808	pJD521	EST2 PRF sequence at 1653 inserted in dual luciferase reporter, viral context, mutated slip site
pJD1805	pJD1018	EST2 PRF sequence at 1215 inserted in dual luciferase reporter, viral context, mutated slip site
pJD1806	pJD1019	EST2 PRF sequence at 1326 inserted in dual luciferase reporter, viral context, mutated slip site
pJD1807	pJD1039	STN1 PRF sequence at 1203 inserted in dual luciferase reporter, viral context, mutated slip site
pJD1808	pJD1041	EST1 PRF sequence at 1272 inserted in dual luciferase reporter, viral context, mutated slip site
pJD1809	pJD1043	EST1 PRF sequence at 1920 inserted in dual luciferase

		reporter, viral context, mutated slip site
pJD641	pJD638	Full length EST2 low copy plasmid
pJD796	pJD641	Mutated full length EST2 low copy plasmid
pJD972(T7)	pTNT	Yeast telomeric sequence under T7 promoter control
pJD972(M13)	pBC6	Yeast telomeric sequence flanked by M13
pJD985	pJD641	Full length EST2 low copy plasmid with mutations to the positions 72,1215,1326,1653 PRF sequence
pJD1048	pRS313	CBF5 wild-type in pRS313 (a,l)
pJD1049	pRS313	CBF5 D95A in pRS313 (a,l)

Table 5. Yeast based plasmids used in chapters 2 and 3.

Appendix 3: Mammalian plasmids

Plasmid Name	Backbone Plasmid	Description
pJD0175f	P2luci (206)	pJD175f is identical to p2luci
pJD0187	P2luci	Insertion of the HIV-1 PRF signal into the dual luciferase plasmid
pJD0827	pJD175e	Insertion of the <i>CCR5</i> PRF signal into the dual luciferase plasmid
pJD0835	pJD175e	Insertion of the <i>homo sapiens IL7α</i> PRF signal into the dual luciferase plasmid
pJD1525	pJD175f	Dual luciferase vector with an in-frame UAA codon after <i>Renilla</i> .
pJD1526	pJD175f	Dual luciferase vector with an in-frame UAG codon after <i>Renilla</i> .
pJD1527	pJD175f	Dual luciferase vector with an in-frame UGA codon after <i>Renilla</i> .
pJD1800	pJD175f	Insertion of the <i>IL2Rγ</i> PRF signal into the dual luciferase plasmid
pJD1529	pJD175f	Insertion of the eIF2B3 PRF signal into the dual luciferase plasmid
pJD1530	pJD175f	Insertion of the RASA4 PRF signal into the dual luciferase plasmid
pJD1532	pJD175f	Insertion of the PARP1 PRF signal into the dual luciferase plasmid
pJD1533	pJD175f	Insertion of the TERF2 PRF signal into the dual luciferase plasmid
pJD1534	pJD175f	Insertion of the TERF2IP PRF signal into the dual luciferase plasmid
pJD1535	pJD175f	Insertion of the SMG6 PRF signal into the dual luciferase plasmid
pJD1536	pJD175f	Insertion of the IPO11 PRF signal into the dual luciferase plasmid
pJD1537	pJD175f	Insertion of the <i>eIF5B</i> PRF signal into the dual luciferase plasmid
pJD1538	pJD175f	Insertion of the ATG7 PRF signal into the dual luciferase plasmid
pJD1539	pJD175f	Insertion of the SelL PRF signal into the dual luciferase plasmid
pJD1540	pJD175f	Insertion of the <i>COL8A1</i> PRF signal into the dual luciferase plasmid
pJD1541	pJD175f	Insertion of the RBBP4 PRF signal into the dual luciferase plasmid
pJD1542	pJD175f	Insertion of the MTAP PRF signal into the dual luciferase plasmid
pJD1543	pJD175f	Insertion of the RET PRF signal into the dual luciferase plasmid

pJD1544	pJD175f	Insertion of the PKHD1 PRF signal into the dual luciferase plasmid
pJD1545	pJD175f	Insertion of the PDCD7 PRF signal into the dual luciferase plasmid
pJD1546	pJD175f	Insertion of the ARRB1 PRF signal into the dual luciferase plasmid

Table 6. Mammalian plasmids used in the study.

Appendix 4: Oligonucleotides for Cloning

Oligo name	Clone	Sequence
YLR318W, forward	pJD521	5'TCGACAAAAAATCAAATGGGTTTTTCGTTAGATCT CAATATTTCTTCAATACCAATACAGGTGTATTGAAGT TATTTAATGTTGTTAACGCTG3'
YLR318W, reverse	pJD521	5'GATCCAGCGTTAACAACATTAATAACTTCAATAC ACCTGTATTGGTATTGAAGAAATATTGAGATCTAAC GAAAAACCCATTGATTTTTTG3'
EST2 PRF1	pJD659	5'CCCATTTTCGTTCTTCAGGGCATCCTTGAG3'
EST2 PRF2	pJD660	5'GATACTTGAATAAACTTATCACTCCATTCATCGT AGAATATTTTAAGACG3'
EST2 PRF3	pJD661	5'GCAAAATGAGGATTATACCTAAGAAGAGTAATAA TGAGTTCAGG3'
EST2 PRF4	pJD662	5'GAGGATACTCAAGGATGCGCTGAAGAACGAAAAT GGG3'
EST2 PRF5	pJD667	5'GCCAGTCCTAGCCAGGACACATTAATATTGAAGCT GGCTGACGATTTCC3'
GC - EST2 PRF1	pJD659	5'CGAGGCCATTGAAGTGACCACACTTCAAGTTCTCT TTGTAAGTACTGTTGG3'
GC - EST2 PRF2	pJD660	5'CGTCTTAAAATATTCTACGATGAATGGAGTGATAA GTTTATTCCAAGTATC3'
GC - EST2 PRF3	pJD661	5'CCTGAACTCATTATTACTCTTCTTAGGTATAATCCT CATTTTGC3'
GC - EST2 PRF4	pJD662	5'CCCATTTTCGTTCTTCAGCGCATCCTTGAGTATCCT C3'
GC - EST2 PRF5	pJD667	5'GGAAATCGTCAGCCAGCTTCAATATTAATGTGTCC TGGCTAGGACTGGC3'
LEFT KPN1 DLR	pJD753	5'CCCCGGTACCTCGTTCGTTGAGCGAGTTC3'
RIGHT KPN1 DLR	pJD753	5'CCCCGGTACCGGCGTCTTCCATGAGCTC3'
left DLR MCS KPN1 Amp.	pJD753 based	5'CCCCGGTACCTCGTTCGTTGAGCGAGTTC3'
right DLR MCS KPN1 Amp.	pJD753 based	5'CCCCGGTACCGGCGTCTTCCATGAGCTC3'
EST2 CDS Left	pJD641	5'CCCCGGATCCCTGATTTATACTCATGAAAATCTTAT TCG3'
EST2 CDS Right	pJD641	5'CCCCCTGCAGTCCTTATCAGCATCATAAGC3'
est2-72 fwd- cloning	pJD1017	5'AAAAGTCGACCATTGATCTACAGACCAACAGTACT TACAAAG3'
est2-72 rev- cloning	pJD1017	5'AAAAGGATCCGCCAAATGTTAGTACGTTGTTGTAT AATTCG3'
est2-1215 fwd-cloning	pJD1018	5'AAAAGTCGACTTACTTTAGACATGATACTTGGAAAT AAACTTATCA3'
est2-1215	pJD1018	5'AAAAGGATCCTGTGAATTCTTCTTCGTCTGCC3'

rev-cloning		
est2-1326 fwd-cloning	pJD1019	5'AAAAGTCGACGTTGTCCAATTTCAATCATAGCAAA ATGAGG3'
est2-1326 rev-cloning	pJD1019	5'AAAAGGATCCTATTTGCGTTGGAGAATATATTTTA GTAAAACACTAGTCG3'
est2-1995 fwd-cloning	pJD1020	5'AAAAGTCGACTTATAGCGAGTTTAAAGCCAGTCCT AGC3'
est2-1995 rev-cloning	pJD1020	5'AAAAGGATCCTATGTGCATTGCACAAAATTGAATA ACCG3'
clone_5p stn1_885	pJD1000	5'AAAAGTCGACTGATCAAATTGACAACGGCAATGA CG3'
clone_3p stn1_885	pJD1000	5'AAAAGGATCCCGATGCTAAGCTAGTTACTACGCTG CGTACTTCC3'
clone_5p stn1_1203	pJD1001	5'AAAGTCGACATTA AAAAGATAAAAACAAGTGAGACA TTTGATTTGCTTCC3'
clone_3p stn1_1203	pJD1001	5'AAAAGGATCCCCACCAATTTTTTAGTACCTCAGGA TACTGTTTCTTTGTCC3'
clone_5p est1_1203	pJD1002	5'AAAAGTCGACCAAATATGCAGATTTGAGTGAGCGC CAGG3'
clone_3p est1_1203	pJD1002	5'AAAAGGATCCGCTATATATATTTTCTGAACAATTC AGTGGACTATTTATCAAGTCG3'
clone_5p est1_1272	pJD1003	5'AAAAGTCGACGACGTCGTCATCAAACCTCCTGGC 3'
clone_3p est1_1272	pJD1003	5'AAAAGGATCCCCTGAAAATAATATCTTCTCTAAAA AGATAGCTTCTTTTCGG3'
clone_5p est1_1920	pJD1004	5'AAAAGTCGACGACAGA ACTGGAAAAACAATTTGC AAATGTCCGG3'
clone_3p est1_1920	pJD1004	5'AAAAGGATCCTGGCACTTGGACGGTGATGTCCTC3'
clone_5p cdc13_1272	pJD1005	5'AAAAGTCGACGAGATCGTTATCCCGACGAGAGAG CGAATCTGTGAGC3'
clone_3p cdc13_1272	pJD1005	5'AAAAGGATCCGGGGTCTTTCCTTGCCATTTGCTCA TCC3'

Table 7. Oligos used for cloning.

Appendix 5: Oligonucleotides for Site-Directed Mutagenesis

Oligo name	Template	Sequence
SDM_3p est2 pos72 del1bp	pJD1017	5'CGAGGCCATTGAAGTGACCACTTTTAAATTTTCTTT GTAAGTAC3'
SDM_3p est2 pos1215 del1bp	pJD1018	5'CGTCTTAAAATATTCTACGAAAAAGGGTGATAAG TTTATTCC3'
SDM_3p est2 pos1326 del1bp	pJD1019	5'CCTGAACTCATTATTCTTTTTTTTTGGTATAATCCTC ATTTTGC3'
SDM_3p est2 pos1995 del1bp	pJD1020	5'GGAAATCGTCAGCCATTTTAAAATTAATGTGTCCT GGC3'
est1 1203 minus1bp	pJD1040	5'GAGTGAGCGCCAGGTTTTTTTTTTAGATTGAGCTTT GATTTTATTGC3'
est1 1272 minus1bp	pJD1041	5'CCCTCCTGGCAAAAAACAGGAAGACTTTCGATAT CTAGCC3'
est1 1920 minus1bp	pJD1043	5'GCAAATGTCCGGAGAACAAAAAATGTCTCCGCTC CCAGAAAAAGATGG3'
CDC13_DL_ SDM1_Fwd	pJD1005	5'CTCAAAAATGAACAAATGTTCGACGATCGTTATCCC GACGA3'
CDC13_DL_ SDM1_Rev	pJD1005	5'GGGATAACGATCGTCGACATTTGTTCATTTTTGAG AACTCG3'
CDC13_DL_ SDM2_Fwd	pJD1005	5'CTTCGGTGTTTTAAACCATGTCAAAGCGACAAGA3'
CDC13_DL_ SDM2_Rev	pJD1005	5'CGCTTTGACATGGTTTTAAAACACCGAAGAGCTCA3'
pJD521 SS_F	pJD0808	5'CAAATGTCGACGAAGAACCAAATGGGTTTTTCGTT AGATCTC3'
pJD521 SS_R	pJD0808	5'GAGATCTAACGAAAAACCCATTTGGTTCTTCGTCC ACATTTG3'
Est2_PRF@1 215_ssMut_f w	pJD1809	5'AAACTTATCACTCCATTCTCGTAGAATATTTAAGA CG3'
Est2_PRF@1 215_ssMut_r e	pJD1809	5'CGACTAAGTACGTCTTAAAATATTCTACGAGAATG GAGTGATAAG3'
stn1@1203_ DLssMut_Fw d	pJD1807	5'GATTTGCTTCCTCGAAGAACTTTTTGAATATGCTG 3'
stn1@1203_ DLssMut_Rev	pJD1807	5'TCAAAAAAGTTCTTCGAGGAAGCAAATCAAATGTC TC3'
est1@1272_ DLssMut_Fw d	pJD1808	5'ACCCTCCTGGCAAAGAAAAATGGAAGACTTTCGAT ATCTAG3'
est1@1272_ DLssMut_Rev	pJD1808	5'CGAAAGTCTTCATTTTCTTTGCCAGGAGGGTTG ATGAC3'

est1@1920_ DLssMut_Fw d	pJD1809	5'ATGTCCGGAGAAGAACAAGATGTCTCCGCTCC3'
est1@1920_ DLssMut_Re v	pJD1809	5'AGCGGAGACATCTTCTTGTCTCCGGACATTTGCA 3'
cdc13@1272 DLssMut_Fw	pJD1005	5'CGGTGTCTTCAACCATGTCAAAGCGACAAGA3'
cdc13@1272 DLssMut_Re v	pJD1005	5'CGCTTTGACATGGTTGAAGACACCGAAGAGCTC3'

Table 8. Oligos used for site-directed mutagenesis.

Appendix 6: Oligonucleotides used for qPCR.

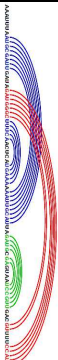
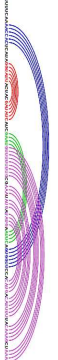
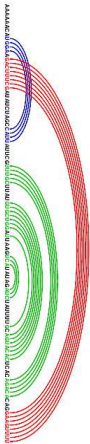
Name	Template	Sequence
yEST2 qPCR Fwd	Yeast cDNA	5'TGGTCGGTACATACGCATTC3'
yEST2 qPCR Rev	Yeast cDNA	5'CGGCAGATGAGGTTTCGTTAC3'
yEST1 qPCR Fwd	Yeast cDNA	5'ATTCCGTGATACCATTGGTTC3'
yEST1 qPCR Rev	Yeast cDNA	5'CTTTCTTCTGTTACTTAGTCGCA3'
ySTN1 qPCR Fwd	Yeast cDNA	5'ACAGCAAATACACCTTATTGGC3'
ySTN1 qPCR Rev	Yeast cDNA	5'ACCAATGAAGAGTCTGAAGTACA3'
yCDC13 qPCR Fwd	Yeast cDNA	5'TGGTAAGTGTGATAAGCAC3'
yCDC13 qPCR Rev	Yeast cDNA	5'AGATATCCACAAGTGAGTTGT3'
yPGK1- DLR qPCR Rev	Exogenous PGK1	5'GTTTCGTTGAGCGAGTTCTCA3'
yPGK1- DLR qPCR Fwd	Exogenous PGK1	5'GGTACCGGCGTCTTCCAT3'
U3 Forward	Yeast cDNA	5'TCCAACCTTGGTTGATGAGTCC3'
U3 Reverse	Yeast cDNA	5'CGAACCGCTAAGGATTGC3'
yCCR4 qPCR Fwd	Yeast cDNA	5' AGCAATCTCACATTGCAGAAGC 3'
yCCR4 qPCR Rev	Yeast cDNA	5' CGTAGGTTGTTGTTTCTTTGCT 3'
yGCN4 qPCR Fwd	Yeast cDNA	5' ACATTCCAGTTACCACTGACGATGT 3'
yGCN4 qPCR Rev	Yeast cDNA	5' GGG TAAGAATGAAGTTGTCGAGACTTC 3'
yTel Fwd	Yeast gDNA	5'CAGTGGTGTGGGTGTGCATGGTGGTGTGGGTGTGT GG 3'
yTel Rev	Yeast gDNA	5'GCCACAACCACACCCAACACATCCCACACCACC AC 3'
Gapdh 5p_qper forward	Human cDNA	TCGGAGTCAACGGATTTGGTTCG
Gapdh 5p qper_reverse	Human cDNA	TAAACCATGTAGTTGAGGTCAATGAAGG
Gapdh 3p qper_forwar d	Human cDNA	AAGCTCATTTCTGGTATGACAACG

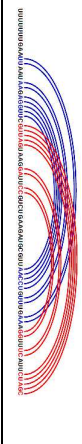
Gapdh 3p qpcr reverse	Human cDNA	TCTTCCTCTTGTGCTCTTGCTGG
hDKC1 qPCR Fwd	Human cDNA	5' CAAGATTATGCTTCCAGGTGTTCTT 3'
hDKC1 qPCR Rev	Human cDNA	5' TGTGGTCATTAATGCAATAGCCATG 3'

Table 9. Oligos used for qPCR in this study.

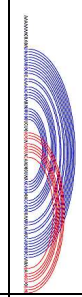
Appendix 7: Phylogenetic analysis of predicted -1 PRF signals in ORFs involved in yeast telomere maintenance

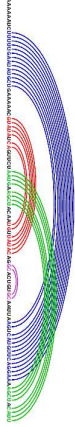

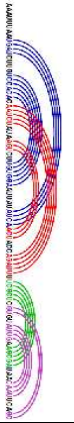
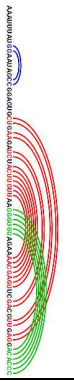
EST1 -1 PRF signals in *Saccharomyces* species

<i>S. cerevisiae</i>	Yeast species	Slippery site location of similar frameshift signal	Slippery site	Predicted MFE (Minimum Free Energy) Kcal/mol	Predicted pseudoknot structure
EST1 -1 PRF signal @ 1272	<i>Saccharomyces paradoxus</i>	480	AAAUUUA	-12.75	
Slippery Site: AAAAAA U MFE: -20.8 Kcal/mol	<i>Saccharomyces bayanus</i>	378	UUUUUUC	-19.7	
	<i>Saccharomyces castellii</i> No predicted -1 PRF	NA	-	-	-
EST1 -1 PRF signal @ 1920 Slippery	<i>Saccharomyces kluyveri</i> No predicted -1 PRF	NA	-	-	-


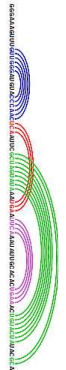
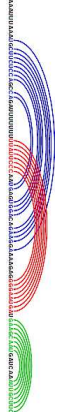

Site: AAAAAA A MFE: -21.2 Kcal/mol	<i>Saccharomyces kudriavzevii</i> No predicted -1 PRF	NA	-	-	-
	<i>Saccharomyces mikatae</i>	774	UUUUUUU	-17.7	

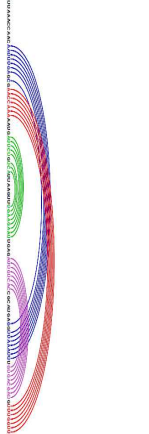
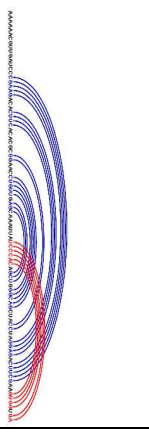
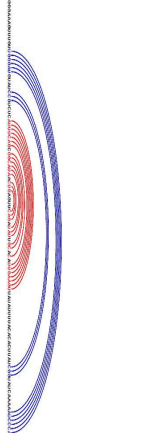
STN1 -1 PRF signals in *Saccharomyces* species

<i>S. cerevisiae</i>	Yeast species	Slippery site location of similar frameshifting signal	Slippery site	Predicted MFE (Minimum Free Energy) Kcal/mol	Predicted pseudoknot structure
STN1 -1 PRF signal @ 1203 Slippery Site: AAAAAAU MFE: -20.08 Kcal/mol	<i>Saccharomyces paradoxus</i>	1203	AAAAAAA	-19.7	
	<i>Saccharomyces bayanus</i>	1071	AAAUUUA	-20.7	

					
	<i>Saccharomyces castellii</i>	939	AAAUUUA	-19	
	<i>Saccharomyces kluyveri</i>	723	AAAUUUA	-19	
	<i>Saccharomyces kudriavzevii</i> No predicted -1 PRF	NA	-	-	-
	<i>Saccharomyces mikatae</i> No predicted -1 PRF	NA	-	-	-

CDC13 -1 PRF signals in *Saccharomyces* species

<i>S. cerevisiae</i> CDC13 -1 PRF signal @ 1272	Yeast species	Slippery site location of similar frameshifting signal	Slippery site	Predicted MFE (Minimum Free Energy) Kcal/mol	Predicted pseudokno t structure
Slippery Site: UUUAAAC MFE: -21.3 Kcal/mol 	<i>Saccharomyce s paradoxus</i>	1092	GGGAAA G	-13.49	
	<i>Saccharomyce s banayus</i> No predicted - 1 PRF	NA	-	-	-
	<i>Saccharomyce s castellii</i>	972	AAAUUU A	-26.6	
		975	UUUAAA U	-17.9	

		1389	UUUAAA C	-21.2	
	<i>Saccharomyces kluyveri</i>	2421	AAAAAA C	-24.5	
	<i>Saccharomyces kudriavzevii</i> No predicted - 1 PRF	NA	-	-	-
	<i>Saccharomyces mikatae</i>	1080	GGGAAA G	-18.55	
		1266	UUUAAA C	-17.42	

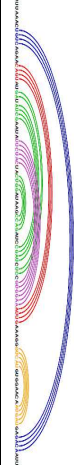
					
--	--	--	--	--	---

Table 10. Phylogenetic analysis of predicted -1 PRF signals in ORFs involved in yeast telomere maintenance.

The orthologs of *EST1*, *STN1* and *CDC13* from *Saccharomyces cerevisiae*, *S. paradoxus*, *S. mikatae*, *S. bayanus*, *S. castellii*, *S. kudriavzevii* and *S. kluyveri* were queried for -1 PRF signals. The information in this table includes each slippery site, its location, predicted downstream mRNA pseudoknot secondary structures and their predicted Minimum Free Energies (MFE) as obtained from PRFdb (<http://prfdb.umd.edu/>). The sequences were queried for the potential - 1 PRF signals as described in ^[1]. Similar analysis for *EST2* is described in^[2]. Slippery site locations are hyperlinked to URLs for all potential folding solutions for each potential -1 PRF signal (186).

Appendix 8: RNAi Oligonucleotides

Name	Sequence
hEIF2C1 (argonaute 1)	Target: 5' TA GTC TTA ACA TAA AGC CGA A 3' Sense: 5' GUC UUA ACA UAA AGC CGA Att 3' Anti: 3' at CAG AAU UGU AUU UCG GCU U 5'
hRENT1 (UPF1)	Target: 5' CA CCA TGA GCG TGG AGG CGT A 3' Sense: 5' CCA UGA GCG UGG AGG CGU Att 3' Anti: 3' gt GGU ACU CGC ACC UCC GCA U 5'
Scrambled	Target: 5' AAT TCT CCG AAC GTG TCA CGT 3' Sense: 5' UUC UCC GAA CGU GUC ACG Utt 3' Anti: 3' ACG UGA CAC GUU CGG AGA Att 5'

Table 11. RNAi oligonucleotides used in this study.

The siRNA oligonucleotides include both sense and anti-sense RNA strands with two base pair DNA overhangs.

Appendix 9: Additional validated -1 PRF signals in Humans

	Gene name	Annotation	Position	% -1 PRF (\pm error)
pJD1536	IPO11	Importin 11	898	2.46% \pm 0.14%
pJD1538	ATG7	Autophagy related 7	80	10.45% \pm .42%
pJD1539	SelL	Selectin L	753	0.89% \pm 0.03%
pJD1540	COL8A1	Collagen, type VIII, alpha 1	1710	2.88% \pm 0.34%
pJD1541	RBBP4	Retinoblastoma Binding Protein 4	725	1.95% \pm 0.21%
pJD1542	MTAP	Methylthioadenosine Phosphorylase	245	0.63% \pm 0.03%
pJD1543	RET	Ret proto-oncogene	3024	3.31% \pm 0.67%
pJD1544	PKHD1	Polycystic Kidney and Hepatic Disease 1	9387	5.82% \pm 0.14%
pJD1545	PDCD7	Programmed Cell Death 7	193	6.45% \pm 0.59%
pJD1529	eIF2B3	eukaryotic translation initiation factor 2B, subunit 3 gamma	541	2.34% \pm 0.41%
pJD1530	RASA2	RAS p21 protein Activator 4	3024	1.41% \pm 0.11%
pJD1532	PARP1	poly (ADP-ribose) polymerase family, member 1	654	1.48% \pm 0.33%
pJD1546	ARRB1	arrestin, beta 1, transcript variant 1, mRNA	143	4.19% \pm 0.85%

Table 12. Additional validated -1 PRF signals in Humans.

Computationally identified putative -1 PRF signals were cloned in the dual luciferase reporter and -1 PRF efficiencies were assayed in HeLa cells. These frameshift signals were cloned by undergraduate students Tyler Thrasher, Yousuf Khan, Kristen Langan, Avan Anita and Swaksha Raichura. The errors denoted SEM (n=2).

Appendix 10: Summary of the additional validated -1 PRF signals in Humans

Importin 11 (IPO11) – It belongs to the karyopherin/importin-beta family that are receptors involved in nucleocytoplasmic transport (207). Its function by docking the importin/substrate complex to the nuclear pore complex (NPC) and transport is achieved by Ran-dependent mechanism (208). It is involved in transport of large subunit (LSU) ribosomal protein L12.

Autophagy related (factor) 7 (ATG7) - E1-like activating enzyme required for cytoplasm to vacuole transport and autophagy (209). Association of ATG7 with ATG12 (Autophagy related (factor) 12) activates the ATG8 family proteins required for autophagy by inhibition of caspase-8 (210)(211).

Selectin L (SELL) – It belongs to the family of adhesion/homing receptors (212). The protein has C-type lectin-like and calcium-binding epidermal growth factor-like domains (213)(214) . It facilitates the adhesion of leucocytes on endothelial cells. A SNP in the SELL gene is associated with immunoglobulin A nephropathy (215).

Collagen, Type VIII, Alpha (COL8A) - It's a major component of the sub endothelial Descemet's membrane and endothelia of blood vessels (216). It is involved in the smooth muscle cell migration and proliferation, thus playing an important role atherogenesis (216). Diseases associated with COL8A include posterior polymorphous corneal dystrophy and fuchs' endothelial dystrophy (217)(218).

Retinoblastoma Binding Protein 4 (RBBP4) – It is a component of many complexes that include chromatin assembly factor 1 (CAF-1) complex, the histone deacetylase (HDAC) complex, the nucleosome remodeling and histone deacetylase (NuRD) complex (219)(220) . All these complexes are important for chromatin homeostasis. Diseases associated with RBBP4 include retinoblastoma and intermediate charcot-marie-tooth neuropathy (221)(222)(223).

Methylthioadenosine Phosphorylase (MTAP) – It is involved in the breakdown of catalyzes the phosphorylation of S-methyl-5'-thioadenosine (MTA) by catalyzing the phosphorylation of MTA to adenine and 5-methylthioribose-1-phosphate (224). MTA is a major by product polyamine biosynthesis. Diseases associated with MTAP include diaphyseal medullary stenosis with malignant fibrous histiocytoma, and acute lymphoblastic leukemia (225)(226)(227).

Ret Proto-Oncogene (RET) – It is a member of the cadherin superfamily and encodes for receptor tyrosine kinase involved in cell migration, proliferation and differentiation (228). It also plays a major role in neuronal navigation(228). Diseases associated with RET include familial papillary thyroid carcinoma, Central hypoventilation syndrome, congenital, renal agenesis and lichen amyloidosis (229)(230).

Polycystic Kidney And Hepatic Disease 1 (PKHD1) – It is a transmembrane protein involved in tubulogenesis during cell division (231)(232). Mutations

in PKHD1 result in autosomal recessive polycystic kidney disease, also known as polycystic kidney and hepatic disease-1 (233).

Programmed Cell Death 7 (PDCD7) – It is a component of the U12 spliceosome complex and overexpression leads to cell apoptosis(234)(235). Its expression is selectively regulated during the apoptosis of T-cell thymoma cells (236).

Eukaryotic translation initiation factor 2B, subunit 3 gamma (eIF2B3) - It is one of the subunits of eukaryotic initiation factor 2B which catalyzes the exchange of eukaryotic initiation factor 2-bound GDP for GTP (237). Diseases associated with EIF2B3 include eif2b3-related childhood ataxia with central nervous system hypomyelination/vanishing white matter and childhood ataxia with central nervous system hypomyelination/vanishing white matter (238)(239).

RAS p21 Protein Activator 2 (RASA2) – It belongs to the family of the GTP-ase activating proteins and it stimulates the GTPase activity if the RAS p21 acting as a suppressor of the RAS function(240)(241). RASA2 is associated neurofibromatosis (242).

Poly (ADP-ribose) polymerase family, member 1 (PARP1) – It is involved in the poly-ADP-ribosylation of multiple nuclear proteins. It plays an important role in cell division, proliferation, DNA damage repair and tumor formation (243)(244) . PARP1 is associated with squamous cell carcinoma (245).

Arrestin Beta 1 (ARRB1) – It's a member of the beta-arrestin protein family and involved in the agonist-mediated desensitization of G-protein-coupled receptors (246)(247). Recently it has been identified as a cofactor in the beta-adrenergic receptor kinase (BARK) mediated desensitization of beta-adrenergic receptors.

Appendix 11: Human -1 PRF being cloned by the FIRE class

ORF	Gene annotation	Position	Slippery site
eIF4G	eukaryotic translation initiation factor 4 gamma	3806	GGGAAAA
eIF4G	eukaryotic translation initiation factor 4 gamma	1347	CCCUUUG
eIF5B	eukaryotic translation initiation factor 5B	3637	AAAAAAA
eIF5B	eukaryotic translation initiation factor 5B	2242	AAAUUUU
eIF4B	eukaryotic translation initiation factor 4B	1811	CCCAAAA
EIF3E	eukaryotic translation initiation factor 3 E	480	UUUUUUU
EIF2AK4	eukaryotic translation initiation factor 2 alpha kinase 4	326	AAAAAAU
CHST14	carbohydrate (N-acetylgalactosamine 4-0) sulfotransferase 14	233	CCCAAU
EBF1	early B-cell factor 1	908	GGGAAAC
PDZD2	PDZ domain containing 2	6880	GGGAAAA
PTPN11	Homo sapiens protein tyrosine phosphatase, non-receptor type 11 (Noonan syndrome 1)	227	CCCAAU
WASL	Wiskott-Aldrich syndrome-like	1544	AAAAAAA
ZFH3	Zinc finger homeobox protein 3	5694	CCCUUUC
MAP4K3	mitogen-activated protein kinase kinase kinase kinase 3	527	CCCAAU
MAP4K3	mitogen-activated protein kinase kinase kinase kinase 3	2459	CCCUUUA
MAP4K5	mitogen-activated protein kinase kinase kinase	1151	CCCAAAA

	kinase 5		
EIF1A	eukaryotic translation initiation factor 1A	406	AAAAAAG
RASIP1	Pas interacting protein 1	2235	CCCUUUC
BCL9	B-cell CLL/lymphoma 9	2603	CCCAAAC
BCL9	B-cell CLL/lymphoma 9	2549	AAAUUUU
BCL9	B-cell CLL/lymphoma 9	4247	GGGUUUC
CDH16	cadherin 16	928	GGGAAAC
CDH16	cadherin 16	178	AAAUUUC
ABL1	tyrosine-protein kinase ABL1	951	CCCAAAG
CDH13	cadherin-13	477	GGGAAAC
BAG3	BCL2-associated athanogene 3	1259	CCCAAAA
BAG3	BCL2-associated athanogene 3	338	CCCUUUC
BCL2L11	BCL2-like 11	483	CCCUUUU
GATA5	GATA binding protein 5	341	CCCUUUC
FOXJ2	forkhead box J2	2129	GGGAAAG
FOXI3	forkhead box I3	1152	CCCUUUC
FOXL1	forkhead box L1	1019	GGGAAAG
BMP5	bone morphogenetic protein 5	748	GGGUUUC
GPR31	G protein-coupled receptor 31	9	CCCAAAC
AEN	interferon stimulated exonuclease gene 20kDa-like 1	740	CCCAAAC
SLC52A1	G protein-coupled receptor 172B	844	GGGAAAC
GRK 4	G protein-coupled receptor kinase 4	1847	CCCUUUC

Table 13. Additional -1 PRF signals being cloned by the FIRE class.

Computationally identified potential -1 PRF signals mentioned in the table above are being cloned in the dual luciferase reporter by the First-Year Innovative and Research Experience (FIRE) stream – Found in Translation (FIT). -1 PRF efficiencies of the successful cloned sequences assayed in HeLa cells by dual luciferase assays during the Fall2015 semester

References

1. Dinman JD. Control of gene expression by translational recoding. *Adv Protein Chem Struct Biol* [Internet]. 2012 Jan [cited 2015 Mar 5];86:129–49. Available from: <http://www.sciencedirect.com/science/article/pii/B9780123864970000049>
2. Dinman JD. Mechanisms and implications of programmed translational frameshifting. *Wiley Interdiscip Rev RNA* [Internet]. Jan [cited 2015 Mar 4];3(5):661–73. Available from: <http://www.pubmedcentral.nih.gov/articlerender.fcgi?artid=3419312&tool=pmcentrez&rendertype=abstract>
3. Atkins J, Gesteland R, Dinman JD, Connor MO, Farabaugh PJ. Recoding: expansion of decoding rules enriches gene expression. *Nucleic Acids Mol Biol* [Internet]. 2010;24:221–47. Available from: <http://link.springer.com/10.1007/978-0-387-89382-2>
<http://www.springerlink.com/index/10.1007/978-0-387-89382-2>
4. Drummond DA, Wilke CO. The evolutionary consequences of erroneous protein synthesis. *Nat Rev Genet* [Internet]. Nature Publishing Group; 2009 Oct [cited 2014 Dec 25];10(10):715–24. Available from: <http://dx.doi.org/10.1038/nrg2662>
5. De Keersmaecker K, Sulima SO, Dinman JD. Ribosomopathies and the paradox of cellular hypo- to hyperproliferation. *Blood* [Internet]. American Society of Hematology; 2015 Jan 9 [cited 2015 Jan 29];125(9):1377–82. Available from: <http://www.bloodjournal.org/content/early/2015/01/09/blood-2014-10-569616.abstract>
6. Nevins JR. The pathway of eukaryotic mRNA formation. *Annu Rev Biochem* [Internet]. Annual Reviews 4139 El Camino Way, P.O. Box 10139, Palo Alto, CA 94303-0139, USA; 1983 Jan 28 [cited 2015 Mar 6];52:441–66. Available from: <http://www.annualreviews.org/doi/abs/10.1146/annurev.bi.52.070183.002301>
7. Sonenberg N. Cap-binding proteins of eukaryotic messenger RNA: functions in initiation and control of translation. *Prog Nucleic Acid Res Mol Biol* [Internet]. 1988 Jan [cited 2015 Mar 6];35:173–207. Available from: <http://www.ncbi.nlm.nih.gov/pubmed/3065823>
8. Hinnebusch AG. The scanning mechanism of eukaryotic translation initiation. *Annu Rev Biochem* [Internet]. Annual Reviews; 2014 Jan 6 [cited 2015 Mar 6];83:779–812. Available from:

<http://www.annualreviews.org/doi/abs/10.1146/annurev-biochem-060713-035802>

9. Jackson RJ, Hellen CUT, Pestova T V. The mechanism of eukaryotic translation initiation and principles of its regulation. *Nat Rev Mol Cell Biol* [Internet]. Nature Publishing Group; 2010 Feb [cited 2014 Jul 10];11(2):113–27. Available from: <http://dx.doi.org/10.1038/nrm2838>
10. Rodnina M V, Wintermeyer W. Fidelity of aminoacyl-tRNA selection on the ribosome: kinetic and structural mechanisms. *Annu Rev Biochem* [Internet]. Annual Reviews 4139 El Camino Way, P.O. Box 10139, Palo Alto, CA 94303-0139, USA; 2001 Jan 28 [cited 2015 Jan 19];70:415–35. Available from: <http://www.annualreviews.org/doi/abs/10.1146/annurev.biochem.70.1.415>
11. Valle M, Sengupta J, Swami NK, Grassucci RA, Burkhardt N, Nierhaus KH, et al. Cryo-EM reveals an active role for aminoacyl-tRNA in the accommodation process. *EMBO J* [Internet]. 2002 Jul 1 [cited 2015 Mar 9];21(13):3557–67. Available from: <http://www.pubmedcentral.nih.gov/articlerender.fcgi?artid=126079&tool=pmc-entrez&rendertype=abstract>
12. Pape T, Wintermeyer W, Rodnina M V. Complete kinetic mechanism of elongation factor Tu-dependent binding of aminoacyl-tRNA to the A site of the *E. coli* ribosome. *EMBO J* [Internet]. 1998 Dec 15 [cited 2015 Feb 15];17(24):7490–7. Available from: <http://www.pubmedcentral.nih.gov/articlerender.fcgi?artid=1171092&tool=pm-centrez&rendertype=abstract>
13. Schuette J-C, Murphy F V, Kelley AC, Weir JR, Giesebrecht J, Connell SR, et al. GTPase activation of elongation factor EF-Tu by the ribosome during decoding. *EMBO J* [Internet]. 2009 Mar 18 [cited 2015 Mar 9];28(6):755–65. Available from: <http://www.pubmedcentral.nih.gov/articlerender.fcgi?artid=2666022&tool=pm-centrez&rendertype=abstract>
14. Kapp LD, Lorsch JR. The molecular mechanics of eukaryotic translation. *Annu Rev Biochem* [Internet]. Annual Reviews 4139 El Camino Way, P.O. Box 10139, Palo Alto, CA 94303-0139, USA; 2004 Jan 9 [cited 2015 Feb 20];73:657–704. Available from: <http://www.annualreviews.org/doi/abs/10.1146/annurev.biochem.73.030403.080419>
15. Noller HF, Yusupov MM, Yusupova GZ, Baucom A, Cate JHD. Translocation of tRNA during protein synthesis. *FEBS Lett* [Internet]. 2002 Mar [cited 2015

- Mar 18];514(1):11–6. Available from:
<http://www.sciencedirect.com/science/article/pii/S001457930202327X>
16. Nureki O. Enzyme Structure with Two Catalytic Sites for Double-Sieve Selection of Substrate. *Science* (80-) [Internet]. 1998 Apr 24 [cited 2015 Mar 9];280(5363):578–82. Available from:
<http://www.sciencemag.org/content/280/5363/578.abstract>
 17. Fischer N, Konevega AL, Wintermeyer W, Rodnina M V, Stark H. Ribosome dynamics and tRNA movement by time-resolved electron cryomicroscopy. *Nature* [Internet]. Nature Publishing Group, a division of Macmillan Publishers Limited. All Rights Reserved.; 2010 Jul 15 [cited 2014 Nov 2];466(7304):329–33. Available from: <http://dx.doi.org/10.1038/nature09206>
 18. Spahn CMT, Beckmann R, Eswar N, Penczek PA, Sali A, Blobel G, et al. Structure of the 80S Ribosome from *Saccharomyces cerevisiae*—tRNA-Ribosome and Subunit-Subunit Interactions. *Cell* [Internet]. 2001 Nov [cited 2015 Mar 15];107(3):373–86. Available from:
<http://www.sciencedirect.com/science/article/pii/S0092867401005396>
 19. Spahn CMT, Gomez-Lorenzo MG, Grassucci RA, Jørgensen R, Andersen GR, Beckmann R, et al. Domain movements of elongation factor eEF2 and the eukaryotic 80S ribosome facilitate tRNA translocation. *EMBO J* [Internet]. 2004 Mar 10 [cited 2015 Mar 4];23(5):1008–19. Available from:
<http://emboj.embopress.org/cgi/doi/10.1038/sj.emboj.7600102>
 20. Frank J, Gao H, Sengupta J, Gao N, Taylor DJ. The process of mRNA-tRNA translocation. *Proc Natl Acad Sci U S A* [Internet]. 2007 Dec 11 [cited 2015 Mar 15];104(50):19671–8. Available from:
<http://www.pnas.org/content/104/50/19671.short>
 21. Schmeing TM, Ramakrishnan V. What recent ribosome structures have revealed about the mechanism of translation. *Nature* [Internet]. Macmillan Publishers Limited. All rights reserved; 2009 Oct 29 [cited 2015 Feb 13];461(7268):1234–42. Available from:
<http://dx.doi.org/10.1038/nature08403>
 22. Kisselev LL, Buckingham RH. Translational termination comes of age. *Trends Biochem Sci* [Internet]. 2000 Nov [cited 2015 Mar 15];25(11):561–6. Available from:
<http://www.sciencedirect.com/science/article/pii/S0968000400016698>
 23. Nakamura Y, Ito K. tRNA mimicry in translation termination and beyond. *Wiley Interdiscip Rev RNA* [Internet]. Jan [cited 2015 Mar 15];2(5):647–68. Available from: <http://www.ncbi.nlm.nih.gov/pubmed/21823227>

24. Song H, Mugnier P, Das AK, Webb HM, Evans DR, Tuite MF, et al. The Crystal Structure of Human Eukaryotic Release Factor eRF1—Mechanism of Stop Codon Recognition and Peptidyl-tRNA Hydrolysis. *Cell* [Internet]. 2000 Feb [cited 2015 Feb 18];100(3):311–21. Available from: <http://www.sciencedirect.com/science/article/pii/S0092867400806674>
25. Pisarev A V, Skabkin MA, Pisareva VP, Skabkina O V, Rakotondrafara AM, Hentze MW, et al. The role of ABCE1 in eukaryotic posttermination ribosomal recycling. *Mol Cell* [Internet]. 2010 Jan 29 [cited 2015 Mar 18];37(2):196–210. Available from: <http://www.sciencedirect.com/science/article/pii/S1097276509009691>
26. Eyler DE, Green R. Distinct response of yeast ribosomes to a miscoding event during translation. *RNA* [Internet]. 2011 May 1 [cited 2015 Mar 17];17(5):925–32. Available from: <http://rnajournal.cshlp.org/content/17/5/925.short>
27. Jacks T, Varmus H. Expression of the Rous sarcoma virus pol gene by ribosomal frameshifting. *Science* (80-) [Internet]. 1985 Dec 13 [cited 2015 Mar 17];230(4731):1237–42. Available from: <http://www.sciencemag.org/content/230/4731/1237.abstract>
28. Jacks T, Madhani HD, Masiarz FR, Varmus HE. Signals for ribosomal frameshifting in the rous sarcoma virus gag-pol region. *Cell* [Internet]. 1988 Nov [cited 2015 Mar 17];55(3):447–58. Available from: <http://www.sciencedirect.com/science/article/pii/0092867488900311>
29. Biswas P, Jiang X, Pacchia AL, Dougherty JP, Peltz SW. The Human Immunodeficiency Virus Type 1 Ribosomal Frameshifting Site Is an Invariant Sequence Determinant and an Important Target for Antiviral Therapy. *J Virol* [Internet]. 2004 Jan 27 [cited 2015 Mar 17];78(4):2082–7. Available from: <http://jvi.asm.org/content/78/4/2082.short>
30. Marra MA, Jones SJM, Astell CR, Holt RA, Brooks-Wilson A, Butterfield YSN, et al. The Genome sequence of the SARS-associated coronavirus. *Science* [Internet]. 2003 May 30 [cited 2015 Mar 10];300(5624):1399–404. Available from: <http://www.sciencemag.org/content/300/5624/1399.abstract>
31. Dinman JD, Icho T, Wickner RB. A -1 ribosomal frameshift in a double-stranded RNA virus of yeast forms a gag-pol fusion protein. *Proc Natl Acad Sci* [Internet]. 1991 Jan 1 [cited 2015 Mar 17];88(1):174–8. Available from: <http://www.pnas.org/content/88/1/174.abstract>
32. Dinman JD, Wickner RB. Ribosomal frameshifting efficiency and gag/gag-pol ratio are critical for yeast M1 double-stranded RNA virus propagation. *J Virol*

- [Internet]. 1992 Jun 1 [cited 2015 Mar 17];66(6):3669–76. Available from: <http://jvi.asm.org/content/66/6/3669.short>
33. Harger JW, Meskauskas A, Dinman JD. An “integrated model” of programmed ribosomal frameshifting. *Trends Biochem Sci* [Internet]. 2002 Sep [cited 2015 Mar 17];27(9):448–54. Available from: <http://www.sciencedirect.com/science/article/pii/S0968000402021497>
 34. PLANT EP. The 9-A solution: How mRNA pseudoknots promote efficient programmed -1 ribosomal frameshifting. *RNA* [Internet]. 2003 Feb 1 [cited 2015 Mar 17];9(2):168–74. Available from: <http://rnajournal.cshlp.org/content/9/2/168.short>
 35. Namy O, Moran SJ, Stuart DI, Gilbert RJC, Brierley I. A mechanical explanation of RNA pseudoknot function in programmed ribosomal frameshifting. *Nature* [Internet]. 2006 May 11 [cited 2015 Mar 17];441(7090):244–7. Available from: <http://dx.doi.org/10.1038/nature04735>
 36. Leger M, Dulude D, Steinberg S V., Brakier-Gingras L. The three transfer RNAs occupying the A, P and E sites on the ribosome are involved in viral programmed -1 ribosomal frameshift. *Nucleic Acids Res* [Internet]. 2007 Aug 17 [cited 2015 Mar 17];35(16):5581–92. Available from: <http://nar.oxfordjournals.org/content/35/16/5581.short>
 37. Belew AT, Dinman JD. Cell cycle control (and more) by programmed –1 ribosomal frameshifting: implications for disease and therapeutics [Internet]. *Cell Cycle*. Taylor & Francis; 2015 [cited 2015 Mar 18]. Available from: <http://www.tandfonline.com/doi/full/10.4161/15384101.2014.989123#abstract>
 38. Cleland WW. Partition analysis and concept of net rate constants as tools in enzyme kinetics. *Biochemistry* [Internet]. American Chemical Society; 1975 Jul [cited 2015 Mar 17];14(14):3220–4. Available from: <http://dx.doi.org/10.1021/bi00685a029>
 39. Liao P-Y, Choi YS, Dinman JD, Lee KH. The many paths to frameshifting: kinetic modelling and analysis of the effects of different elongation steps on programmed -1 ribosomal frameshifting. *Nucleic Acids Res* [Internet]. 2011 Jan 1 [cited 2015 Mar 17];39(1):300–12. Available from: <http://nar.oxfordjournals.org/content/39/1/300.full>
 40. Hammell AB, Taylor RC, Peltz SW, Dinman JD. Identification of Putative Programmed -1 Ribosomal Frameshift Signals in Large DNA Databases. *Genome Res* [Internet]. 1999 May 1 [cited 2015 Mar 17];9(5):417–27. Available from: <http://genome.cshlp.org/content/9/5/417.abstract>

41. Baranov P V. RECODE 2003. *Nucleic Acids Res* [Internet]. 2003 Jan 1 [cited 2015 Mar 17];31(1):87–9. Available from: <http://nar.oxfordjournals.org/content/31/1/87.short>
42. Moon S, Byun Y, Han K. FSDB: A frameshift signal database. *Comput Biol Chem* [Internet]. 2007 Aug [cited 2015 Mar 17];31(4):298–302. Available from: <http://www.sciencedirect.com/science/article/pii/S1476927107000795>
43. Han K. PSEUDOVIEWER2: visualization of RNA pseudoknots of any type. *Nucleic Acids Res* [Internet]. 2003 Jul 1 [cited 2015 Mar 17];31(13):3432–40. Available from: <http://nar.oxfordjournals.org/content/31/13/3432.short>
44. Belew AT, Hepler NL, Jacobs JL, Dinman JD. PRFdb: a database of computationally predicted eukaryotic programmed -1 ribosomal frameshift signals. *BMC Genomics* [Internet]. 2008 Jan [cited 2014 Oct 15];9(1):339. Available from: <http://www.biomedcentral.com/1471-2164/9/339>
45. Jacobs JL, Belew AT, Rakauskaitė R, Dinman JD. Identification of functional, endogenous programmed -1 ribosomal frameshift signals in the genome of *Saccharomyces cerevisiae*. *Nucleic Acids Res* [Internet]. 2007 Jan 12 [cited 2015 Mar 17];35(1):165–74. Available from: <http://nar.oxfordjournals.org/content/35/1/165.abstract?keytype=ref&ijkey=x0ZyxmvIlvTV2Yp>
46. Farabaugh PJ, Zhao H, Vimaladithan A. A novel programmed frameshift expresses the POL3 gene of retrotransposon Ty3 of yeast: Frameshifting without tRNA slippage. *Cell* [Internet]. 1993 Jul [cited 2015 Mar 17];74(1):93–103. Available from: <http://www.sciencedirect.com/science/article/pii/0092867493902974>
47. Wang X, Wong S-M, Liu DX. Identification of Hepta- and Octo-Uridine stretches as sole signals for programmed +1 and -1 ribosomal frameshifting during translation of SARS-CoV ORF 3a variants. *Nucleic Acids Res* [Internet]. 2006 Jan 25 [cited 2015 Mar 4];34(4):1250–60. Available from: <http://nar.oxfordjournals.org/content/34/4/1250.short>
48. Craigen WJ, Caskey CT. Expression of peptide chain release factor 2 requires high-efficiency frameshift. *Nature* [Internet]. Nature Publishing Group; 1986 Jan 17 [cited 2015 Mar 17];322(6076):273–5. Available from: <http://www.nature.com/nature/journal/v322/n6076/abs/322273a0.html#close>
49. Vimaladithan A, Farabaugh PJ. Special peptidyl-tRNA molecules can promote translational frameshifting without slippage. *Mol Cell Biol* [Internet]. 1994 Dec 1 [cited 2015 Mar 17];14(12):8107–16. Available from: <http://mcb.asm.org/content/14/12/8107.short>

50. Asakura T, Sasaki T, Nagano F, Satoh A, Obaishi H, Nishioka H, et al. Isolation and characterization of a novel actin filament-binding protein from *Saccharomyces cerevisiae*. *Oncogene* [Internet]. 1998 Jan 21 [cited 2015 Mar 17];16(1):121–30. Available from: <http://europepmc.org/abstract/med/9467951>
51. MATSUFUJI S. Autoregulatory frameshifting in decoding mammalian ornithine decarboxylase antizyme. *Cell* [Internet]. 1995 Jan [cited 2015 Mar 17];80(1):51–60. Available from: <http://www.sciencedirect.com/science/article/pii/0092867495904506>
52. Clare J, Farabaugh P. Nucleotide sequence of a yeast Ty element: evidence for an unusual mechanism of gene expression. *Proc Natl Acad Sci* [Internet]. 1985 May 1 [cited 2015 Mar 17];82(9):2829–33. Available from: <http://www.pnas.org/content/82/9/2829.short>
53. Boeke JD, Garfinkel DJ, Styles CA, Fink GR. Ty elements transpose through an RNA intermediate. *Cell* [Internet]. 1985 Mar [cited 2015 Mar 17];40(3):491–500. Available from: <http://www.sciencedirect.com/science/article/pii/0092867485901977>
54. Morris DK, Lundblad V. Programmed translational frameshifting in a gene required for yeast telomere replication. *Curr Biol* [Internet]. 1997 Dec [cited 2015 Mar 17];7(12):969–76. Available from: <http://www.sciencedirect.com/science/article/pii/S0960982206004167>
55. Namy O, Rousset J-P, Naphine S, Brierley I. Reprogrammed Genetic Decoding in Cellular Gene Expression. *Mol Cell* [Internet]. 2004 Jan [cited 2015 Mar 17];13(2):157–68. Available from: <http://www.sciencedirect.com/science/article/pii/S1097276504000310>
56. Pegg AE. Recent advances in the biochemistry of polyamines in eukaryotes. *Biochem J* [Internet]. 1986 Mar 1 [cited 2015 Mar 17];234(2):249–62. Available from: <http://www.pubmedcentral.nih.gov/articlerender.fcgi?artid=1146560&tool=pmcentrez&rendertype=abstract>
57. Ivanov IP. Conservation of polyamine regulation by translational frameshifting from yeast to mammals. *EMBO J* [Internet]. 2000 Apr 17 [cited 2015 Mar 17];19(8):1907–17. Available from: <http://www.pubmedcentral.nih.gov/articlerender.fcgi?artid=302018&tool=pmcentrez&rendertype=abstract>
58. Balasundaram D, Dinman JD, Tabor CW, Tabor H. SPE1 and SPE2: two essential genes in the biosynthesis of polyamines that modulate +1 ribosomal frameshifting in *Saccharomyces cerevisiae*. *J Bacteriol* [Internet]. 1994 Nov 1

[cited 2015 Mar 17];176(22):7126–8. Available from:
<http://jb.asm.org/content/176/22/7126.short>

59. Hoffmann PR, Berry MJ. Selenoprotein Synthesis: A Unique Translational Mechanism Used by a Diverse Family of Proteins. *Thyroid* [Internet]. Mary Ann Liebert, Inc. 2 Madison Avenue Larchmont, NY 10538 USA; 2005 Aug 30 [cited 2015 Mar 17];15(8):769–75. Available from:
<http://online.liebertpub.com/doi/abs/10.1089/thy.2005.15.769>
60. Hatfield DL, Gladyshev VN. How Selenium Has Altered Our Understanding of the Genetic Code. *Mol Cell Biol* [Internet]. 2002 Jun 1 [cited 2015 Mar 17];22(11):3565–76. Available from:
<http://mcb.asm.org/content/22/11/3565.short>
61. Tujebajeva RM, Copeland PR, Xu X-M, Carlson BA, Harney JW, Driscoll DM, et al. Decoding apparatus for eukaryotic selenocysteine insertion. *EMBO Rep* [Internet]. 2000 Aug 1 [cited 2015 Mar 17];1(2):158–63. Available from:
<http://embor.embopress.org/cgi/doi/10.1093/embo-reports/kvd033>
62. Wills NM, Gesteland RF, Atkins JF. Pseudoknot-dependent read-through of retroviral gag termination codons: importance of sequences in the spacer and loop 2. *EMBO J* [Internet]. 1994 Sep 1 [cited 2015 Mar 17];13(17):4137–44. Available from:
<http://www.pubmedcentral.nih.gov/articlerender.fcgi?artid=395336&tool=pmc-entrez&rendertype=abstract>
63. Alam SL, Wills NM, Ingram JA, Atkins JF, Gesteland RF. Structural studies of the RNA pseudoknot required for readthrough of the gag-termination codon of murine leukemia virus. *J Mol Biol* [Internet]. 1999 May [cited 2015 Mar 17];288(5):837–52. Available from:
<http://www.sciencedirect.com/science/article/pii/S0022283699927134>
64. Goff SP. Retrovirus restriction factors. *Mol Cell* [Internet]. 2004 Dec 22 [cited 2015 Mar 17];16(6):849–59. Available from:
<http://www.sciencedirect.com/science/article/pii/S1097276504007555>
65. Eswarappa SM, Potdar AA, Koch WJ, Fan Y, Vasu K, Lindner D, et al. Programmed Translational Readthrough Generates Antiangiogenic VEGF-Ax. *Cell* [Internet]. 2014 Jun 19 [cited 2014 Jul 10];157(7):1605–18. Available from: <http://www.sciencedirect.com/science/article/pii/S0092867414006126>
66. Maquat LE. When cells stop making sense: effects of nonsense codons on RNA metabolism in vertebrate cells. *RNA* [Internet]. 1995 Jul 1 [cited 2015 Mar 18];1(5):453–65. Available from:
<http://rnajournal.cshlp.org/content/1/5/453.short>

67. Culbertson MR, Leeds PF. Looking at mRNA decay pathways through the window of molecular evolution. *Curr Opin Genet Dev* [Internet]. 2003 Apr [cited 2015 Mar 18];13(2):207–14. Available from: <http://www.sciencedirect.com/science/article/pii/S0959437X03000145>
68. Lykke-Andersen J. mRNA quality control: Marking the message for life or death. *Curr Biol* [Internet]. 2001 Feb [cited 2015 Mar 18];11(3):R88–91. Available from: <http://www.sciencedirect.com/science/article/pii/S0960982201000367>
69. Hilleren P, Parker R. Mechanisms of mRNA surveillance in eukaryotes. *Annu Rev Genet* [Internet]. Annual Reviews 4139 El Camino Way, P.O. Box 10139, Palo Alto, CA 94303-0139, USA; 1999 Jan 28 [cited 2015 Mar 18];33:229–60. Available from: <http://www.annualreviews.org/doi/abs/10.1146/annurev.genet.33.1.229>
70. Morrison M, Harris KS, Roth MB. smg mutants affect the expression of alternatively spliced SR protein mRNAs in *Caenorhabditis elegans*. *Proc Natl Acad Sci* [Internet]. 1997 Sep 2 [cited 2015 Mar 18];94(18):9782–5. Available from: <http://www.pnas.org/content/94/18/9782.short>
71. Moriarty PM, Reddy CC, Maquat LE. Selenium Deficiency Reduces the Abundance of mRNA for Se-Dependent Glutathione Peroxidase 1 by a UGA-Dependent Mechanism Likely To Be Nonsense Codon-Mediated Decay of Cytoplasmic mRNA. *Mol Cell Biol* [Internet]. 1998 May 1 [cited 2015 Mar 18];18(5):2932–9. Available from: <http://mcb.asm.org/content/18/5/2932.short>
72. Sun X, Li X, Moriarty PM, Henics T, LaDuca JP, Maquat LE. Nonsense-mediated Decay of mRNA for the Selenoprotein Phospholipid Hydroperoxide Glutathione Peroxidase Is Detectable in Cultured Cells but Masked or Inhibited in Rat Tissues. *Mol Biol Cell* [Internet]. 2001 Apr 1 [cited 2015 Mar 18];12(4):1009–17. Available from: <http://www.molbiolcell.org/content/12/4/1009.short>
73. Bühler M, Steiner S, Mohn F, Paillusson A, Mühlemann O. EJC-independent degradation of nonsense immunoglobulin- μ mRNA depends on 3' UTR length. *Nat Struct Mol Biol* [Internet]. 2006 May [cited 2015 Mar 18];13(5):462–4. Available from: <http://dx.doi.org/10.1038/nsmb1081>
74. Amrani N, Ganesan R, Kervestin S, Mangus DA, Ghosh S, Jacobson A. A faux 3'-UTR promotes aberrant termination and triggers nonsense-mediated mRNA decay. *Nature* [Internet]. 2004 Nov 4 [cited 2015 Mar 3];432(7013):112–8. Available from: <http://dx.doi.org/10.1038/nature03060>

75. Hogg JR, Goff SP. Upf1 senses 3'UTR length to potentiate mRNA decay. *Cell* [Internet]. 2010 Oct 29 [cited 2015 Mar 18];143(3):379–89. Available from: <http://www.sciencedirect.com/science/article/pii/S0092867410011414>
76. Leeds P, Wood JM, Lee BS, Culbertson MR. Gene products that promote mRNA turnover in *Saccharomyces cerevisiae*. *Mol Cell Biol* [Internet]. 1992 May 1 [cited 2015 Mar 18];12(5):2165–77. Available from: <http://mcb.asm.org/content/12/5/2165.short>
77. Czaplinski K, Ruiz-Echevarria MJ, Paushkin S V., Han X, Weng Y, Perlick HA, et al. The surveillance complex interacts with the translation release factors to enhance termination and degrade aberrant mRNAs. *Genes Dev* [Internet]. Cold Spring Harbor Lab; 1998 Jun 1 [cited 2015 Mar 18];12(11):1665–77. Available from: <http://genesdev.cshlp.org/content/12/11/1665/F8.expansion.html>
78. Min EE, Roy B, Amrani N, He F, Jacobson A. Yeast Upf1 CH domain interacts with Rps26 of the 40S ribosomal subunit. *RNA* [Internet]. 2013 Aug [cited 2015 Mar 18];19(8):1105–15. Available from: <http://www.pubmedcentral.nih.gov/articlerender.fcgi?artid=3708530&tool=pmcentrez&rendertype=abstract>
79. Celik A, Kervestin S, Jacobson A. NMD: At the crossroads between translation termination and ribosome recycling. *Biochimie* [Internet]. 2014 Nov 13 [cited 2014 Dec 4]; Available from: <http://www.sciencedirect.com/science/article/pii/S0300908414003290>
80. Mitchell P, Tollervey D. An NMD Pathway in Yeast Involving Accelerated Deadenylation and Exosome-Mediated 3'→5' Degradation. *Mol Cell* [Internet]. 2003 May [cited 2015 Mar 18];11(5):1405–13. Available from: <http://www.sciencedirect.com/science/article/pii/S1097276503001904>
81. Nagy E, Maquat LE. A rule for termination-codon position within intron-containing genes: when nonsense affects RNA abundance. *Trends Biochem Sci* [Internet]. 1998 Jun [cited 2015 Feb 4];23(6):198–9. Available from: <http://www.ncbi.nlm.nih.gov/pubmed/9644970>
82. Popp MW-L, Maquat LE. Organizing principles of mammalian nonsense-mediated mRNA decay. *Annu Rev Genet* [Internet]. 2013 Jan [cited 2015 Feb 6];47:139–65. Available from: <http://www.pubmedcentral.nih.gov/articlerender.fcgi?artid=4148824&tool=pmcentrez&rendertype=abstract>
83. Gong C, Kim YK, Woeller CF, Tang Y, Maquat LE. SMD and NMD are competitive pathways that contribute to myogenesis: effects on PAX3 and myogenin mRNAs. *Genes Dev* [Internet]. 2009 Jan 1 [cited 2015 Mar

6];23(1):54–66. Available from:
<http://www.pubmedcentral.nih.gov/articlerender.fcgi?artid=2632170&tool=pmcentrez&rendertype=abstract>

84. Kashima I, Yamashita A, Izumi N, Kataoka N, Morishita R, Hoshino S, et al. Binding of a novel SMG-1-Upf1-eRF1-eRF3 complex (SURF) to the exon junction complex triggers Upf1 phosphorylation and nonsense-mediated mRNA decay. *Genes Dev* [Internet]. 2006 Feb 1 [cited 2015 Mar 3];20(3):355–67. Available from:
<http://www.pubmedcentral.nih.gov/articlerender.fcgi?artid=1361706&tool=pmcentrez&rendertype=abstract>
85. Fukuhara N, Ebert J, Unterholzner L, Lindner D, Izaurralde E, Conti E. SMG7 is a 14-3-3-like adaptor in the nonsense-mediated mRNA decay pathway. *Mol Cell* [Internet]. 2005 Feb 18 [cited 2015 Mar 14];17(4):537–47. Available from: <http://www.ncbi.nlm.nih.gov/pubmed/15721257>
86. Lejeune F, Li X, Maquat LE. Nonsense-mediated mRNA decay in mammalian cells involves decapping, deadenylation, and exonucleolytic activities. *Mol Cell* [Internet]. 2003 Sep [cited 2015 Mar 18];12(3):675–87. Available from: <http://www.ncbi.nlm.nih.gov/pubmed/14527413>
87. Wilke CO. Transcriptional robustness complements nonsense-mediated decay in humans. *PLoS Genet* [Internet]. 2011 Oct 13 [cited 2015 Mar 18];7(10):e1002296. Available from:
<http://journals.plos.org/plosgenetics/article?id=10.1371/journal.pgen.1002296>
88. Brogna S, Wen J. Nonsense-mediated mRNA decay (NMD) mechanisms. *Nat Struct Mol Biol* [Internet]. Nature Publishing Group; 2009 Feb [cited 2014 Jul 17];16(2):107–13. Available from: <http://dx.doi.org/10.1038/nsmb.1550>
89. Hosoda N, Kobayashi T, Uchida N, Funakoshi Y, Kikuchi Y, Hoshino S, et al. Translation termination factor eRF3 mediates mRNA decay through the regulation of deadenylation. *J Biol Chem* [Internet]. 2003 Oct 3 [cited 2015 Mar 18];278(40):38287–91. Available from:
<http://www.jbc.org/content/278/40/38287.short>
90. Matsuda D, Hosoda N, Kim YK, Maquat LE. Failsafe nonsense-mediated mRNA decay does not detectably target eIF4E-bound mRNA. *Nat Struct Mol Biol* [Internet]. Nature Publishing Group; 2007 Oct [cited 2015 Mar 18];14(10):974–9. Available from: <http://dx.doi.org/10.1038/nsmb1297>
91. Chan W-K, Huang L, Gudikote JP, Chang Y-F, Imam JS, MacLean JA, et al. An alternative branch of the nonsense-mediated decay pathway. *EMBO J* [Internet]. EMBO Press; 2007 Apr 4 [cited 2015 Mar 18];26(7):1820–30. Available from: <http://emboj.embopress.org/content/26/7/1820.abstract>

92. He F, Li X, Spatrick P, Casillo R, Dong S, Jacobson A. Genome-Wide Analysis of mRNAs Regulated by the Nonsense-Mediated and 5' to 3' mRNA Decay Pathways in Yeast. *Mol Cell* [Internet]. 2003 Dec [cited 2015 Mar 18];12(6):1439–52. Available from: <http://www.sciencedirect.com/science/article/pii/S1097276503004465>
93. Avery P, Vicente-Crespo M, Francis D, Nashchekina O, Alonso CR, Palacios IM. Drosophila Upf1 and Upf2 loss of function inhibits cell growth and causes animal death in a Upf3-independent manner. *RNA* [Internet]. 2011 Apr [cited 2015 Mar 18];17(4):624–38. Available from: <http://www.pubmedcentral.nih.gov/articlerender.fcgi?artid=3062174&tool=pmcentrez&rendertype=abstract>
94. Vicente-Crespo M, Palacios IM. Nonsense-mediated mRNA decay and development: shoot the messenger to survive? *Biochem Soc Trans* [Internet]. 2010 Dec [cited 2015 Mar 18];38(6):1500–5. Available from: <http://www.pubmedcentral.nih.gov/articlerender.fcgi?artid=3432441&tool=pmcentrez&rendertype=abstract>
95. Holbrook JA, Neu-Yilik G, Hentze MW, Kulozik AE. NMD and Human Disease [Internet]. *Landes Bioscience*; 2000 [cited 2015 Mar 18]. Available from: <http://www.ncbi.nlm.nih.gov/books/NBK6093/>
96. Plant EP, Wang P, Jacobs JL, Dinman JD. A programmed -1 ribosomal frameshift signal can function as a cis-acting mRNA destabilizing element. *Nucleic Acids Res* [Internet]. 2004 Jan 3 [cited 2015 Apr 6];32(2):784–90. Available from: <http://nar.oxfordjournals.org/content/32/2/784.abstract>
97. Belew AT, Advani VM, Dinman JD. Endogenous ribosomal frameshift signals operate as mRNA destabilizing elements through at least two molecular pathways in yeast. *Nucleic Acids Res* [Internet]. 2011 Apr 1 [cited 2014 Oct 14];39(7):2799–808. Available from: <http://nar.oxfordjournals.org/content/39/7/2799.long>
98. Smogorzewska A, de Lange T. Regulation of telomerase by telomeric proteins. *Annu Rev Biochem* [Internet]. 2004 Jan [cited 2015 Jan 7];73:177–208. Available from: <http://www.ncbi.nlm.nih.gov/pubmed/15189140>
99. Belew AT, Meskauskas A, Musalgaonkar S, Advani VM, Sulima SO, Kasprzak WK, et al. Ribosomal frameshifting in the CCR5 mRNA is regulated by miRNAs and the NMD pathway. *Nature* [Internet]. Nature Publishing Group, a division of Macmillan Publishers Limited. All Rights Reserved.; 2014 Jul 9 [cited 2014 Jul 9];512(7514):265–9. Available from: <http://dx.doi.org/10.1038/nature13429>

100. Fromont-Racine M, Senger B, Saveanu C, Fasiolo F. Ribosome assembly in eukaryotes. *Gene* [Internet]. 2003 Aug [cited 2015 Mar 18];313:17–42. Available from: <http://www.sciencedirect.com/science/article/pii/S0378111903006292>
101. Kressler D, Linder P, de la Cruz J. Protein trans-Acting Factors Involved in Ribosome Biogenesis in *Saccharomyces cerevisiae*. *Mol Cell Biol* [Internet]. 1999 Dec 1 [cited 2015 Mar 18];19(12):7897–912. Available from: <http://mcb.asm.org/content/19/12/7897.short>
102. Granneman S, Baserga SJ. Ribosome biogenesis: of knobs and RNA processing. *Exp Cell Res* [Internet]. 2004 May 15 [cited 2015 Mar 18];296(1):43–50. Available from: <http://www.sciencedirect.com/science/article/pii/S0014482704001284>
103. Decatur WA, Fournier MJ. rRNA modifications and ribosome function. *Trends Biochem Sci* [Internet]. 2002 Jul [cited 2015 Feb 28];27(7):344–51. Available from: <http://www.sciencedirect.com/science/article/pii/S0968000402021096>
104. Kressler D, Hurt E, Bassler J. Driving ribosome assembly. *Biochim Biophys Acta* [Internet]. 2010 Jun [cited 2014 Dec 8];1803(6):673–83. Available from: <http://www.ncbi.nlm.nih.gov/pubmed/19879902>
105. Nakhoul H, Ke J, Zhou X, Liao W, Zeng SX, Lu H. Ribosomopathies: mechanisms of disease. *Clin Med insights Blood Disord* [Internet]. 2014 Jan [cited 2015 Mar 18];7:7–16. Available from: <http://www.pubmedcentral.nih.gov/articlerender.fcgi?artid=4251057&tool=pmcentrez&rendertype=abstract>
106. Jack K, Bellodi C, Landry DM, Niederer RO, Meskauskas A, Musalgaonkar S, et al. rRNA pseudouridylation defects affect ribosomal ligand binding and translational fidelity from yeast to human cells. *Mol Cell* [Internet]. Elsevier; 2011 Nov 18 [cited 2014 Sep 23];44(4):660–6. Available from: <http://www.cell.com/article/S1097276511008161/fulltext>
107. Hekman KE, Yu G-Y, Brown CD, Zhu H, Du X, Gervin K, et al. A conserved eEF2 coding variant in SCA26 leads to loss of translational fidelity and increased susceptibility to proteostatic insult. *Hum Mol Genet* [Internet]. 2012 Dec 15 [cited 2014 Oct 14];21(26):5472–83. Available from: <http://hmg.oxfordjournals.org/content/21/26/5472.long>
108. Kontos H, Napthine S, Brierley I. Ribosomal pausing at a frameshifter RNA pseudoknot is sensitive to reading phase but shows little correlation with frameshift efficiency. *Mol Cell Biol* [Internet]. 2001 Dec [cited 2015 Apr 6];21(24):8657–70. Available from:

<http://www.pubmedcentral.nih.gov/articlerender.fcgi?artid=100026&tool=pmc-entrez&rendertype=abstract>

109. Lopinski JD, Dinman JD, Bruenn JA. Kinetics of Ribosomal Pausing during Programmed -1 Translational Frameshifting. *Mol Cell Biol* [Internet]. 2000 Feb 15 [cited 2015 Apr 7];20(4):1095–103. Available from: <http://mcb.asm.org/content/20/4/1095.short>
110. Baril M, Dulude D, Steinberg S V, Brakier-Gingras L. The Frameshift Stimulatory Signal of Human Immunodeficiency Virus Type 1 Group O is a Pseudoknot. *J Mol Biol* [Internet]. 2003 Aug [cited 2015 Apr 7];331(3):571–83. Available from: <http://www.sciencedirect.com/science/article/pii/S0022283603007848>
111. Kollmus H, Hentze MW, Hauser H. Regulated ribosomal frameshifting by an RNA-protein interaction. *RNA* [Internet]. 1996 Apr [cited 2015 Apr 7];2(4):316–23. Available from: <http://www.pubmedcentral.nih.gov/articlerender.fcgi?artid=1369374&tool=pmc-entrez&rendertype=abstract>
112. Matsufuji S, Matsufuji T, Wills NM, Gesteland RF, Atkins JF. Reading two bases twice: mammalian antizyme frameshifting in yeast. *EMBO J* [Internet]. 1996 Mar 15 [cited 2015 Apr 7];15(6):1360–70. Available from: <http://www.pubmedcentral.nih.gov/articlerender.fcgi?artid=450040&tool=pmc-entrez&rendertype=abstract>
113. Morris DR, Geballe AP. Upstream Open Reading Frames as Regulators of mRNA Translation. *Mol Cell Biol* [Internet]. 2000 Dec 1 [cited 2015 Apr 7];20(23):8635–42. Available from: <http://mcb.asm.org/content/20/23/8635.short>
114. Shigemoto K, Brennan J, Walls E, Watson CJ, Stott D, Rigby PWJ, et al. Identification and characterisation of a developmentally regulated mammalian gene that utilises -1 programmed ribosomal frameshifting. *Nucleic Acids Res* [Internet]. 2001 Oct 1 [cited 2015 Apr 7];29(19):4079–88. Available from: <http://nar.oxfordjournals.org/content/29/19/4079.short>
115. Manktelow E, Shigemoto K, Brierley I. Characterization of the frameshift signal of Edr, a mammalian example of programmed -1 ribosomal frameshifting. *Nucleic Acids Res* [Internet]. 2005 Jan 14 [cited 2015 Apr 7];33(5):1553–63. Available from: <http://nar.oxfordjournals.org/content/33/5/1553.short>
116. Wills NM, Moore B, Hammer A, Gesteland RF, Atkins JF. A functional -1 ribosomal frameshift signal in the human paraneoplastic Ma3 gene. *J Biol*

- Chem [Internet]. 2006 Mar 17 [cited 2015 Apr 7];281(11):7082–8. Available from: <http://www.jbc.org/content/281/11/7082.short>
117. Shah AA, Giddings MC, Parvaz JB, Gesteland RF, Atkins JF, Ivanov IP. Computational identification of putative programmed translational frameshift sites. *Bioinformatics* [Internet]. 2002 Aug 1 [cited 2015 Apr 7];18(8):1046–53. Available from: <http://bioinformatics.oxfordjournals.org/content/18/8/1046.short>
 118. GAO X. Translational recoding signals between gag and pol in diverse LTR retrotransposons. *RNA* [Internet]. 2003 Dec 1 [cited 2015 Apr 7];9(12):1422–30. Available from: <http://rnajournal.cshlp.org/content/9/12/1422.short>
 119. Moon S, Byun Y, Kim HJ, Jeong S. Predicting genes expressed via –1 and +1 frameshifts. *Nucleic Acids Res* [Internet]. 2004 [cited 2011 Jun 6];32(16):4884–92. Available from: <http://nar.oxfordjournals.org/content/32/16/4884.short>
 120. Namy O, Rousset J, Naphtine S, Brierley I. Reprogrammed genetic decoding in cellular gene expression. *Mol Cell* [Internet]. Elsevier; 2004 Jan [cited 2011 Jun 6];13(2):157–68. Available from: <http://www.sciencedirect.com/science/article/pii/S1097276504000310>
 121. Guan Q, Zheng W, Tang S, Liu X, Zinkel RA, Tsui K-W, et al. Impact of nonsense-mediated mRNA decay on the global expression profile of budding yeast. Kruglyak L, editor. *PLoS Genet* [Internet]. Public Library of Science; 2006 Nov 24 [cited 2014 Jul 28];2(11):e203. Available from: <http://dx.plos.org/10.1371/journal.pgen.0020203>
 122. Harger JW, Dinman JD. An in vivo dual-luciferase assay system for studying translational recoding in the yeast *Saccharomyces cerevisiae* An in vivo dual-luciferase assay system for studying translational recoding in the yeast *Saccharomyces cerevisiae*. 2003;1019–24.
 123. Jacks T, Madhani HD, Masiarz FR, Varmus HE. Signals for ribosomal frameshifting in the Rous sarcoma virus gag-pol region. *Cell* [Internet]. Elsevier; 1988 Nov [cited 2011 Jun 5];55(3):447–58. Available from: <http://linkinghub.elsevier.com/retrieve/pii/0092867488900311>
 124. Dinman JD, Connor MO. Mutants That Affect Recoding. *Nucleic Acids Mol Biol*. 2010;321–44.
 125. Meskauskas A, Harger JW, Jacobs KL. Decreased peptidyltransferase activity correlates with increased programmed – 1 ribosomal frameshifting and viral maintenance defects in the yeast *Saccharomyces cerevisiae* Decreased

peptidyltransferase activity correlates with increased programmed – 1 rib. 2003;

126. Meskauskas A, Dinman JD. A molecular clamp ensures allosteric coordination of peptidyltransfer and ligand binding to the ribosomal A-site. *Nucleic Acids Res.* Oxford Univ Press; 2010;38(21):7800–13.
127. Sulima SO, Patchett S, Advani VM, De Keersmaecker K, Johnson AW, Dinman JD. Bypass of the pre-60S ribosomal quality control as a pathway to oncogenesis. *Proc Natl Acad Sci U S A* [Internet]. 2014 Apr 15 [cited 2014 Oct 27];111(15):5640–5. Available from: <http://www.pnas.org/content/111/15/5640.short>
128. Dinman JD, Ruiz-Echevarria MJ, Czaplinski K, Peltz SW. Peptidyl-transferase inhibitors have antiviral properties by altering programmed- 1 ribosomal frameshifting efficiencies: Development of model systems. *Proc Natl Acad Sci* [Internet]. National Acad Sciences; 1997 [cited 2011 Jun 4];94(13):6606. Available from: <http://www.pnas.org/content/94/13/6606.short>
129. Jacobs JL, Belew AT, Rakauskaitė R, Dinman JD. Identification of functional, endogenous programmed -1 ribosomal frameshift signals in the genome of *Saccharomyces cerevisiae*. *Nucleic Acids Res* [Internet]. 2007 Jan [cited 2012 Mar 1];35(1):165–74. Available from: <http://www.pubmedcentral.nih.gov/articlerender.fcgi?artid=1802563&tool=pmcentrez&rendertype=abstract>
130. Belew AT, Hepler NL, Jacobs JL, Dinman JD. PRFdb: A database of computationally predicted eukaryotic programmed -1 ribosomal frameshift signals. *BMC Genomics* [Internet]. 2008;9(1):339–47. Available from: <http://www.biomedcentral.com/1471-2164/9/339>
131. Dahlseid JN, Lew-Smith J, Lelivelt MJ, Enomoto S, Ford A, Desruisseaux M, et al. mRNAs Encoding Telomerase Components and Regulators Are Controlled by UPF Genes in *Saccharomyces cerevisiae*. *Eukaryot Cell* [Internet]. 2003 Feb 1 [cited 2015 Mar 14];2(1):134–42. Available from: <http://ec.asm.org/content/2/1/134.short>
132. He F, Li X, Spatrick P, Castillo R, Dong S, Jacobson A. Genome-wide analysis of mRNAs regulated by the nonsense-mediated and 5' to 3' mRNA decay pathways in yeast. *Mol Cell.* 2003;12(3):1439–52.
133. Dahlseid JN, Lew-Smith J, Lelivelt MJ, Enomoto S, Ford A, Desruisseaux M, et al. mRNAs encoding telomerase components and regulators are controlled by UPF genes in *Saccharomyces cerevisiae*. *Eukaryot Cell* [Internet]. *Am Soc Microbiol*; 2003 Feb [cited 2012 Feb 1];2(1):134–42. Available from: <http://ec.asm.org/cgi/content/abstract/2/1/134>

134. Lew JEE, Enomoto S, Berman J. Telomere length regulation and telomeric chromatin require the nonsense-mediated mRNA decay pathway. *Mol Cell Biol* [Internet]. Am Soc Microbiol; 1998 Oct [cited 2011 Jun 4];18(10):6121. Available from: <http://mcb.asm.org/cgi/content/abstract/18/10/6121>
135. Teo SH, Jackson SP. Telomerase subunit overexpression suppresses telomere-specific checkpoint activation in the yeast yku80 mutant. *EMBO Rep* [Internet]. Nature Publishing Group; 2001 Mar [cited 2011 Jun 6];2(3):197–202. Available from: <http://www.nature.com/embor/journal/v2/n3/abs/embor470.html>
136. Belew AT, Advani VM, Dinman JD. Endogenous ribosomal frameshift signals operate as mRNA destabilizing elements through at least two molecular pathways in yeast. *Nucleic Acids Res* [Internet]. Oxford Univ Press; 2011 [cited 2011 Jun 4];39(7):2799–808. Available from: <http://nar.oxfordjournals.org/content/39/7/2799.short>
137. Lydall D. Hiding at the ends of yeast chromosomes: telomeres, nucleases and checkpoint pathways. *J Cell Sci* [Internet]. The Company of Biologists Ltd; 2003 Oct [cited 2011 Jun 6];116(20):4057. Available from: <http://jcs.biologists.org/content/116/20/4057.short>
138. Broccoli D, Smogorzewska A, Chong L, de Lange T. Human telomeres contain two distinct Myb-related proteins, TRF1 and TRF2. *Nat Genet* [Internet]. 1997 Oct [cited 2015 Apr 7];17(2):231–5. Available from: <http://www.ncbi.nlm.nih.gov/pubmed/9326950>
139. Van Steensel B, Smogorzewska A, de Lange T. TRF2 protects human telomeres from end-to-end fusions. *Cell* [Internet]. 1998 Feb 6 [cited 2015 Mar 19];92(3):401–13. Available from: <http://www.ncbi.nlm.nih.gov/pubmed/9476899>
140. Griffith JD, Comeau L, Rosenfield S, Stansel RM, Bianchi A, Moss H, et al. Mammalian telomeres end in a large duplex loop. *Cell* [Internet]. 1999 May 14 [cited 2015 Apr 5];97(4):503–14. Available from: <http://www.ncbi.nlm.nih.gov/pubmed/10338214>
141. Lieb JD, Liu X, Botstein D, Brown PO. Promoter-specific binding of Rap1 revealed by genome-wide maps of protein-DNA association. *Nat Genet* [Internet]. 2001 Aug [cited 2015 Feb 25];28(4):327–34. Available from: <http://www.ncbi.nlm.nih.gov/pubmed/11455386>
142. Sfeir A, Kabir S, van Overbeek M, Celli GB, de Lange T. Loss of Rap1 induces telomere recombination in the absence of NHEJ or a DNA damage signal. *Science* [Internet]. 2010 Mar 26 [cited 2015 Mar 31];327(5973):1657–61. Available from:

<http://www.pubmedcentral.nih.gov/articlerender.fcgi?artid=2864730&tool=pmcentrez&rendertype=abstract>

143. Snow BE, Erdmann N, Cruickshank J, Goldman H, Gill RM, Robinson MO, et al. Functional conservation of the telomerase protein Est1p in humans. *Curr Biol* [Internet]. 2003 Apr 15 [cited 2015 Apr 7];13(8):698–704. Available from: <http://www.ncbi.nlm.nih.gov/pubmed/12699629>
144. Azzalin CM, Reichenbach P, Khoriantuli L, Giulotto E, Lingner J. Telomeric repeat containing RNA and RNA surveillance factors at mammalian chromosome ends. *Science* [Internet]. 2007 Nov 2 [cited 2015 Feb 26];318(5851):798–801. Available from: <http://www.ncbi.nlm.nih.gov/pubmed/17916692>
145. Zakian VA. Telomeres: The beginnings and ends of eukaryotic chromosomes. *Exp Cell Res* [Internet]. 2012 Jul 15 [cited 2015 Apr 4];318(12):1456–60. Available from: <http://www.pubmedcentral.nih.gov/articlerender.fcgi?artid=3372703&tool=pmcentrez&rendertype=abstract>
146. Bianchi A, Shore D. How telomerase reaches its end: mechanism of telomerase regulation by the telomeric complex. *Mol Cell* [Internet]. Elsevier; 2008 Jul [cited 2011 Jun 4];31(2):153–65. Available from: <http://linkinghub.elsevier.com/retrieve/pii/S1097276508004310>
147. Mozdy AD, Cech TR. Low abundance of telomerase in yeast: implications for telomerase haploinsufficiency. *RNA* [Internet]. Cold Spring Harbor Lab; 2006 Sep [cited 2012 Feb 1];12(9):1721–37. Available from: <http://rnajournal.cshlp.org/content/12/9/1721.short>
148. Teixeira MT, Arneric M, Sperisen P, Lingner J. Telomere Length Homeostasis Is Achieved via a Switch between Telomerase- Extendible and -Nonextendible States. *Cell* [Internet]. 2004 Apr [cited 2015 Mar 14];117(3):323–35. Available from: <http://www.sciencedirect.com/science/article/pii/S0092867404003344>
149. Lew JE, Enomoto S, Berman J. Telomere Length Regulation and Telomeric Chromatin Require the Nonsense-Mediated mRNA Decay Pathway. *Cell* [Internet]. 1998;18(10):1171–81. Available from: <http://www.sciencedirect.com/science/article/pii/S0092867498001171>
150. Morris DK, Lundblad V. Programmed translational frameshifting in a gene required for yeast telomere replication. *Curr Biol* [Internet]. Elsevier; 1997 [cited 2012 Feb 1];7(12):969–76. Available from: [http://linkinghub.elsevier.com/retrieve/pii/s0960-9822\(06\)00416-7](http://linkinghub.elsevier.com/retrieve/pii/S0960-9822(06)00416-7)

151. Liao XH, Zhang ML, Yang CP, Xu LX, Zhou JQ. Characterization of recombinant *Saccharomyces cerevisiae* telomerase core enzyme purified from yeast. *Biochem J* [Internet]. Portland Press Ltd; 2005 [cited 2012 Feb 1];390(Pt 1):169. Available from: <http://scholar.google.com/scholar?hl=en&btnG=Search&q=intitle:Characterization+of+recombinant+Saccharomyces+cerevisiae+telomerase+core+enzyme+purified+from+yeast#0>
152. Ito H, Fukuda Y, Murata K, Kimura A. Transformation of intact yeast cells treated with alkali cations. *J Bacteriol* [Internet]. 1983 Jan 1 [cited 2015 Apr 7];153(1):163–8. Available from: <http://jb.asm.org/content/153/1/163.short>
153. Sambrook J, Russell DW. *Molecular cloning: a laboratory manual* [Internet]. Cold Spring Harbor, NY: Cold spring harbor laboratory press; 2001 [cited 2011 Jun 6]. Available from: http://books.google.com/books?hl=en&lr=&id=Bosc5JVxNpkC&oi=fnd&pg=PR21&dq=Molecular+cloning,+a+laboratory+manual.&ots=eecSmIASgP&sig=zOqDQpXk_NE49WSdjvd6Y2wwgtE
154. Wickner RB, Leibowitz MJ. Two chromosomal genes required for killing expression in killer strains of *Saccharomyces cerevisiae*. *Genetics* [Internet]. Genetics Soc America; 1976 Mar [cited 2011 Jun 5];82(3):429. Available from: <http://www.genetics.org/content/82/3/429.short>
155. Byrne KPP, Wolfe KHH. The Yeast Gene Order Browser: combining curated homology and syntenic context reveals gene fate in polyploid species. *Genome Res* [Internet]. Cold Spring Harbor Lab; 2005 [cited 2011 Jun 3];15(10):1456. Available from: <http://genome.cshlp.org/content/15/10/1456.short>
156. Jacobs JL, Dinman JD. Systematic analysis of bicistronic reporter assay data. *Nucleic Acids Res*. 2004 Jan;32(20):e160.
157. Warner JR. The economics of ribosome biosynthesis in yeast. *Trends Biochem Sci* [Internet]. 1999 Nov [cited 2015 Mar 22];24(11):437–40. Available from: <http://www.sciencedirect.com/science/article/pii/S0968000499014607>
158. Verschoor A, Warner JR, Srivastava S, Grassucci RA, Frank J. Three-dimensional structure of the yeast ribosome. *Nucleic Acids Res* [Internet]. 1998 Jan 1 [cited 2015 Mar 22];26(2):655–61. Available from: <http://nar.oxfordjournals.org/content/26/2/655.short>
159. Warner JR. *The Yeast Ribosome: Structure, Function, and Synthesis* [Internet]. Cold Spring Harbor Monograph Archive. 1982 [cited 2015 Mar 22]. p. 529–60. Available from: <https://cshmonographs.org/csh/index.php/monographs/article/view/4273>

160. Cantley LC, Neel BG. New insights into tumor suppression: PTEN suppresses tumor formation by restraining the phosphoinositide 3-kinase/AKT pathway. *Proc Natl Acad Sci* [Internet]. 1999 Apr 13 [cited 2015 Mar 22];96(8):4240–5. Available from: <http://www.pnas.org/content/96/8/4240.short>
161. Gingras AC, Raught B, Sonenberg N. Regulation of translation initiation by FRAP/mTOR. *Genes Dev* [Internet]. 2001 Apr 1 [cited 2015 Mar 22];15(7):807–26. Available from: <http://genesdev.cshlp.org/content/15/7/807.full>
162. Ruggero D, Pandolfi PP. Does the ribosome translate cancer? *Nat Rev Cancer* [Internet]. 2003 Mar [cited 2014 Dec 5];3(3):179–92. Available from: <http://dx.doi.org/10.1038/nrc1015>
163. Stumpf CR, Ruggero D. The cancerous translation apparatus. *Curr Opin Genet Dev* [Internet]. 2011 Aug [cited 2015 Mar 22];21(4):474–83. Available from: <http://www.sciencedirect.com/science/article/pii/S0959437X11000670>
164. Barlow JL, Drynan LF, Trim NL, Erber WN, Warren AJ, McKenzie ANJ. New insights into 5q- syndrome as a ribosomopathy. *Cell Cycle* [Internet]. Taylor & Francis; 2014 Oct 27 [cited 2015 Mar 22];9(21):4286–93. Available from: <http://www.tandfonline.com/doi/abs/10.4161/cc.9.21.13742#.VQ5L1vnF8kM>
165. Boria I, Garelli E, Gazda HT, Aspesi A, Quarello P, Pavesi E, et al. The ribosomal basis of Diamond-Blackfan Anemia: mutation and database update. *Hum Mutat* [Internet]. 2010 Dec [cited 2015 Mar 11];31(12):1269–79. Available from: <http://www.ncbi.nlm.nih.gov/pubmed/20960466>
166. Gazda HT, Grabowska A, Merida-Long LB, Latawiec E, Schneider HE, Lipton JM, et al. Ribosomal protein S24 gene is mutated in Diamond-Blackfan anemia. *Am J Hum Genet* [Internet]. 2006 Dec [cited 2015 Mar 22];79(6):1110–8. Available from: <http://www.sciencedirect.com/science/article/pii/S0002929707634740>
167. Vlachos A, Ball S, Dahl N, Alter BP, Sheth S, Ramenghi U, et al. Diagnosing and treating Diamond Blackfan anaemia: results of an international clinical consensus conference. *Br J Haematol* [Internet]. 2008 Sep [cited 2015 Mar 11];142(6):859–76. Available from: <http://www.pubmedcentral.nih.gov/articlerender.fcgi?artid=2654478&tool=pmcentrez&rendertype=abstract>
168. Knight SW, Heiss NS, Vulliamy TJ, Greschner S, Stavrides G, Pai GS, et al. X-linked dyskeratosis congenita is predominantly caused by missense mutations in the DKC1 gene. *Am J Hum Genet* [Internet]. 1999 Jul [cited 2015 Mar 22];65(1):50–8. Available from: <http://www.sciencedirect.com/science/article/pii/S0002929707637276>

169. Alter BP, Giri N, Savage SA, Rosenberg PS. Cancer in dyskeratosis congenita. *Blood* [Internet]. 2009 Jun 25 [cited 2015 Mar 22];113(26):6549–57. Available from: <http://www.pubmedcentral.nih.gov/articlerender.fcgi?artid=2710915&tool=pmcentrez&rendertype=abstract>
170. Dokal I. Dyskeratosis congenita in all its forms. *Br J Haematol* [Internet]. 2000 Sep [cited 2015 Mar 22];110(4):768–79. Available from: <http://doi.wiley.com/10.1046/j.1365-2141.2000.02109.x>
171. Wong JMY, Collins K. Telomerase RNA level limits telomere maintenance in X-linked dyskeratosis congenita. *Genes Dev* [Internet]. 2006 Oct 15 [cited 2015 Mar 22];20(20):2848–58. Available from: <http://genesdev.cshlp.org/content/20/20/2848.short>
172. Vulliamy TJ, Knight SW, Mason PJ, Dokal I. Very short telomeres in the peripheral blood of patients with X-linked and autosomal dyskeratosis congenita. *Blood Cells Mol Dis* [Internet]. Jan [cited 2015 Mar 26];27(2):353–7. Available from: <http://www.ncbi.nlm.nih.gov/pubmed/11259155>
173. Ofengand J. Ribosomal RNA pseudouridines and pseudouridine synthases. *FEBS Lett* [Internet]. 2002 Mar [cited 2015 Mar 22];514(1):17–25. Available from: <http://www.sciencedirect.com/science/article/pii/S0014579302023050>
174. Liang B, Li H. Structures of ribonucleoprotein particle modification enzymes. *Q Rev Biophys* [Internet]. Cambridge University Press; 2011 Feb 1 [cited 2015 Mar 26];44(01):95–122. Available from: http://journals.cambridge.org/abstract_S0033583510000235
175. Roovers M, Hale C, Tricot C, Terns MP, Terns RM, Grosjean H, et al. Formation of the conserved pseudouridine at position 55 in archaeal tRNA. *Nucleic Acids Res* [Internet]. 2006 Jan 1 [cited 2015 Feb 23];34(15):4293–301. Available from: <http://nar.oxfordjournals.org/content/34/15/4293.abstract>
176. Lafontaine DLJ, et al. (1998) | SGD [Internet]. [cited 2015 Mar 26]. Available from: <http://www.yeastgenome.org/reference/S000048923/overview>
177. Carlile TM, Rojas-Duran MF, Zinshteyn B, Shin H, Bartoli KM, Gilbert W V. Pseudouridine profiling reveals regulated mRNA pseudouridylation in yeast and human cells. *Nature* [Internet]. Nature Publishing Group, a division of Macmillan Publishers Limited. All Rights Reserved.; 2014 Sep 5 [cited 2014 Sep 7];515(7525):143–6. Available from: <http://dx.doi.org/10.1038/nature13802>
178. Jeanteur P, Amaldi F, Attardi G. Partial sequence analysis of ribosomal RNA from HeLa cells. *J Mol Biol* [Internet]. 1968 May [cited 2015 Mar

22];33(3):757–75. Available from:
<http://www.sciencedirect.com/science/article/pii/S0022283668903185>

179. Liang X-H, Liu Q, Fournier MJ. Loss of rRNA modifications in the decoding center of the ribosome impairs translation and strongly delays pre-rRNA processing. *RNA* [Internet]. 2009 Sep 1 [cited 2015 Mar 22];15(9):1716–28. Available from: <http://rnajournal.cshlp.org/content/15/9/1716.abstract>
180. Zebarjadian Y, King T, Fournier MJ, Clarke L, Carbon J. Point mutations in yeast CBF5 can abolish in vivo pseudouridylation of rRNA. *Mol Cell Biol* [Internet]. 1999 Nov 1 [cited 2015 Mar 26];19(11):7461–72. Available from: <http://mcb.asm.org/content/19/11/7461.abstract>
181. Decatur WA, Schnare MN. Different mechanisms for pseudouridine formation in yeast 5S and 5.8S rRNAs. *Mol Cell Biol* [Internet]. 2008 May 15 [cited 2015 Mar 26];28(10):3089–100. Available from: <http://mcb.asm.org/content/28/10/3089.abstract>
182. Jobert L, Skjeldam HK, Dalhus B, Galashevskaya A, Vågbø CB, Bjørås M, et al. The human base excision repair enzyme SMUG1 directly interacts with DKC1 and contributes to RNA quality control. *Mol Cell* [Internet]. 2013 Jan 24 [cited 2015 Mar 26];49(2):339–45. Available from: <http://www.ncbi.nlm.nih.gov/pubmed/23246433>
183. Craig K, Keers SM, Archibald K, Curtis A, Chinnery PF. Molecular epidemiology of spinocerebellar ataxia type 6. *Ann Neurol* [Internet]. 2004 May [cited 2015 Apr 2];55(5):752–5. Available from: <http://www.ncbi.nlm.nih.gov/pubmed/15122720>
184. Manto M-U. The wide spectrum of spinocerebellar ataxias (SCAs). *Cerebellum* [Internet]. 2005 Jan [cited 2015 Jan 7];4(1):2–6. Available from: <http://www.ncbi.nlm.nih.gov/pubmed/15895552>
185. Yu G-Y, Howell MJ, Roller MJ, Xie T-D, Gomez CM. Spinocerebellar ataxia type 26 maps to chromosome 19p13.3 adjacent to SCA6. *Ann Neurol* [Internet]. 2005 Mar [cited 2015 Apr 2];57(3):349–54. Available from: <http://www.ncbi.nlm.nih.gov/pubmed/15732118>
186. Advani VM, Belew AT, Dinman JD. Yeast telomere maintenance is globally controlled by programmed ribosomal frameshifting and the nonsense-mediated mRNA decay pathway. *Transl (Austin, Tex)* [Internet]. 2013 Apr 1 [cited 2014 Oct 14];1(1):e24418. Available from: <http://www.pubmedcentral.nih.gov/articlerender.fcgi?artid=3908577&tool=pmcentrez&rendertype=abstract>

187. Czaplinski K, Ruiz-Echevarria MJ, Paushkin S V., Han X, Weng Y, Perlick HA, et al. The surveillance complex interacts with the translation release factors to enhance termination and degrade aberrant mRNAs. *Genes Dev* [Internet]. 1998 Jun 1 [cited 2015 Mar 18];12(11):1665–77. Available from: <http://genesdev.cshlp.org/content/12/11/1665.short>
188. Stansfield I, Jones KM, Kushnirov V V, Dagkesamanskaya AR, Poznyakovski AI, Paushkin S V, et al. The products of the SUP45 (eRF1) and SUP35 genes interact to mediate translation termination in *Saccharomyces cerevisiae*. *EMBO J* [Internet]. 1995 Sep 1 [cited 2015 Mar 9];14(17):4365–73. Available from: <http://www.pubmedcentral.nih.gov/articlerender.fcgi?artid=394521&tool=pmcentrez&rendertype=abstract>
189. Keeling KM, Lanier J, Du M, Salas-Marco J, Gao L, Kaenjak-Angeletti A, et al. Leaky termination at premature stop codons antagonizes nonsense-mediated mRNA decay in *S. cerevisiae*. *RNA* [Internet]. 2004 Apr [cited 2015 Mar 22];10(4):691–703. Available from: <http://www.pubmedcentral.nih.gov/articlerender.fcgi?artid=1262634&tool=pmcentrez&rendertype=abstract>
190. Ellenberger TE, Brandl CJ, Struhl K, Harrison SC. The GCN4 basic region leucine zipper binds DNA as a dimer of uninterrupted α Helices: Crystal structure of the protein-DNA complex. *Cell* [Internet]. 1992 Dec [cited 2015 Apr 1];71(7):1223–37. Available from: <http://www.sciencedirect.com/science/article/pii/S0092867405800704>
191. Tucker M, Valencia-Sanchez MA, Staples RR, Chen J, Denis CL, Parker R. The transcription factor associated Ccr4 and Caf1 proteins are components of the major cytoplasmic mRNA deadenylase in *Saccharomyces cerevisiae*. *Cell* [Internet]. 2001 Feb 9 [cited 2015 Apr 1];104(3):377–86. Available from: <http://www.ncbi.nlm.nih.gov/pubmed/11239395>
192. Thireos G, Penn MD, Greer H. 5' untranslated sequences are required for the translational control of a yeast regulatory gene. *Proc Natl Acad Sci* [Internet]. 1984 Aug 1 [cited 2015 Apr 1];81(16):5096–100. Available from: <http://www.pnas.org/content/81/16/5096.short>
193. Caliskan N, Katunin VI, Belardinelli R, Peske F, Rodnina M V. Programmed -1 frameshifting by kinetic partitioning during impeded translocation. *Cell* [Internet]. 2014 Jun 19 [cited 2014 Aug 20];157(7):1619–31. Available from: <http://www.sciencedirect.com/science/article/pii/S0092867414006588>
194. Dunn JG, Foo CK, Belletier NG, Gavis ER, Weissman JS. Ribosome profiling reveals pervasive and regulated stop codon readthrough in *Drosophila melanogaster*. *Elife* [Internet]. eLife Sciences Publications Limited; 2013 Jan 3

[cited 2015 Jan 16];2:e01179. Available from:
<http://elifesciences.org/content/2/e01179.abstract>

195. Jungreis I, Lin MF, Spokony R, Chan CS, Negre N, Victorsen A, et al. Evidence of abundant stop codon readthrough in *Drosophila* and other metazoa. *Genome Res* [Internet]. 2011 Dec [cited 2015 Mar 4];21(12):2096–113. Available from:
<http://www.pubmedcentral.nih.gov/articlerender.fcgi?artid=3227100&tool=pmcentrez&rendertype=abstract>
196. Sato H, Hosoda N, Maquat LE. Efficiency of the pioneer round of translation affects the cellular site of nonsense-mediated mRNA decay. *Mol Cell* [Internet]. Elsevier; 2008 Feb 1 [cited 2015 Apr 2];29(2):255–62. Available from: <http://www.cell.com/article/S109727650700860X/fulltext>
197. Jolly LA, Homan CC, Jacob R, Barry S, Gecz J. The UPF3B gene, implicated in intellectual disability, autism, ADHD and childhood onset schizophrenia regulates neural progenitor cell behaviour and neuronal outgrowth. *Hum Mol Genet* [Internet]. 2013 Dec 1 [cited 2015 Apr 2];22(23):4673–87. Available from: <http://hmg.oxfordjournals.org/content/22/23/4673.short>
198. Lou CH, Shao A, Shum EY, Espinoza JL, Huang L, Karam R, et al. Posttranscriptional control of the stem cell and neurogenic programs by the nonsense-mediated RNA decay pathway. *Cell Rep* [Internet]. 2014 Feb 27 [cited 2014 Oct 27];6(4):748–64. Available from:
<http://www.sciencedirect.com/science/article/pii/S221112471400045X>
199. Weischenfeldt J, Damgaard I, Bryder D, Theilgaard-Mönch K, Thoren LA, Nielsen FC, et al. NMD is essential for hematopoietic stem and progenitor cells and for eliminating by-products of programmed DNA rearrangements. *Genes Dev* [Internet]. 2008 May 15 [cited 2014 Aug 20];22(10):1381–96. Available from: <http://genesdev.cshlp.org/content/22/10/1381>
200. Jacobs JL, Dinman JD. Systematic analysis of bicistronic reporter assay data. *Nucleic Acids Res*. 2008;32:e160–70.
201. Rose MD, Winston FM, Heiter P. *Methods in yeast genetics: a laboratory course manual*. Cold Spring Harbor Laboratory Press; 1990 [cited 2015 Apr 7]; Available from: <http://agris.fao.org/agris-search/search.do?recordID=US9140801>
202. Schluns KS, Lefrançois L. Cytokine control of memory T-cell development and survival. *Nat Rev Immunol* [Internet]. 2003 Apr [cited 2015 Feb 20];3(4):269–79. Available from: <http://dx.doi.org/10.1038/nri1052>

203. Firth AE, Chung BY, Fleeton MN, Atkins JF. Discovery of frameshifting in Alphavirus 6K resolves a 20-year enigma. *Virology J* [Internet]. 2008 Jan [cited 2015 Apr 4];5(1):108. Available from: <http://www.virologyj.com/content/5/1/108>
204. Kirsch M, Hülseweh B, Nacke C, Rülker T, Schirrmann T, Marschall H-J, et al. Development of human antibody fragments using antibody phage display for the detection and diagnosis of Venezuelan equine encephalitis virus (VEEV). *BMC Biotechnol* [Internet]. 2008 [cited 2015 Apr 4];8(1):66. Available from: <http://www.biomedcentral.com/1472-6750/8/66>
205. Ito H, Fukuda Y, Murata K, Kimura A. Transformation of intact yeast cells treated with alkali cations. *J Bacteriol. Am Soc Microbiol*; 1983;153(1):163–8.
206. Grentzmann G, Ingram JA, Kelley PJ, Gesteland RF, Atkins JF. A dual-luciferase reporter system for studying recoding signals. *RNA*. Cambridge Univ Press; 1998;4(04):479–86.
207. Plafker SM, Macara IG. Importin-11, a nuclear import receptor for the ubiquitin-conjugating enzyme, UbcM2. *EMBO J* [Internet]. EMBO Press; 2000 Oct 16 [cited 2015 Apr 8];19(20):5502–13. Available from: <http://emboj.embopress.org/content/19/20/5502.abstract>
208. Plafker SM, Macara IG. Ribosomal Protein L12 Uses a Distinct Nuclear Import Pathway Mediated by Importin 11. *Mol Cell Biol* [Internet]. 2002 Feb 15 [cited 2015 Apr 8];22(4):1266–75. Available from: <http://mcb.asm.org/content/22/4/1266.long>
209. Tanida I, Tanida-Miyake E, Komatsu M, Ueno T, Kominami E. Human Apg3p/Aut1p Homologue Is an Authentic E2 Enzyme for Multiple Substrates, GATE-16, GABARAP, and MAP-LC3, and Facilitates the Conjugation of hApg12p to hApg5p. *J Biol Chem* [Internet]. 2002 Apr 19 [cited 2015 Apr 8];277(16):13739–44. Available from: <http://www.jbc.org/content/277/16/13739.long>
210. Sanjuan MA, Dillon CP, Tait SWG, Moshiah S, Dorsey F, Connell S, et al. Toll-like receptor signalling in macrophages links the autophagy pathway to phagocytosis. *Nature* [Internet]. Nature Publishing Group; 2007 Dec 20 [cited 2014 Jul 10];450(7173):1253–7. Available from: <http://dx.doi.org/10.1038/nature06421>
211. Yu L, Alva A, Su H, Dutt P, Freundt E, Welsh S, et al. Regulation of an ATG7-beclin 1 program of autophagic cell death by caspase-8. *Science* [Internet]. 2004 Jun 4 [cited 2015 Apr 8];304(5676):1500–2. Available from: <http://www.sciencemag.org/content/304/5676/1500.abstract>

212. Lasky LA, Singer MS, Dowbenko D, Imai Y, Henzel WJ, Grimley C, et al. An endothelial ligand for L-selectin is a novel mucin-like molecule. *Cell* [Internet]. 1992 Jun 12 [cited 2015 Apr 8];69(6):927–38. Available from: <http://www.ncbi.nlm.nih.gov/pubmed/1376638>
213. Smigiel KS, Richards E, Srivastava S, Thomas KR, Dudda JC, Klonowski KD, et al. CCR7 provides localized access to IL-2 and defines homeostatically distinct regulatory T cell subsets. *J Exp Med* [Internet]. 2014 Jan 13 [cited 2015 Mar 4];211(1):121–36. Available from: <http://www.pubmedcentral.nih.gov/articlerender.fcgi?artid=3892972&tool=pmcentrez&rendertype=abstract>
214. Endo Y, Iwamura C, Kuwahara M, Suzuki A, Sugaya K, Tumes DJ, et al. Eomesodermin Controls Interleukin-5 Production in Memory T Helper 2 Cells through Inhibition of Activity of the Transcription Factor GATA3. *Immunity* [Internet]. 2011 Nov 23 [cited 2015 Apr 8];35(5):733–45. Available from: <http://www.ncbi.nlm.nih.gov/pubmed/22118525>
215. Iida A, Nakamura Y. High-resolution SNP map in the 55-kb region containing the selectin gene family on chromosome 1q24-q25. *J Hum Genet* [Internet]. 2003 Jan [cited 2015 Apr 8];48(3):150–4. Available from: <http://www.ncbi.nlm.nih.gov/pubmed/12624727>
216. Yamaguchi N, Benya PD, van der Rest M, Ninomiya Y. The cloning and sequencing of alpha 1(VIII) collagen cDNAs demonstrate that type VIII collagen is a short chain collagen and contains triple-helical and carboxyl-terminal non-triple-helical domains similar to those of type X collagen. *J Biol Chem* [Internet]. 1989 Sep 25 [cited 2015 Apr 8];264(27):16022–9. Available from: <http://www.ncbi.nlm.nih.gov/pubmed/2476437>
217. Nag A, Bochukova EG, Kremeyer B, Campbell DD, Muller H, Valencia-Duarte A V, et al. CNV analysis in Tourette syndrome implicates large genomic rearrangements in COL8A1 and NRXN1. *PLoS One* [Internet]. 2013 Jan [cited 2015 Mar 2];8(3):e59061. Available from: <http://www.pubmedcentral.nih.gov/articlerender.fcgi?artid=3606459&tool=pmcentrez&rendertype=abstract>
218. Fritsche LG, Chen W, Schu M, Yaspan BL, Yu Y, Thorleifsson G, et al. Seven new loci associated with age-related macular degeneration. *Nat Genet* [Internet]. 2013 Apr [cited 2015 Apr 8];45(4):433–9, 439e1–2. Available from: <http://www.pubmedcentral.nih.gov/articlerender.fcgi?artid=3739472&tool=pmcentrez&rendertype=abstract>
219. Qian YW, Wang YC, Hollingsworth RE, Jones D, Ling N, Lee EY. A retinoblastoma-binding protein related to a negative regulator of Ras in yeast.

- Nature [Internet]. 1993 Aug 12 [cited 2015 Apr 8];364(6438):648–52.
Available from: <http://www.ncbi.nlm.nih.gov/pubmed/8350924>
220. Zhang Y, Sun ZW, Iratni R, Erdjument-Bromage H, Tempst P, Hampsey M, et al. SAP30, a novel protein conserved between human and yeast, is a component of a histone deacetylase complex. *Mol Cell* [Internet]. 1998 Jun [cited 2015 Apr 8];1(7):1021–31. Available from: <http://www.ncbi.nlm.nih.gov/pubmed/9651585>
221. Nicolas E, Morales V, Magnaghi-Jaulin L, Harel-Bellan A, Richard-Foy H, Trouche D. RbAp48 belongs to the histone deacetylase complex that associates with the retinoblastoma protein. *J Biol Chem* [Internet]. 2000 Mar 31 [cited 2015 Apr 8];275(13):9797–804. Available from: <http://www.ncbi.nlm.nih.gov/pubmed/10734134>
222. Jordanova A, Irobi J, Thomas FP, Van Dijck P, Meerschaert K, Dewil M, et al. Disrupted function and axonal distribution of mutant tyrosyl-tRNA synthetase in dominant intermediate Charcot-Marie-Tooth neuropathy. *Nat Genet* [Internet]. 2006 Feb [cited 2015 Apr 8];38(2):197–202. Available from: <http://www.ncbi.nlm.nih.gov/pubmed/16429158>
223. Ach RA, Taranto P, Gruissem W. A conserved family of WD-40 proteins binds to the retinoblastoma protein in both plants and animals. *Plant Cell* [Internet]. 1997 Sep [cited 2015 Apr 8];9(9):1595–606. Available from: <http://www.pubmedcentral.nih.gov/articlerender.fcgi?artid=157036&tool=pmc-entrez&rendertype=abstract>
224. Della Ragione F, Takabayashi K, Mastropietro S, Mercurio C, Oliva A, Russo GL, et al. Purification and characterization of recombinant human 5'-methylthioadenosine phosphorylase: definite identification of coding cDNA. *Biochem Biophys Res Commun* [Internet]. 1996 Jun 25 [cited 2015 Apr 8];223(3):514–9. Available from: <http://www.ncbi.nlm.nih.gov/pubmed/8687427>
225. Watanabe F, Takao M, Inoue K, Nishioka J, Nobori T, Shiraishi T, et al. Immunohistochemical diagnosis of methylthioadenosine phosphorylase (MTAP) deficiency in non-small cell lung carcinoma. *Lung Cancer* [Internet]. 2009 Jan [cited 2015 Apr 8];63(1):39–44. Available from: <http://www.ncbi.nlm.nih.gov/pubmed/18555557>
226. Dreyling MH, Roulston D, Bohlander SK, Vardiman J, Olopade OI. Codeletion of CDKN2 and MTAP genes in a subset of non-Hodgkin's lymphoma may be associated with histologic transformation from low-grade to diffuse large-cell lymphoma. *Genes Chromosomes Cancer* [Internet]. 1998 May [cited 2015 Apr 8];22(1):72–8. Available from: <http://www.ncbi.nlm.nih.gov/pubmed/9591637>

227. Nobori T, Takabayashi K, Tran P, Orvis L, Batova A, Yu AL, et al. Genomic cloning of methylthioadenosine phosphorylase: a purine metabolic enzyme deficient in multiple different cancers. *Proc Natl Acad Sci U S A* [Internet]. 1996 Jun 11 [cited 2015 Apr 8];93(12):6203–8. Available from: <http://www.pubmedcentral.nih.gov/articlerender.fcgi?artid=39214&tool=pmcentrez&rendertype=abstract>
228. Attié-Bitach T, Abitbol M, Gérard M, Delezoide AL, Augé J, Pelet A, et al. Expression of the RET proto-oncogene in human embryos. *Am J Med Genet* [Internet]. 1998 Dec 28 [cited 2015 Apr 8];80(5):481–6. Available from: <http://www.ncbi.nlm.nih.gov/pubmed/9880212>
229. PLAZAMENACHO I, BURZYNSKI G, GROOT J, EGGEN B, HOFSTRA R. Current concepts in RET-related genetics, signaling and therapeutics. *Trends Genet* [Internet]. 2006 Nov [cited 2015 Apr 8];22(11):627–36. Available from: <http://www.ncbi.nlm.nih.gov/pubmed/16979782>
230. Hofstra RM, Sijmons RH, Stelwagen T, Stulp RP, Kousseff BG, Lips CJ, et al. RET mutation screening in familial cutaneous lichen amyloidosis and in skin amyloidosis associated with multiple endocrine neoplasia. *J Invest Dermatol* [Internet]. 1996 Aug [cited 2015 Apr 8];107(2):215–8. Available from: <http://www.ncbi.nlm.nih.gov/pubmed/8757765>
231. Zhang M-Z, Mai W, Li C, Cho S, Hao C, Moeckel G, et al. PKHD1 protein encoded by the gene for autosomal recessive polycystic kidney disease associates with basal bodies and primary cilia in renal epithelial cells. *Proc Natl Acad Sci U S A* [Internet]. 2004 Feb 24 [cited 2015 Apr 8];101(8):2311–6. Available from: <http://www.pubmedcentral.nih.gov/articlerender.fcgi?artid=356947&tool=pmcentrez&rendertype=abstract>
232. Kaimori J, Nagasawa Y, Menezes LF, Garcia-Gonzalez MA, Deng J, Imai E, et al. Polyductin undergoes notch-like processing and regulated release from primary cilia. *Hum Mol Genet* [Internet]. 2007 Apr 15 [cited 2015 Apr 8];16(8):942–56. Available from: <http://www.pubmedcentral.nih.gov/articlerender.fcgi?artid=1955383&tool=pmcentrez&rendertype=abstract>
233. Bergmann C, Senderek J, Sedlacek B, Pegiazoglou I, Puglia P, Eggermann T, et al. Spectrum of mutations in the gene for autosomal recessive polycystic kidney disease (ARPKD/PKHD1). *J Am Soc Nephrol* [Internet]. 2003 Jan [cited 2015 Apr 8];14(1):76–89. Available from: <http://www.ncbi.nlm.nih.gov/pubmed/12506140>
234. Will CL, Schneider C, Hossbach M, Urlaub H, Rauhut R, Elbashir S, et al. The human 18S U11/U12 snRNP contains a set of novel proteins not found in the

- U2-dependent spliceosome. RNA [Internet]. 2004 Jun [cited 2015 Mar 24];10(6):929–41. Available from: <http://www.pubmedcentral.nih.gov/articlerender.fcgi?artid=1370585&tool=pmcentrez&rendertype=abstract>
235. Abdelmohsen K, Srikantan S, Yang X, Lal A, Kim HH, Kuwano Y, et al. Ubiquitin-mediated proteolysis of HuR by heat shock. EMBO J [Internet]. 2009 May 6 [cited 2015 Mar 12];28(9):1271–82. Available from: <http://www.pubmedcentral.nih.gov/articlerender.fcgi?artid=2683047&tool=pmcentrez&rendertype=abstract>
236. Park EJ, Kim JH, Seong RH, Kim CG, Park SD, Hong SH. Characterization of a novel mouse cDNA, ES18, involved in apoptotic cell death of T-cells. Nucleic Acids Res [Internet]. 1999 Mar 15 [cited 2015 Apr 8];27(6):1524–30. Available from: <http://www.pubmedcentral.nih.gov/articlerender.fcgi?artid=148348&tool=pmcentrez&rendertype=abstract>
237. Fogli A, Schiffmann R, Hugendubler L, Combes P, Bertini E, Rodriguez D, et al. Decreased guanine nucleotide exchange factor activity in eIF2B-mutated patients. Eur J Hum Genet [Internet]. 2004 Jul [cited 2015 Apr 5];12(7):561–6. Available from: <http://www.ncbi.nlm.nih.gov/pubmed/15054402>
238. Matsukawa T, Wang X, Liu R, Wortham NC, Onuki Y, Kubota A, et al. Adult-onset leukoencephalopathies with vanishing white matter with novel missense mutations in EIF2B2, EIF2B3, and EIF2B5. Neurogenetics [Internet]. 2011 Aug [cited 2015 Apr 8];12(3):259–61. Available from: <http://www.ncbi.nlm.nih.gov/pubmed/21484434>
239. Van der Knaap MS, Leegwater PAJ, Könst AAM, Visser A, Naidu S, Oudejans CBM, et al. Mutations in each of the five subunits of translation initiation factor eIF2B can cause leukoencephalopathy with vanishing white matter. Ann Neurol [Internet]. 2002 Feb [cited 2015 Mar 13];51(2):264–70. Available from: <http://www.ncbi.nlm.nih.gov/pubmed/11835386>
240. Gaul U, Mardon G, Rubin GM. A putative Ras GTPase activating protein acts as a negative regulator of signaling by the Sevenless receptor tyrosine kinase. Cell [Internet]. 1992 Mar 20 [cited 2015 Apr 8];68(6):1007–19. Available from: <http://www.ncbi.nlm.nih.gov/pubmed/1547500>
241. Jiang Y, Ma W, Wan Y, Kozasa T, Hattori S, Huang XY. The G protein G α 12 stimulates Bruton's tyrosine kinase and a rasGAP through a conserved PH/BM domain. Nature [Internet]. 1998 Oct 22 [cited 2015 Apr 8];395(6704):808–13. Available from: <http://www.ncbi.nlm.nih.gov/pubmed/9796816>

242. Morrison H, Sperka T, Manent J, Giovannini M, Ponta H, Herrlich P. Merlin/neurofibromatosis type 2 suppresses growth by inhibiting the activation of Ras and Rac. *Cancer Res* [Internet]. 2007 Jan 15 [cited 2015 Apr 8];67(2):520–7. Available from: <http://www.ncbi.nlm.nih.gov/pubmed/17234759>
243. Loetscher P, Alvarez-Gonzalez R, Althaus FR. Poly(ADP-ribose) may signal changing metabolic conditions to the chromatin of mammalian cells. *Proc Natl Acad Sci U S A* [Internet]. 1987 Mar [cited 2015 Apr 8];84(5):1286–9. Available from: <http://www.pubmedcentral.nih.gov/articlerender.fcgi?artid=304412&tool=pmc-entrez&rendertype=abstract>
244. Yu S-W, Wang H, Poitras MF, Coombs C, Bowers WJ, Federoff HJ, et al. Mediation of poly(ADP-ribose) polymerase-1-dependent cell death by apoptosis-inducing factor. *Science* [Internet]. 2002 Jul 12 [cited 2015 Apr 8];297(5579):259–63. Available from: <http://www.ncbi.nlm.nih.gov/pubmed/12114629>
245. Hao L-X, Wang Y-L, Cai L, Li Y-Y. [Inhibitory effect of 5-aminoisoquinolinone on PARP activity in colon carcinoma cell line HT-29]. *Ai Zheng* [Internet]. 2007 Jun [cited 2015 Apr 8];26(6):566–71. Available from: <http://www.ncbi.nlm.nih.gov/pubmed/17562258>
246. Parruti G, Peracchia F, Sallese M, Ambrosini G, Masini M, Rotilio D, et al. Molecular analysis of human beta-arrestin-1: cloning, tissue distribution, and regulation of expression. Identification of two isoforms generated by alternative splicing. *J Biol Chem* [Internet]. 1993 May 5 [cited 2015 Apr 8];268(13):9753–61. Available from: <http://www.ncbi.nlm.nih.gov/pubmed/8486659>
247. Kang J, Shi Y, Xiang B, Qu B, Su W, Zhu M, et al. A nuclear function of beta-arrestin1 in GPCR signaling: regulation of histone acetylation and gene transcription. *Cell* [Internet]. 2005 Dec 2 [cited 2015 Apr 8];123(5):833–47. Available from: <http://www.ncbi.nlm.nih.gov/pubmed/16325578>